**UNIVERSIDADE FEDERAL DO RIO GRANDE DO SUL**

**INSTITUTO DE QUÍMICA**

# ADSORÇÃO DE CORANTES TÊXTEIS UTILIZANDO BIOSSORVENTES ALTERNATIVOS

Doutoranda: **Natalí Farias Cardoso**

**Dezembro de 2012**

**Porto Alegre, RS**

**UNIVERSIDADE FEDERAL DO RIO GRANDE DO SUL**

**INSTITUTO DE QUÍMICA**

# ADSORÇÃO DE CORANTES TÊXTEIS UTILIZANDO BIOSSORVENTES ALTERNATIVOS

Doutoranda: ***Natalí Farias Cardoso***

Orientador: Prof. Dr. Éder Cláudio Lima

*Tese de doutorado submetido ao Programa de Pós-Graduação em Química como parte dos requisitos para obtenção do título de Doutora em Química.*

**Dezembro de 2012**

**Porto Alegre, RS**

A presente tese foi realizada inteiramente pela autora, exceto as colaborações as quais serão devidamente citadas nos agradecimentos, no período entre abril/2010 e novembro/2012, no Instituto de Química da Universidade Federal do Rio Grande do Sul, sob Orientação do Professor Doutor Éder Cláudio Lima. A tese foi julgada adequada para a obtenção do título de Doutora em Química pela seguinte banca examinadora:

**Comissão Examinadora:**

Prof. Dra. Débora Simone Figueredo Gay

Prof. Dra. Leliz Ticona Arenas

Prof. Dr. Fernando Machado Machado

Prof. Dra. Tânia Haas Costa

Prof. Dr. Éder Cláudio Lima

Natalí Farias Cardoso

À memória de uma pessoa que, por infortúnio do destino, partiu cedo, aos 28 anos, poucos meses antes de concluir o doutorado, cujo trabalho havia sido selecionado no Programa TOP USA Santander 2010. Sem dúvidas, uma profissional com futuro promissor. Para os familiares, ela sempre foi muito mais do que isso... Companheira de todas as horas, amiga e confidente, que por diversas vezes me foi exemplo de conduta e caminho a seguir: minha irmã Flávia.

À mulher forte que me educou, me passou valores e sempre me incentivou a estudar: minha mãe Marli.

.... Dedico

# Agradecimentos

Agradeço principalmente ao meu orientador Éder Cláudio Lima. Sem a sua confiança no início do mestrado, o seu esforço ao submeter projeto solicitando bolsa para que eu pudesse me manter e me dedicar aos estudos, nada disso seria possível. Pela interminável compreensão nos momentos difíceis, pela torcida, pelos ensinamentos e pelo auxílio ao longo destes cinco anos de convivência.

Aos professores que compuseram a comissão examinadora da tese e da qualificação pelas sugestões a respeito do trabalho: Débora Figueredo, Fernando Machado, Irene T. Santos Garcia, Leliz Ticona Arenas, Tânia Maria Haas Costa e Tatiana Calvete.

A todos que fizeram parte do grupo de pesquisa do laboratório de tecnologia ambiental e analítica neste período: Jorge Brasil, Júlio Vaghetti, Betina Royer, Tatiana Calvete, Wagner Alencar, Fernando Machado, Rodrigo Pinto, Bruna Cunha, Nathália Simon, Bruna Martins, Camila Amavisca, Thaís Fernandes, Marta Cunha, Bruna dos Santos, Felipe Souza, e Elie Akayanka, pelo auxílio no desenvolvimento do trabalho e companheirismo. Em especial, a Tatiana, pelas diversas sugestões ao longo do mestrado e doutorado, pelas correções de texto e apresentações, pelo carinho e pela amizade.

Ao Wagner Alencar e a sua orientadora Simone Pereira, por nos enviarem os Biossorventes amazônicos e pelo trabalho em parceria.

Ao Guilherme Dotto, que produziu a microalga e ao seu orientador, professor Luiz Pinto, pelo trabalho em parceria.

Aos meus pais, que sempre me incentivaram a estudar fazendo tudo que estava ao alcance. Em especial, à minha mãe, pelo apoio e incentivo diário.

À minha irmã Flávia, por ter me convencido a prestar vestibular para Química e não para Matemática. Pelo apoio, pela amizade, pelo companheirismo, pelas brincadeiras, gargalhadas e até mesmo pelas brigas, por todos os momentos nesses vinte e seis anos que Deus me permitiu estar ao seu

lado.

Ao Júlio Silva, que me acompanhou durante boa parte de minha jornada acadêmica, fazendo parte da minha vida nos momentos mais bipolares: fim do EF, EM, fim de graduação, entrada no mercado de trabalho, mudanças de cidade, todo período de mestrado, ingresso no doutorado, aprovação no concurso, conclusão das disciplinas do doutorado e a encantada qualificação. Eu agradeço todas as palavras de conforto, o apoio, a compreensão e o companheirismo nos inúmeros finais de semana trancados em casa porque eu tinha de estudar, os dezesseis anos de amizade e finalmente, por acreditar mais em mim do que eu mesma.

À irmã que escolhi: Fabiane Porto. Dupla inseparável dos tempos da graduação, parceira nas diversas madrugadas em claro elaborando relatórios. Grande amiga: agradeço os conselhos, as palavras de apoio, a ajuda em todos os momentos difíceis, o carinho e a interminável paciência.

Ao meu namorado Leonardo Soares, pela compreensão nos momentos de ausência, pelo carinho e apoio.

A todos os meus amigos e colegas de trabalho. Em especial, a Ana Geller, a Carolina Trindade, Caroline Wille, Elder Latosinski, Fabiana Zaffalon, Luciana Scaglioni, Marina Laranjo, Ricardo Conrado e a Vera Haas pelos abraços, pelas palavras de apoio e pela amizade. A Lydia Mulling e a Carla Vianna, pelos auxílios na escrita, pelo apoio e carinho.

Aos colegas da pós-graduação. Em especial, ao Álvaro Duarte, Carolina Trindade, Felipe Kessler, Jaqueline Rodrigues, Marina Laranjo e Patrícia Ferreira, pelos grupos de estudo e materiais emprestados.

A todos os professores que contribuíram para a minha formação acadêmica. Em especial, aos professores Caciano Zapatan e Silvio Dias, pelas contribuições no mestrado.

Ao CNPq e à Capes, pelo financiamento.

A todos aqueles que, de alguma forma, contribuíram: muito obrigada.

# Lista de trabalhos Gerados

- Cardoso, Natali F.; Lima, Eder C.; Pinto, Isis S.; Amavisca, Camila V.; Royer, Betina; Pinto, Rodrigo B.; Alencar, Wagner S.; Pereira, Simone F.P. **Application of cupuassu shell as biosorbent for the removal of textile dyes from aqueous solution.** *Journal of Environmental Management*, v. 92, p. 1237-1247, **2011**.

- Cardoso, Natali F.; Lima, Eder C.; Calvete, Tatiana; Pinto, Isis S.; Amavisca, Camila V.; Fernandes, T. H. M.; Pinto, Rodrigo B.; Alencar, Wagner S. **Application of Aqai Stalks as Biosorbents for the Removal of the Dyes Reactive Black 5 and Reactive Orange 16 from Aqueous Solution.** *Journal of Chemical and Engineering Data*, v. 56, p. 1857-1868, **2011**.

- Cardoso, Natali. F.; Lima, Eder. C.; Royer, Betina; Bach, Marta. V.; Dotto, Guilherme. L.; Pinto, Luiz. A. A.; Calvete, Tatiana.; **Comparison of Spirulina platensis microalgae and commercial activated carbon as adsorbents for the removal of Reactive Red 120 dye from aqueous effluents.** *J. Hazard. Mater.,* v. 241-242, p. 146-153, **2012**.

## Publicações de N.F. Cardoso no Grupo de Pesquisa LATAMA

1. Vaghetti, J.C.P., Lima E.C., Royer B., Brasil, J.L., da Cunha, B.M., Simon, N.M., Cardoso, N.F., Noreña, C.P. Z., "*Application of Brazilian-pine fruit coat as a biosorbent to removal of Cr(VI) from aqueous solution. Kinetics and equilibrium study*". **Biochemical Engineering Journal, 2008,** v.42, pp 67-76. Autor Correspondente: **Lima, E.C.** DOI: 10.1016/j.bej.2008.05.021
2. Vaghetti, J.C.P., Lima, E.C., Royer, B., da Cunha, B.M., Cardoso, N.F., Brasil, J. L., Dias, S.L.P. "*Pecan nutshell as biosorbent to remove Cu(II), Mn(II) and Pb(II) from aqueous solutions*". **Journal of Hazardous Materials**, **2009,** v.162, PP 270-280. Autor Correspondente: **Lima, E.C.** DOI: 10.1016/j.jhazmat.2008.05.039
3. Vaghetti, J.C.P., Lima, E.C., Royer, B., Cardoso, N.F., Martins, B., Calvete, T. "*Pecan nutshell as biosorbent to remove toxic metals from aqueous solution*", **Separation Science and Technology**, **2009**, v. 44, pp. 615-644. Autor Correspondente: **Lima, E.C.** DOI: 10.1080/01496390802634331
4. Royer, B., Cardoso, N.F., Lima, E.C., Vaghetti, J.C.P., Simon, N.M., Calvete, T., Veses, R.C., "*Applications of Brazilian-pine fruit shell in natural and carbonized forms as adsorbents to removal of methylene blue from aqueous solutions - Kinetic and equilibrium study*". **Journal of Hazardous Materials**, **2009**, v. 164, pp. 1213-1222. Autor Correspondente: **Lima, E.C.** DOI: 10.1016/j.jhazmat.2008.05.039
5. Royer, B., Cardoso, N.F., Lima, E.C., Ruiz, V.S.O., Macedo, T.R., Airoldi, C. "*Organofunctionalized kenyaite for dye removal from aqueous solution*". **Journal of Colloid and Interface Science, 2009**, v.336, pp. 398-405. Autor Correspondente: **Lima, E.C** DOI:10.1016/j.jcis.2009.04.025
6. Calvete, T, Lima, E.C., Cardoso, N.F., Dias, S.L.P., Pavan, F.A., "*Application of carbon adsorbents prepared from the Brazilian-pine fruit shell for removal of Procion Red MX 3B from aqueous solution - Kinetic, equilibrium, and thermodynamic studies*". **Chemical Engineering Journal, 2009**, v.155, pp. 627-636. Autor Correspondente: **Lima, E.C** DOI:10.1016/j.cej.2009.08.019
7. Royer, B., Lima, E.C., Cardoso, N.F., Calvete, T., Bruns, R.E., "*Statistical design of experiments for optimization of batch adsorption conditions for removal of*

*reactive red 194 textile dye from aqueous effluents*". **Chemical Engineering Communications, 2010**, v.197, pp. 775-790**.** Autor Correspondente: **Lima, E.C** DOI: 10.1080/00986440903359004

8. Royer, B., Cardoso, N.F., Lima, E.C., Macedo, T.R., Airoldi, C. "*Sodic and acidic crystalline lamellar magadiite adsorbents for removal of methylene blue from aqueous solutions. Kinetic and equilibrium studies."* **Separation Science and Technology, 2010**, v.45, pp.129-141. Autor Correspondente: **Lima, E.C** DOI: 10.1080/01496390903256257.
9. Gay, D.S.F., Fernandes, T.H.M., Amavisca, C.V., Cardoso, N.F., Benvenutti, E.V., Costa, T.M.H., Lima, E.C. "*Silica grafted with a silsesquioxane containing the positively charged 1,4-diazoniabicyclo[2.2.2]octane group used as adsorbent for anionic dye removal.*" **Desalination**, **2010**, v.258, pp.128-135. Autor Correspondente: **Lima, E.C** DOI:10.1016/j.desal.2010.03.026
10. Calvete, T, Lima, E.C., Cardoso, N.F., Vaghetti, J.C.P., Dias, S.L.P., Pavan, F.A. "*Application of carbon adsorbents prepared from Brazilian-pine fruit shell for the removal of reactive orange 16 from aqueous solution: Kinetic, equilibrium, and thermodynamic studies*". **Journal of Environmental Management**, **2010**, v.91, pp 1695-1706. Autor Correspondente: **Lima, E.C** DOI:10.1016/j.jenvman.2010.03.013.
11. Royer, B., Cardoso, N.F., Lima, E.C., Macedo, T.R., Airoldi, C., "*A useful organofunctionalized layered silicate for textile dye removal*". **Journal of Hazardous Materials, 2010**, v.181, pp 366-374. Autor Correspondente: **Lima, E.C** DOI:10.1016/j.jhazmat.2010.05.019
12. Calvete, T., Lima, E.C., Cardoso, N.F., Dias, S.L.P., Ribeiro, E.S., "*Removal of brilliant green dye from aqueous solutions using home made activated carbons".* **Clean: Air, Soil, Water***, 2010, v.38, pp. 521-532*. Autor Correspondente: **Lima, E.C** DOI: 10.1002/clen.201000027
13. Cardoso, N.F., Lima, E.C., Pinto I.S., Amavisca C.V., Royer B., Pinto R.B., Alencar W.S., Pereira S.F.P., "*Application of cupuassu shell as biosorbent for the removal of textile dyes from aqueous solution"*. **Journal of Environmental Management**, **2011**, v.92, pp. 1237-1247. Autor Correspondente: **Lima, E.C** DOI:10.1016/j.jenvman.2010.12.010
14. Cardoso, N.F., Pinto, R.B., Lima, E.C., Calvete, T., Amavisca, C.V., Royer, B., Cunha, M.L., Fernandes, T.H.M., Pinto, I.S., "*Removal of remazol black B textile*

*dye from aqueous solution by adsorption*", **Desalination**, **2011**, v.269, pp. 92-103 Autor Correspondente: **Lima, E.C.** DOI:10.1016/j.desal.2010.10.047

**15.** Cardoso, N.F., Lima, E.C., Calvete, T., Pinto, I.S., Amavisca, C.V., Fernandes, T.H.M., Pinto, R.B., Alencar, W.S., "*Application of aqai stalks as biosorbents for the removal of the dyes Reactive Black 5 and Reactive Orange 16 from aqueous solution*". **Journal of Chemical & Engineering Data**, **2011**, v.56, pp 1857-1868. Autor Correspondente: **Lima, E.C.** DOI:10.1021/je100866c

**16.** Cardoso, N.F., Lima, E.C., Royer, B., Bach, M.V., Dotto, G.L., Pinto, L.A.A., Calvete, T.," *Comparison of Spirulina platensis microalgae and commercial activated carbon as adsorbents for the removal of Reactive Red 120 dye from aqueous effluents*", Journal of Hazardous Materials, **2012**, v. 241-242, p. 146-153. Autor Correspondente: **Lima, E.C.** DOI: 10.1016/j.jhazmat.2012.09.026

# Sumário

# LISTA DE FIGURAS

# LISTA DE TABELAS

# ABREVIATURAS

AS: Talo do açaí

AAS: Talo do açaí acidificado

CS: Casca de cupuaçu

SP: Microalga verde azulada *S. platensis*

RB-5: Corante Preto reativo 5

RO-16: Corante Laranja reativo 16

RR-194: Corante Vermelho reativo 194

RR-120: Corante Vermelho reativo 120

DB-53: Corante Azul direto 53

$R^2_{adj}$: Função ajustada

$F_{error}$: Função objetiva

FTIR: Espectroscopia vibracional na região do infravermelho com transformada de Fourier

MEV: Microscopia eletrônica de varredura

BET: Método de Brunuer, Emmet e Teller para determinação de áreas superficiais

BJH: Método de Barret, Joyner e Halenda para determinação de tamanho de poros

## Resumo

Os efluentes têxteis, quando lançados nos corpos hídricos, reduzem a penetração da luz solar prejudicando os processos de fotossíntese. Além disso, os corantes têm sido apontados como substâncias potencialmente tóxicas.

Em geral, os processos de remoção estão fundamentados em sistemas físico-químicos seguidos de tratamento biológico. O processo de adsorção, além de apresentar alta eficiência de remoção, ainda apresenta como vantagem a facilidade de operação e a possibilidade de utilização de adsorventes de baixo custo.

Neste trabalho foram utilizados quatro novos adsorventes alternativos para remoção dos corantes têxteis presentes em soluções aquosas ou efluentes sintéticos. O estudo foi segmentado em três etapas de trabalho. Para a remoção dos corantes RR-194 e DB-53, RB-5 e RO-16 de soluções aquosas, foram testados como adsorventes os seguintes materiais: casca de cupuaçu (CS), talo do açaí (AS) e talo do açaí acidificado (AAS), respectivamente. Para a remoção do corante RR-120 do efluente sintético, foi avaliada a capacidade adsorvente da microalga verde azulada *S. platensis* (SP). Com o intuito de comparar a eficiência de remoção da microalga, os testes também foram realizados com carvão ativo comercial. A dessorção do corante RR-120 e a reutilização da microalga foi analisada.

Os biossorventes foram caracterizados por espectroscopia FTIR, MEV e curvas de adsorção e dessorção de nitrogênio. Foram realizados estudos cinéticos e de equilíbrio para os sistemas. Para avaliar a capacidade de remoção do corante RR-120 da microalga *S. platensis* e do carvão ativo comercial, foram analisados os aspectos termodinâmicos do processo.

Os estudos utilizando a casca do cupuaçu, o talo do açaí, o talo do açaí acidificado e a microalga *S. platensis* mostraram que os novos adsorventes são ótimas alternativas de baixo custo para remoção dos corantes têxteis RR-194 e DB-53, RB-5 e RO-16, e RR-120.

Todos os adsorventes apresentaram elevada eficiência de remoção. Os experimentos de dessorção utilizando solução de NaOH 0,50 mol.$L^{-1}$demonstraram que a microalga *S. platensis* pode ser reutilizada, com pouca perda de eficiência de remoção, diferentemente do carvão ativo, que, apesar de apresentar uma boa

eficiência de remoção, forneceu uma porcentagem de dessorção de cerca de 13%, impossibilitando sua reutilização.

A caracterização dos biossorventes mostrou que os grupos hidroxila presentes nos compostos fenólicos e alcoólicos e os carboxilatos devem participar efetivamente do mecanismo de biossorção.

Os resultados obtidos com os biossorventes CS, AS e AAS foram mais bem representados pelo modelo de ordem fracionária de Avrami, enquanto que o biossorvente SP foi adequadamente ajustado pelo modelo de ordem geral. O modelo de difusão intra-partícula sugere que a biossorção ocorreu em múltiplas etapas.

O equilíbrio foi atingido após 10 e 4 horas de contato dos biossorventes AS e AAS, respectivamente, com os corantes RB-5 e RO-16. O tempo necessário para atingir o equilíbrio entre os corantes RR-194 e DB-53 e o biossorvente CS foi de 8 e 18 horas, respectivamente, enquanto que, para remoção do corante RR-120 com o adsorvente SP e AC, foram necessárias 3 horas.

O modelo de isoterma de Sips foi o que melhor representou os sistemas de adsorção utilizando CS, AS e AAS como biossorventes. Para o carvão ativo e para o biossorvente SP, o modelo que melhor se ajustou aos dados experimentais foi o de Liu.

A capacidade máxima de adsorção dos corantes RB-5 e RO-16 foi de 52,3 $mg.g^{-1}$ e 61,3 $mg.g^{-1}$, respectivamente, utilizando AS como biossorvente e 72,3 $mg.g^{-1}$ e 156 $mg.g^{-1}$, respectivamente, utilizando AAS como biossorvente.

A capacidade máxima de adsorção de RR-194 e DB-53 foi de 64,1 $mg.g^{-1}$ e 37,5 $mg.g^{-1}$, respectivamente, utilizando CS como biossorvente, enquanto que a capacidade máxima de adsorção do corante RR-120 foi de 482,2 $mg.g^{-1}$ e 267,2 $mg.g^{-1}$, respectivamente, utilizando SP e AC como adsorvente.

## Abstract

The textile effluents when launched into water bodies reduce the penetration of sun light harming the photosynthesis processes. Besides this, the dyes have been pointed out as potentially toxic substances.

In general, the removal processes are based on physicochemical systems followed by biological treatment. The sorption process, besides presenting high removal efficiency, it still has the advantage of easy operation and the possibility of usage of low cost adsorbents.

In this work, four new alternative adsorbents were used for the removal of textile dye found in aqueous solutions or synthetic effluents. The study was divided in three working steps. For the removal of the dyes RR-194 and DB-53, RB-5 and RO-16 of aqueous solutions, the following materials were tested as adsorbents: cupuassu shell (CS), aqai stalk (AS) and acidified aqai stalk (AAS), respectively. For the removal of the dye RR-120 of the synthetic effluent the adsorbing capacity of the blue-green microalgae *S. platensis* (SP) was evaluated. In order to compare the efficiency of microalgae removal, the tests were also performed using commercial activated carbon (AC). The desorption of the dye RR-120 e reusage of the microalgae was analyzed.

The biosorbents were characterized through spectroscopy FTIR, MEV and nitrogen adsorption and desorption curves. Kinetic and balance studies for the systems were developed. To evaluate the removal capacity of the dye RR-120 of *S. platensis* microalgae and the commercial activated carbon, the thermodynamic aspects of the process were analyzed.

The studies using the cupuassu shell, aqai stalk, acidified aqai stalk and the *S. platensis* microalgae showed that the new adsorbents are excelent low cost alternatives for the removal of textile dyes RR-194 and DB-53, RB-5 and RO-16, and RR-120.

All adsorbents presented high removal efficiency. The desorption experiments using NaOH 0.50 mol.$L^{-1}$ solution demonstrated that the *S. platensis* microalgae may be reused, with a small loss of removal efficiency, different from the activated carbon,

which, despite presenting a good removal efficiency, provided a desorption rate of about 13%, preventing its reuse.

The characterization of biosorbents showed that the hydroxyl groups found in phenolic and alcoholic compounds and the carboxylates shall effectively participate in the biosorption mechanism.

The results obtained with the CS, AS and AAS biosorbents were better represented by the Avrami fractional order model, while the SP biosorbent was properly adjusted by the general order model. The intra-particle diffusion model suggests that the biosorption occurred in multiple stages.

The balance was reached after 10 and 4 hours of contact with the biosorbents RB-5 and RO-16 and AS and AAS, respectively. The time needed to reach the balance between the dyes RR-194 and DB-53 and the biosorbent CS was of 8 and 18 hours, respectively, whereas for the removal of the dye RR-120 with the adsorbent SP and AC, 3 hours were needed.

The Sips isotherm model was the one which better represented the adsorption systems using CS, AS and AAS as biosorbents. For the activated carbon and the biosorbent SP the model which best suited the experimental data was the Liu's.

The adsorption maximum capacity of the dyes RB-5 and RO-16 were of 52.3 $mg.g^{-1}$ and 61.3 $mg.g^{-1}$ using AS as biosorbent, respectively, and 72.3 $mg.g^{-1}$ and 156 $mg.g^{-1}$ using AAS as biosorbent, respectively.

The adsorption maximum capacity of RR-194 and DB-53 was of 64.1 $mg.g^{-1}$ and 37.5 $mg.g^{-1}$ using CS as biosorbent, respectively, whereas the adsorption maximum capacity of the dye RR-120 was of 482.2 $mg.g^{-1}$ and 267.2 $mg.g^{-1}$ using SP and AC as adsorbent.

# 1. INTRODUÇÃO

As cores exercem grande fascínio sobre a humanidade. Corantes e pigmentos têm sido cada vez mais utilizados para dar cor ao produto final de diferentes indústrias e, mesmo que muitos não conheçam sua composição química, eles fazem parte da vida de qualquer consumidor moderno. Os pigmentos são responsáveis pela cor de tintas e vernizes utilizados em grande escala, principalmente, por indústrias automotivas e de construção civil. Os pimentos podem ser substâncias orgânicas ou inorgânicas e se diferenciam dos corantes por serem insolúveis em água [1,2].

Os corantes são aplicados em vários segmentos industriais, dentre eles o setor alimentício, que os utiliza para colorir molhos, geleias, biscoitos, sorvetes, temperos e alimentos em geral, a indústria cosmética, para colorir produtos de higiene pessoal, cosméticos e perfumes, e a indústria têxtil, que os utiliza para colorir fibras e tecidos [1,3,4].

As indústrias têxteis geram grandes quantidades de efluentes contaminados com corantes. Os processos de tinturaria e lavagem são as principais fontes de poluição da água, produzindo 45 a 65 litros de efluente por quilograma de tecido processado [5,6].

A composição média dos efluentes têxteis é dada por: sólidos totais na faixa de 1000 $mg.L^{-1}$ a 1600 $mg.L^{-1}$; DBO de 200 $mg.L^{-1}$ a 600 $mg.L^{-1}$, pH alcalino e alcalinidade total de 300 $mg.L^{-1}$ a 900 $mg.L^{-1}$. Esses valores são superiores aos estabelecidos pelas resoluções CONAMA nº 357/2005 e nº 397/2008, que são: 500 $mg.L^{-1}$ de sólidos totais, DBO de até 3 $mg.L^{-1}$ de $O_2$, pH neutro, e 250 $mg.L^{-1}$ de alcalinidade[7,8]. Os efluentes têxteis também apresentam uma forte coloração, uma vez que cerca de 20% do corante inicial não é fixada à fibra durante o processo de tingimento [5,6]. Os corantes são visíveis em concentrações muito baixas, como 1 $mg.L^{-1}$. Os efluentes têxteis possuem concentrações que variam de 10 a 200 $mg.L^{-1}$ dependendo do tipo de corante e fibra utilizados [9]. A presença dessas espécies na água reduz a penetração da luz, interferindo nos processos de fotossíntese da flora aquosa, além de causar um impacto visual e organoléptico [10].

Nos seres humanos, pesquisas têm mostrado que algumas classes de corantes podem causar irritação na pele, nas vias aéreas e, se ingeridos, podem

gerar substâncias com propriedades carcinogênicas e mutagênicas, como, por exemplo, toluidinas, benzidinas, radicais livres, entre outros. Alguns casos de câncer em órgãos como rins, bexiga e fígado foram relatados em trabalhadores de indústrias de corantes [11,12,13]. Por essas razões, o tratamento de efluentes industriais contaminados com corantes tem recebido uma atenção considerável em estudos ambientais [14].

Os corantes são classes de compostos orgânicos que apresentam estruturas moleculares aromáticas complexas tornando-os térmica e quimicamente estáveis, dificultando sua degradação por reagentes químicos oxidantes, tratamento térmico, radiação eletromagnética e decomposição por microrganismos [15,16]. Esses procedimentos de remoção são propensos a gerar espécies incolores com toxicidade muitas vezes superior a do seu precursor, em meio anaeróbio, necessitando de tratamento biológico aeróbio posterior [17].

Alguns procedimentos para o tratamento de efluentes contaminados com corantes são: coagulação e floculação [18], ozonização [19], decomposição por oxidação pelo processo Fenton ($H_2O_2/Fe^{+2}$) [20,21], decomposição assistida por luz [20,21], degradação eletroquímica [22], filtração por membranas [23] e adsorção em carvão ativo [24] e silicatos [25].

O processo de adsorção tem se mostrado uma boa alternativa de tratamento, alcançando altos índices de eficiência de remoção, já que os adsorvatos são transferidos da fase aquosa para a fase sólida, reduzindo consideravelmente a disponibilidade dos corantes para os organismos vivos [25]. O efluente descontaminado pode ser descartado no ambiente ou utilizado em processos industriais que necessitam de água com um menor grau de pureza [26]. O adsorvente pode ser regenerado ou estocado em um local seco após seu uso, sem contato direto com o ambiente [27-28].

O carvão ativo é o adsorvente mais empregado para a remoção de corantes de efluentes devido a sua elevada área superficial [24,29,30]. Contudo, seu uso para a remoção de corantes ainda é muito dispendioso, fato que limita a sua larga aplicação em tratamento de efluentes têxteis [31]. Para contornar essa limitação, há um crescente interesse na utilização de adsorventes alternativos de baixo custo, que apresentem capacidade de adsorção semelhante a do carvão ativo. Preferencialmente,

esses adsorventes devem necessitar de pouco processamento e estar amplamente

disponíveis nas proximidades do local onde serão aplicados.

Entre os adsorventes alternativos, podemos citar: argilas [32]; silicatos [25]; zeólitas naturais [33]; bagaço de frutas [31]; restos de folhas de chá [31]; casca de pinhão [24,26,34]; pele de maracujá [35,36]; pele de tangerina [36]; casca da castanha do Pará [37]; casca de árvore [38]; coroa de abacaxi [39]; mesocarpo do coco de babaçu [40]; resíduo de grama [41]; borra de chá [42]; resíduos de plantas de algodão [43], microrganismos [44].

A casca do cupuaçu e o talo do açaí são oriundos de frutos amazônicos, muito consumidos na forma de sucos, sorvetes, doces e geleias. Estima-se que 2000 toneladas de casca de cupuaçu e 32000 toneladas de talo de açaí sejam produzidos anualmente no Brasil [45,46].

A microalga verde azulada *Spirulina platensis* tem sido amplamente cultivada em todo o mundo. Calcula-se que a produção anual mundial seja de 2000 toneladas. Essa microalga tem sido empregada com sucesso na remoção de metais pesados e corantes alimentícios de soluções aquosas. Apesar disso, não existiam estudos sobre a sua utilização na remoção de corantes têxteis [47,48].

Neste trabalho, os resíduos da casca de cupuaçu, do talo do açaí e a microalga *S. platensis* foram pioneiramente empregados como adsorventes para a remoção de corantes têxteis de solução aquosa ou de efluente sintético.

# 2. OBJETIVO

O objetivo desse trabalho foi testar a aplicação da casca de cupuaçu, do talo do açaí, do talo do açaí acidificado e da microalga *S. platensis* como biossorvente para remoção de corantes reativos, muito utilizados nas indústrias têxteis, bem como avaliar o desempenho cinético e as isotermas de adsorção para o equilíbrio desse tipo de sistema.

# 3. REVISÃO DA LITERATURA

## 3.1. CORANTES E A INDÚSTRIA TÊXTIL

O uso de corantes pela humanidade é bastante antigo, existindo relatos de hábitos de colorir tecidos no Egito há cerca de 3200 a.C e na Índia há 2000 anos a.C. Nessa época, os corantes naturais, provenientes de plantas, predominavam e os processos de tingimento eram bastante rudimentares [49].

Até o século XIX, todos os corantes provinham de origem natural, ou seja, eram obtidos através da extração de vegetais, minerais, insetos e moluscos. Muitos dos corantes naturais utilizados ao longo da história são empregados até hoje, como por exemplo, o índigo, descoberto pelos egípcios e que era extraído das plantas *Isatis tinctoria* e a *Indigofera tinctoria*. O emprego de corantes artificiais teve início em 1856, com William Henry Perkin, um químico inglês, que sintetizou a Mauveína, considerada, então, como o primeiro corante sintético produzido. Os corantes começaram a ser sintetizados em larga escala, a produção de índigo, por exemplo, utilizava anilina como precursor [50].

A indústria têxtil produz fibras, fios e tecidos para, posteriormente, serem transformados em artefatos de vestuário, artigos domésticos e bens industriais. As empresas têxteis recebem e preparam as fibras, convertem os fios em tecidos e os tingem [49].

O segmento da cadeia de produtividade de uma indústria têxtil se divide em: fiação, retorção, tinturaria, estamparia, gomagem, malharia e confecção. A formação do fio e do tecido pouco contribui para a geração dos efluentes líquidos, quando comparados aos processos de tingimento e de lavagem do vestuário [50].

A tecnologia de tingimento consiste de várias etapas que são definidas de acordo com a natureza da fibra têxtil, com as características estruturais, com fatores econômicos, com a classificação e com a disponibilidade do corante para aplicação. Devido às exigências do mercado consumidor em relação à diversidade de cores e tonalidades, bem como à resistência da cor à exposição à luz, à lavagem e à transpiração, estima-se que, somente na indústria têxtil, já estejam catalogados cerca de 8000 corantes sintéticos [50,51,52].

## 3.2. FIXAÇÃO DOS CORANTES

Os corantes são compostos orgânicos utilizados para dar cor às fibras têxteis. Apresentam dois componentes principais em sua estrutura: um grupo cromóforo, responsável pela cor, e um grupo funcional, que promove a sua fixação aos tecidos [53,54]. A fixação da molécula do corante às fibras, geralmente, é feita em solução aquosa e pode envolver, basicamente, quatro tipos de interações: interações iônicas, ligações de hidrogênio, forças de van der Walls e ligações covalentes [51].

### 3.2.1. INTERAÇÕES IÔNICAS

Está baseada na interação entre o centro positivo ou negativo presente na fibra e a carga oposta do corante. Exemplos característicos desse tipo de interação são encontrados na tintura da lã, seda e poliamida [50,51].

### 3.2.2. LIGAÇÕES DE HIDROGÊNIO

As ligações de hidrogênio são oriundas da interação entre os átomos de hidrogênio, ligados covalentemente ao corante, e os pares de elétrons livres de átomos doadores presentes na fibra. Esse tipo de interação é encontrado na tintura da lã, seda e de fibras sintéticas como acetato de celulose [50,51].

.

### 3.2.3. FORÇAS DE VAN DER WAALS

São provenientes da aproximação máxima dos orbitais $\pi$ do corante e da molécula da fibra. Essa atração é especialmente efetiva quando a molécula do corante é linear/longa e/ou achatada, podendo, assim, aproximar-se o máximo possível da molécula da fibra. Esse tipo de interação pode ser encontrado na tintura de lã e de poliéster com corantes com alta afinidade por celulose [50,51].

### 3.2.4. LIGAÇÕES COVALENTES

É baseada na formação de uma ligação covalente entre a molécula do corante contendo um grupo reativo (grupo eletrofílico) e um grupo nucleofílico da

fibra. Exemplos característicos desse tipo de interação são tinturas de fibra de algodão [50,51].

## 3.3. CLASSIFICAÇÃO DOS CORANTES

Os corantes podem ser classificados pela estrutura química ou pela forma com que são fixados à fibra têxtil. A classificação baseada na estrutura química, apresentada na Tabela 1, é o principal sistema adotado pelo *Colour Index* (CI) [5,52].

Tabela 1 - Classificação de corantes conforme a constituição química do Colour Index.

| Classe química | Nº de constituição (CI) |
|---|---|
| Nitroso | 10000 – 10299 |
| Nitro | 10300 – 10999 |
| Monoazo | 11000 – 19999 |
| Diazo | 20000 – 29999 |
| Triazo | 30000 – 34999 |
| Pliazo | 35000 – 36999 |
| Azóico | 37000 – 39999 |
| Estilbenno | 40000 – 40799 |
| Carotenóide | 40800 – 40999 |
| Difenilmetano | 41000 – 41999 |
| Triarilmetano | 42000 – 44999 |
| Xanteno | 45000 – 45999 |
| Acridina | 46000 – 46999 |
| Quinolina | 47000 – 47999 |
| Metina | 48000 – 48999 |
| Triazol | 49000 – 49399 |
| Indamina | 49400 – 49699 |
| Indofenol | 49700 – 49999 |
| Azina | 50000 – 50999 |
| Oxazina | 51000 – 51999 |
| Triazina | 52000 – 52999 |
| Sulfuroso | 53000 – 54999 |
| Lactona | 55000 – 55999 |
| Aminocetona | 56000 – 56999 |
| Hidroxicetona | 57000 – 57999 |
| Antraquinona | 58000 – 72999 |
| Índigo | 73000 – 73999 |
| Ftalocianina | 74000 – 74999 |
| Natural | 75000 – 75999 |
| Base de oxidação | 76000 – 76999 |
| Pigmento inorgânico | 77000 – 77999 |

A tabela 2 apresenta à classificação dos corantes quanto à forma de fixação à fibra têxtil [2,5,55].

Tabela 2 - Classificação de corantes segundo a forma de fixação à fibra têxtil.

| Classificação do corante | Característica | Fibras de aplicação | Porcentagem não fixada |
|---|---|---|---|
| Ácido | Aniônico, altamente solúvel e pouco resistente à lavagem. | Fibras proteicas e poliamidas | 5-20 % |
| Pré-metálico | Aniônico, baixa solubilidade e bem resistente à lavagem. | Fibras proteicas e poliamidas | 2-10% |
| Direto | Aniônico, altamente solúvel e pouco resistente à lavagem. | Fibras celulósicas e viscose | 5-30% |
| Básico | Catiônico e altamente solúvel. | Fibras acrílicas | 0-5% |
| Disperso | Dispersão coloidal, muito pouco solúvel e bem resistente à lavagem. | Fibras sintéticas como: poliéster, nylon, fibras acrílicas e acetato de celulose. | 0-10% |
| Reativo | Aniônico, altamente solúvel e bem resistente à lavagem. | Fibras celulósicas, proteicas e poliamida. | 10-50% |
| Enxofre | Coloidal após reação com a fibra. Insolúvel. | Fibras celulósicas. | 10-40% |
| Vat ou a Cuba | Coloidal após reação com a fibra. Insolúvel. | Fibras celulósicas | 5-20% |
| Azóico | Coloidal após reação com a fibra. Insolúvel. | Fibras celulósicas, seda, viscose e poliamida. | 2-3% |

## 3.4. AGREGAÇÃO DE CORANTES

As moléculas dos corantes têm uma tendência a se auto associarem (agregar) em soluções aquosas [56]. Os corantes iniciam a formação de dímeros em concentrações muito baixas. A aglomeração só se completa quando não existe mais possibilidade de ligações entre as moléculas [57]. A formação de dímeros é afetada pela concentração do corante, temperatura e pelo tipo de solvente utilizado. A agregação dos corantes se dá, principalmente, pela inversão das ligações de hidrogênio intramoleculares, existentes no corante quando ainda estão na forma de monômeros, para ligações intermoleculares, existentes quando estão na forma de dímeros. Um esquema dessas ligações é mostrado nas Figuras 1 e 2 [58].

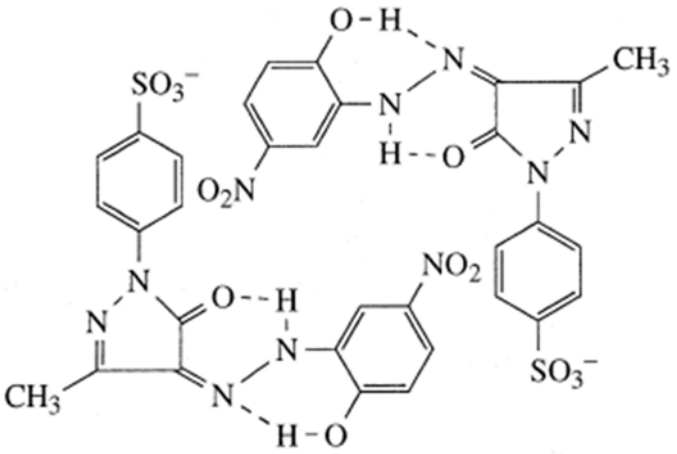


*FIGURA 1. Representação esquemática exemplificando um corante HNAP em solução diluída na forma de monômero.*

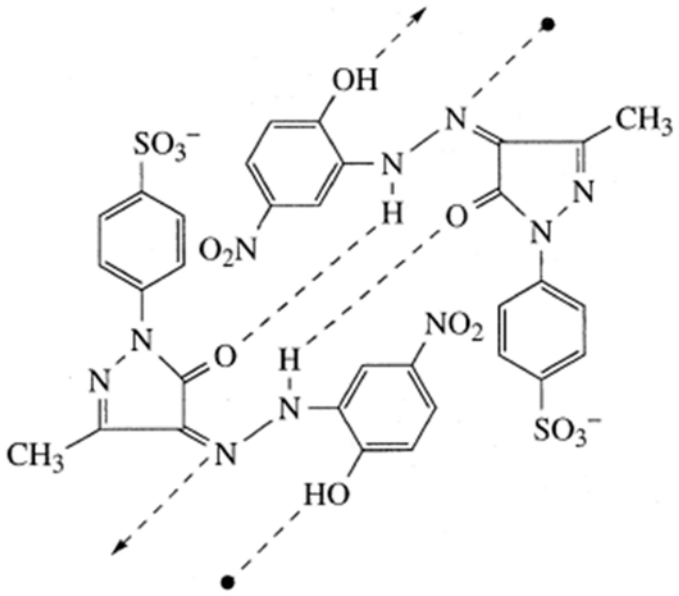


*FIGURA 2. Representação esquemática exemplificando Corante HNAP em solução concentrada na forma de dímero 58.*

Experimentalmente, a agregação pode ser detectada através de varreduras na região UV-Vis. O comprimento de onda no qual se dá o máximo de absorção de radiação é deslocado pelo aumento da concentração. A Tabela 3 mostra um exemplo desse fenômeno [58].

Tabela 3 – Comprimento de onda no UV-Vis que identifica monômeros e dímeros para diferentes corantes.

| Corante | $\lambda_{máx}$ monômero (nm) | $\lambda_{máx}$ dímero (nm) | $\Delta\lambda$ (nm) |
|---|---|---|---|
| HNAP | 480 | 400 | 80 |
| HCAP | 440 | 412 | 28 |
| MNAP | 412 | 395 | 17 |
| HCAN | 527 | 495 | 32 |

A formação de dímeros influenciará principalmente nos processos de sorção das moléculas do corante no adsorvente, uma vez que o adsorvato pode encontrar resistências até atingir o sítio adsorvente [58].

## 3.5. USO DE CORANTES E A GERAÇÃO DE EFLUENTES

O consumo mundial de corantes é estimado em 200 mil toneladas por ano, dividido em diversos segmentos. Cerca de 60 mil toneladas são destinadas à indústria têxtil [2].

No Brasil, a utilização de corantes, pigmentos e branqueadores ópticos por diferentes indústrias vem crescendo, como pode ser observado pelos dados de importações e exportações, apresentados na figura 3 [2].

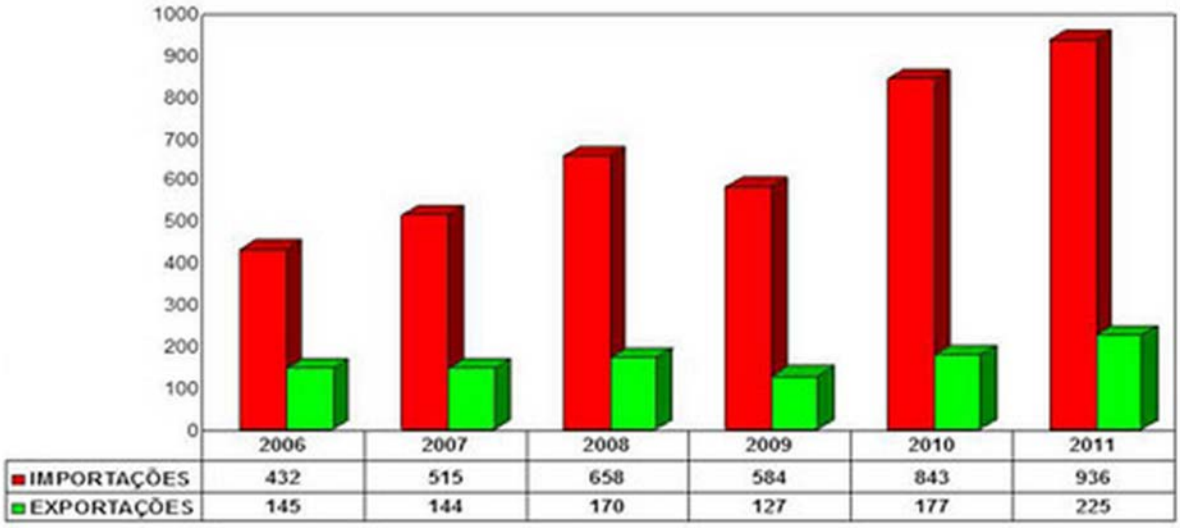


| | 2006 | 2007 | 2008 | 2009 | 2010 | 2011 |
|---|---|---|---|---|---|---|
| IMPORTAÇÕES | 432 | 515 | 658 | 584 | 843 | 936 |
| EXPORTAÇÕES | 145 | 144 | 170 | 127 | 177 | 225 |

*FIGURA 3 – Importações e Exportações brasileiras de corantes, pigmentos e branqueadores ópticos.*

Essas indústrias geram elevado volume de efluentes contaminados com diferentes tipos de corantes. Todos esses efluentes precisam ser tratados antes de serem despejados nos ambientes aquíferos e no solo [2,59].

As indústrias têxteis consomem 45 a 60 litros de água por kg de tecido tingido. Estima-se que até 50% dos corantes utilizados não são fixados às fibras. Os corantes e demais produtos químicos que não são incorporados ao produto final passam a fazer parte das águas residuais [5,55].

Os corantes são visíveis na água em concentrações muito baixas como 1 $mg.L^{-1}$. Os efluentes têxteis, normalmente, possuem corantes em concentrações que variam de 10 a 200 $mg.L^{-1}$, portanto, altamente coloridos [59,60].

Os processos de tingimento industrial lançam, mundialmente nos corpos receptores, cerca de 100.000 toneladas de corantes por ano, e alguns tipos de

corantes são tóxicos e cancerígenos. Por isso, o tratamento de efluentes industriais contaminados com corantes tem recebido uma atenção considerável em estudos ambientais [11,12,14,62].

## 3.6. MÉTODOS DE REMOÇÃO DE CORANTES DE EFLUENTES TÊXTEIS

No tratamento de águas residuais, técnicas tradicionais ou isoladas são ineficazes na remoção de corantes sintéticos, pois a maioria destes compostos é altamente resistente à luz e a agentes oxidantes moderados. O uso de métodos acoplados e de novas técnicas tem sido testado. Portanto, uma ampla gama de métodos vem sendo desenvolvida, incluindo processos físico-químicos e biológicos [63].

### 3.6.1. TRATAMENTO BIOLÓGICO

O tratamento biológico é um método que utiliza microrganismos como bactérias e fungos para degradar as moléculas do corante. A principal vantagem desse tipo de tratamento é o custo, tendo como desvantagem o tempo. O processo pode ser aeróbio, em presença de oxigênio, anaeróbio, na ausência de oxigênio, ou combinado aeróbio-anaeróbio [13,61].

Em condições aeróbias, as enzimas secretadas por bactérias podem quebrar os compostos orgânicos corados. Uma série de corantes, como a magenta, o violeta cristal, o verde brilhante, o verde malaquita e o violeta etílico apresentaram porcentagens de descoloração próximas de 92%, com redução da matéria orgânica superior a 70% utilizando-se o microrganismo *Kurthia sp* [14].

Dentre os vários fungos comumente empregados, o tratamento aeróbio com *Phanerochaete chrysosporium* tem sido extensivamente investigado devido à capacidade de descoloração de uma ampla gama de corantes. Outros microrganismos, tais como *Rhyzopus oryzae, Cyathus bulleri, Coriolus versicolour, Funalia trogii, Laetiporous sulphureus, Streptomyces sp e Trametes versicolour* foram testados, obtendo-se bons resultados na remoção de corantes [31,63].

Estudos apontam que corantes azóicos não são degradados por bactérias

aeróbias, mas podem ser descoloridos por tratamento anaeróbio. Esse tratamento resulta na clivagem da dupla ligação azo e, dentre os fragmentos resultantes, encontram-se as aminas aromáticas, que são comprovadamente cancerígenas. No entanto, a toxicidade desse resíduo pode ser reduzida significativamente com o uso posterior de um tratamento aeróbio, que converte esses compostos em produtos menos nocivos [17,31].

A utilização de bactérias, como *Pseudomonas sp* e *Sphingomonas sp*, tem sido reportada na degradação de corantes. Essas espécies são particularmente úteis na decomposição de azocorantes, pois apresentam a capacidade de realizarem clivagem redutiva das ligações azo, fato este que, geralmente, está associado à enzima azoredutase. Embora os resultados sejam satisfatórios, o tempo necessário para o tratamento com esses microrganismos ainda tem limitado seu uso[13].

### 3.6.2. TRATAMENTO FÍSICO-QUÍMICO

A tecnologia de filtração é um componente importante no tratamento de água potável e residual. O tratamento envolve microfiltrações, ultrafiltrações, nanofiltrações e osmose reversa. Essas técnicas vêm sendo amplamente investigadas para a remoção de coloração de efluentes e, durante seu desenvolvimento, o tipo de membrana a ser utilizado deve ser selecionado previamente, dependendo do objetivo do tratamento de águas. A microfiltração, a ultrafiltração e a nanofiltração são técnicas eficazes para a remoção de todas as classes de corantes. Entretanto, alguns inconvenientes, como o entupimento da membrana e o elevado custo, limitam sua aplicação no tratamento de efluentes industriais [63].

Outro processo adotado para a remoção de poluentes é a osmose reversa. Nesse tratamento, a fase aquosa é forçada a passar, com auxílio de uma membrana impermeável à maioria dos contaminantes, para o lado mais diluído do efluente, reduzindo dessa forma a concentração de contaminantes na fase aquosa. Essa técnica é relativamente bem sucedida para tratamentos de efluentes que não requerem o solvente com um elevado grau de pureza. As principais desvantagens desse processo são as altas pressões de trabalho; o significativo consumo de

energia; o alto custo, a saturação da membrana e o tempo de vida relativamente curto da membrana [13,14].

A aplicação da fotocatálise no tratamento de efluentes têxteis tem sido estudada para a degradação de algumas classes de corantes. Embora a elevada eficiência da fotocatálise heterogênea permita uma rápida mineralização de inúmeras espécies químicas de relevância ambiental, existem vários inconvenientes de ordem prática que têm dificultado bastante a sua consolidação como alternativa de tratamento em grande escala [13]. Dentre as limitações, destacam-se a necessidade de fontes artificiais de radiação, uma vez que grande parte dos fotocatalisadores apresenta uma "*band gap*" com energia correspondente à da região ultravioleta; a dificuldade na penetração da radiação no meio reacional e a dificuldade na separação dos fotocatalisadores, já que esses são empregados na forma de suspensões [13].

O tratamento com agentes coaguladores e floculantes é outra forma de remover corantes de efluentes industriais. O processo envolve a adição de agentes, tais como os íons alumínio ($Al^{3+}$), cálcio ($Ca^{2+}$) ou ferro ($Fe^{3+}$), no efluente para induzir a floculação. Para baixas concentrações e volumes diminutos de efluente, o processo é economicamente viável, mas, para grandes volumes de efluentes ou altas concentrações, o processo se torna oneroso, devido ao custo dos produtos químicos. Com esse tipo de tratamento, são alcançados índices satisfatórios de remoção de corantes dispersos. Essa técnica não é conveniente para o tratamento de efluentes contendo corantes altamente solúveis, tais como os corantes azo, reativos, ácidos e básicos [31].

O termo "POA" é usado para descrever os processos oxidativos em que os radicais hidroxila (•OH), altamente reativos, atuam como oxidantes principais. Geralmente, são empregados de duas formas: oxidação química e oxidação assistida por radiação ultravioleta. A oxidação química normalmente utiliza cloro, água oxigenada, reagente de Fenton ou ozônio como agente oxidante [65,66].

O tratamento por oxidação é mais comumente utilizado para a descoloração de efluentes, uma vez que exigem baixa quantidade de reagente e são relativamente rápidos. Esse tipo de processo é usado para degradar parcialmente ou completamente os corantes de menor peso molecular [31,67].

A combinação de processos oxidativos avançados (POAs), utilizando peróxido de hidrogênio, ozônio e luz ultravioleta, tem sido verificada como alternativa

aos processos de tratamento estabelecidos atualmente, com resultados promissores. Processos físicos utilizando tecnologias de membranas combinadas, principalmente, com ozônio, também têm recebido atenção especial, devido à possibilidade de reuso da água [13,68].

## 3.7. ADSORÇÃO

A adsorção em fase sólida explora a capacidade que certos sólidos têm de agrupar em sua superfície substâncias específicas que estejam presentes em soluções aquosas. O fenômeno de adsorção sólido/líquido consiste na transferência de massa de um soluto, presente em uma fase líquida, para a superfície porosa de uma fase sólida. A adsorção é um processo de interfaces no qual se cria um filme do adsorvato na superfície do material adsorvente [69].

A natureza da interação adsorvente - adsorvato depende das espécies envolvidas. O processo de adsorção é classificado em: adsorção física (fisissorção) e adsorção química (quimissorção) [70]. Na quimissorção, as forças de atração químicas, geralmente ligações covalentes, agem entre a superfície do adsorvente e do adsorvato. Por outro lado, na fisissorção, as forças físicas como forças de van der Waals ou eletrostáticas atuam entre a superfície do adsorvente e do adsorvato. Embora essa distinção seja conceitualmente útil, existem muitos casos intermediários em que nem sempre é possível classificar um determinado sistema de forma inequívoca [71,72]. As características gerais que distinguem a quimissorção da fisissorção são demonstradas na Tabela 4 [73].

Tabela 4 - Características que distinguem fisissorção e quimissorção.

| Fisissorção | Quimissorção |
|---|---|
| Baixo calor de adsorção (< 2 ou 3 vezes o calor latente de evaporação). | Alto calor de adsorção (> 2 ou 3 vezes o calor latente de evaporação) |
| Não específica. | Específica. |
| Monocamada ou multicamadas. | Preferencialmente monocamada. |
| Não ocorre dissociação das espécies adsorvidas. | Pode envolver dissociação. |
| Significativa apenas em temperaturas relativamente baixas. | Possível através de uma ampla faixa de temperatura. |
| Rápida, não ativada e reversível. | Pode ser lenta, ativada e irreversível. |
| Não compartilhamento ou transferência de elétrons e o adsorvato retém sua identidade, embora possa ser deformado pela presença dos campos de força da superfície. | Ocorre uma combinação química entre as superfícies do material adsorvente e do adsorvato, onde os elétrons são compartilhados e/ou transferidos e novas configurações eletrônicas podem se formar através desse processo. |

A remoção da cor de efluente é resultante dos mecanismos de adsorção e de troca iônica (sítios com cargas no adsorvente) e é influenciada por uma série de fatores, tais como o tipo de interação entre o adsorvato e o adsorvente, área superficial do adsorvente, tamanho dos poros do adsorvente, tamanho de partícula, temperatura em que ocorre o processo, acidez do meio (solução do adsorvato) e o tempo de contato entre as fases. Para a seleção adequada do adsorvente a ser empregado para um determinado adsorvato, faz-se necessário ter conhecimento dos dados de equilíbrio e da cinética de adsorção [74].

### 3.7.1. ADSORVENTES

Dentre os diversos adsorventes utilizados industrialmente no processo de adsorção, destacam-se a alumina ativada, a sílica gel, as peneiras moleculares,

algumas argilas ativadas e o carvão ativo [71].

O carvão ativo é o adsorvente mais utilizado para a remoção de corantes de solução aquosa, devido a sua alta capacidade de adsorção e elevada eficiência de remoção [59]. Essa capacidade se deve principalmente a sua característica estrutural que lhe concede uma grande área superficial e a distribuição de tamanho de poros apropriada. Aliada a isso, sua natureza química permite que a superfície do carvão ativo seja facilmente modificada por tratamento químico [75].

Por outro lado, o carvão ativo apresenta várias desvantagens tais como: alto custo, ineficiência com alguns corantes e dificuldade no processo de regeneração [76,77]. Nos últimos anos, devido aos inconvenientes encontrados no uso do carvão ativo, existe um grande interesse em produzir adsorventes alternativos para substituí-lo. A atenção tem sido direcionada para vários materiais sólidos naturais que são capazes de remover poluentes de água contaminada a um custo razoável. Um adsorvente pode ser considerado de baixo custo, se requerer pouco processamento para ser empregado, estiver disponível em abundância na natureza ou apresentar-se como um subproduto industrial [31].

Como alternativa ao carvão ativo, materiais carbonizados não ativados se mostraram eficientes para a remoção de corantes de soluções aquosas. Cabe salientar que esses materiais não exigem um processo de ativação em altas temperaturas, na presença de gases especiais [37], diminuindo o consumo energético.

Resíduos de origem vegetal também podem ser usados como adsorventes de baixo custo. O termo biossorvente é utilizado para definir um adsorvente que seja oriundo de biomassa inativa (sem atividade metabólica) [5].

Os biossorventes apresentam em sua parede celular uma grande variedade de grupos orgânicos, tais como ácidos carboxílicos, ésteres, fenóis, aminas e amidas, que podem reter corantes por troca iônica e atração eletrostática. Os biossorventes também são materiais ricos em celulose, hemicelulose e pectina, servindo para a adsorção de corantes por processos físicos (interação hidrofóbica, ligações de hidrogênio, forças de van der Waals) [5, 63].

Dentre os biossorventes que podem ser utilizados na remoção de corantes de efluentes aquosos contaminados, pode-se citar: casca de coco [38], grão de milho [39], bambu [40], gergelim [41], caroço de cereja [42], caroço de azeitona [43], fibra da casca de coco [44], bagaço de cana de açúcar [59], farelo de trigo [60], serragem de madeira [11], casca de eucalipto [61], pele de maracujá [62], bagaço de maçã [12], raízes de plantas

aquáticas [13], casca de laranja [14], casca de banana [47], casca de amendoim [48], algas [49], quitosana [64], borra de café [90].

O cupuaçu é oriundo de uma árvore amazônica (*Theobroma grandiflorum*). O fruto possui forma esférica ou ovóide, costuma alcançar 20 cm de comprimento e pesar de 1 a 2 kg. Possui casca dura e lisa, de coloração castanho-escura [45].

A polpa é muito apreciada por seu sabor agradável, sendo consumida in natura ou processada, principalmente na forma de sucos, sorvetes, doces e geleias. Além disso, as sementes podem ser usadas para fazer chocolate. A produção anual de sementes de cupuaçu na Amazônia brasileira é de cerca de 5.200 toneladas. Cerca de 40% do peso do cupuaçu é a sua casca, que é um resíduo que não apresenta valor econômico agregado [45].

O açaí é um fruto preto – roxeado que cresce em cachos na palmeira conhecida como açaizeiro, cujo nome cientifico é *Euterpe oleracea*. O açaí é muito consumido como suco, doce, geleias e sorvete. A polpa do açaí, quando batida com xarope de guaraná, origina uma pasta parecida com sorvete muito apreciada e conhecida como açaí na tigela. A produção anual brasileira de açaí é de aproximadamente 160.000 toneladas. Cerca de 20% do peso do açaí é proveniente do talo, que, assim como a casca de cupuaçu, não apresenta valor econômico agregado [46].

A microalga verde azulada *Spirulina platensis* abrange as microalgas eucarióticas e as cianobactérias e é amplamente cultivada em todo o mundo. Estima-se que a produção mundial seja de 2.000 toneladas por ano. Essa microalga tem sido empregada com sucesso na remoção de metais pesados e corantes alimentícios de soluções aquosas, pois apresenta em sua superfície grupos funcionais como as carboxilas, as hidroxila, os sulfatos e os fosfatos, capazes de formar ligação química com o poluente [47,48].

### 3.7.2. ISOTERMAS DE ADSORÇÃO

Enquanto o processo de adsorção se desenvolve, ocorre uma distribuição de soluto entre as duas fases (fluida e sólida), que pode ser mensurada a partir da concentração e da natureza do soluto [73].

As isotermas de adsorção são requisitos básicos para o planejamento de qualquer sistema de adsorção, já que expressam a relação existente entre a

quantidade de adsorvato removido da fase aquosa e a quantidade de adsorvato remanescente na solução a uma temperatura constante [74,78].

As isotermas em batelada são obtidas colocando em contato um volume fixo da solução com uma determinada quantidade de adsorvente, variando-se a concentração de cada solução. O sistema assim formado permanece em agitação até o equilíbrio, para então ser obtida a quantidade adsorvida e a concentração que permanece em solução. Com esses dados, é possível construir o gráfico que relaciona a quantidade de material retido, *q,* em função da concentração da solução em equilibrio *C'*. Na maioria dos casos, observam-se isotermas favoráveis de adsorção de corantes em adsorventes, tais como os carvões ativos, cujos dados de equilíbrio são comumente ajustados aos modelos de Langmuir e Freundlich [74,79].

As formas mais comuns de isotermas estão apresentadas na Figura 4, em que a concentração de equilíbrio em solução (*C'*) é dada em $mg.L^{-1}$ e a quantidade de material retido (*q*) é presentada em $mg.g^{-1}$ [74].

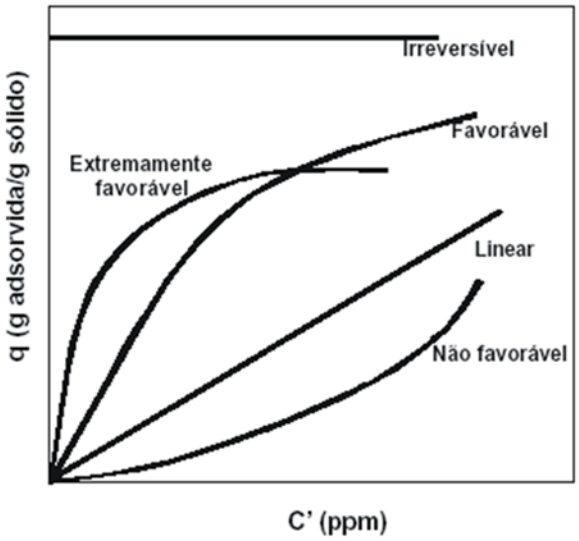


*FIGURA 4 – Tipos de isotermas: q é quantidade máxima de soluto retida no adsorvente no equilíbrio e C' é a concentração de equilíbrio.*

A isoterma linear que sai da origem indica que a quantidade adsorvida é proporcional à concentração do fluido, não indicando uma capacidade máxima para adsorção. As isotermas côncavas são chamadas favoráveis por extrair quantidades relativamente altas, mesmo em baixos níveis de concentração de adsorvato no fluido. As isotermas convexas são chamadas desfavoráveis ou não favoráveis devido à sua baixa capacidade de remoção em baixas concentrações. Isotermas

desfavoráveis são raras, mas muito importantes para entender o processo de regeneração, isto é, transferência de massa do sólido de volta para a fase fluida, quando a isoterma é favorável [74,80].

As isotermas derivadas teórica ou empiricamente podem, frequentemente, ser representadas por equações simples que relacionam diretamente o volume adsorvido em função da pressão e/ou concentração do adsorvato. As isotermas mais utilizadas em estudos da adsorção são as seguintes: Langmuir, Freundlich, Brunauer, Emmett, Teller (B.E.T.), Tóth, Redlich-Peterson, Radke Prausnitz, Sips, Liu, entre outras [79,80].

A descrição matemática precisa da capacidade de adsorção no equilíbrio é indispensável para previsões fidedignas de parâmetros e comparações quantitativas do comportamento de adsorção para diferentes sistemas. Esses parâmetros de isotermas frequentemente podem fornecer informações sobre mecanismos de adsorção, propriedades da superfície e afinidades do adsorvente [79,80].

#### *3.7.2.1. Modelos de isotermas*

*Modelo de isoterma de Langmuir*

O modelo de isoterma de Langmuir é baseado nos seguintes pressupostos [81]:

- os adsorvatos são quimicamente adsorvidos em um número fixo bem definido de sítios;
- um sítio ativo somente interage com uma espécie de adsorvato;
- todos os sítios são energeticamente equivalentes;
- não ocorrem interações entre as espécies de adsorvatos.

A isoterma de Langmuir é dada pela equação:

$$q_e = \frac{Q_{max}.K_L.C_e}{1 + K_L.C_e} \qquad 1)$$

Na qual $C_e$ ($mg.L^{-1}$) é a concentração do sobrenadante após o sistema ter entrado em equilíbrio, $K_L$ é a constante de equilíbrio do processo de adsorção ($L.mg^{-1}$) e $Q_{max}$ é a capacidade máxima de adsorção do adsorvente ($mg.g^{-1}$) assumindo a formação de uma monocamada de adsorvato sobre o adsorvente [81].

*Modelo de isoterma de Freundlich*

O modelo de isoterma de Freundlich [82] assume que a concentração do adsorvato na superfície do adsorvente aumenta infinitamente com a concentração do adsorvato. Teoricamente, esse comportamento é amplamente aplicado a sistemas heterogêneos.

Esse modelo segue um comportamento exponencial dado pela equação:

$$q_e = K_F.C_e^{1/n_F} \qquad 2)$$

Na qual $K_F$ é a constante relacionada com a capacidade de adsorção [$mg.g^{-1}(mg.L^{-1})^{-1/n}$] e $n_F$ é o expoente de Freundlich (adimensional) [82].

*Modelo de isotermas de Sips*

Outro modelo de isotermas de adsorção é o empírico de Sips [83], que é uma combinação matemática dos modelos de isotermas de Langmuir e Freundlich. O modelo de Sips segue a equação:

$$q_e = \frac{Q_{max}.K_S.C_e^{1/n_S}}{1+K_S.C_e^{1/n_S}} \qquad 3)$$

Na qual $K_S$ é a constante de equilíbrio de adsorção de Sips $(mg.L^{-1})^{-1/n}$ , $Q_{max}$ é a capacidade máxima de adsorção ($mg.g^{-1}$), e $n_S$ é o expoente de Sips (adimensional). Em baixas concentrações de adsorvato, esse modelo assume a forma de Freundlich, enquanto que, em altas concentrações, assume a forma de adsorção de Langmuir em monocamadas.

*Modelo de isoterma de Radke e Prausnitz*

A relação empírica proposta por Radke e Prausnitz (1972)[84] foi baseada no modelo de Langmuir. O modelo apresenta a introdução de um novo termo na isoterma de Langmuir e é representado pela seguinte equação [84]:

$$q_e = \frac{Q_{max}.K_{RP}.C_e}{(1+K_{RP}.C_e)^{1/n_{RP}}} \quad 4)$$

Na qual $K_{RP}$ é a constante de Radke e Prausnitz ($L.g^{-1}$) e $n_{RP}$, um número adimensional cujo valor deve ser entre 0 e 1. Em baixas concentrações, a equação se reduz à forma linear. Em altas concentrações de soluto, adquire a forma da isoterma de Freundlich e, no caso especial de $n_{RP}$ = 1, representa a isoterma de Langmuir.

*Modelo de Liu*

Outra proposição para descrever o comportamento de isotermas foi sugerido por Liu *et al* [85]. Esse modelo corresponde à combinação dos modelos de isotermas de Langmuir, Freundlich e Hill e é expresso segundo a equação:

$$q_e = \frac{Q_{max}.(K_g.C_e)^{n_L}}{1+(K_g.C_e)^{n_L}} \quad 5)$$

Onde $k_g$ é a constante de equilíbrio de adsorção de Liu ($L.mg^{-1}$), $n_L$ é o expoente de Liu (adimencional) e $Q_{max}$ é a capacidade máxima de adsorção ($mg.g^{-1}$). Ao contrário do modelo de Sips, o modelo de Liu não prevê restrição quanto ao valor do expoente, o que não o torna limitado [85].

### 3.7.3. MODELOS DE CINÉTICA DE ADSORÇÃO

A cinética de adsorção descreve a velocidade com que as moléculas do adsorvato são adsorvidas pelo adsorvente. Esta velocidade depende das características físico-químicas do adsorvato (natureza do adsorvato, peso molecular, solubilidade e etc.), do adsorvente (natureza, estrutura dos poros) e da solução (pH, temperatura e concentração). Essa cinética de adsorção é de fundamental importância para o projeto de sistemas de tratamento de efluentes em batelada, pois assim podemos determinar o tempo de equilíbrio e a velocidade em

que ocorre a adsorção [86].

O mecanismo da adsorção de corantes sobre adsorventes porosos pode envolver as seguintes etapas [5]:

- difusão das moléculas de corante em solução para a superfície externa do sólido (adsorvente);
- adsorção nos sítios da superfície externa;
- difusão das moléculas da superfície para o interior do sólido até o sítio de adsorção (poros);
- adsorção das moléculas nos sítios ativos disponíveis na superfície interna.

A primeira etapa da adsorção pode ser afetada pela concentração do corante. Portanto, um aumento da concentração inicial do corante pode acelerar a difusão dos corantes da solução para a superfície do sólido. Por outro lado, com concentrações iniciais superiores, teremos concentrações de adsorvato no equilíbrio também superiores, para uma mesma quantidade de adsorvente. A segunda etapa da adsorção é dependente da natureza das moléculas do corante, e a terceira etapa é geralmente considerada a etapa determinante, especialmente no caso de adsorventes microporosos [5,86].

Vários modelos foram desenvolvidos para encontrar as constantes intrínsecas das taxas cinéticas de adsorção. Tradicionalmente, as cinéticas de adsorções dos adsorvatos são descritas pelas expressões originalmente desenvolvidas por Lagergren [87]. Uma cinética de adsorção simples é a equação de pseudo-primeira ordem, dada abaixo:

$$\frac{dq}{dt} = k_f.(q_e - q_t) \qquad 6)$$

Na qual $q_t$ é a quantidade de adsorvato adsorvida em qualquer tempo t ($mg.g^{-1}$), $q_e$ é a quantidade adsorvida no equilíbrio ($mg.g^{-1}$), $k_f$ é a constante da taxa de pseudo-primeira ordem ($min^{-1}$), e t é o tempo de contato (min) entre o adsorvente e o adsorvato. A integração da equação (6) nas condições de contorno, $q_t = 0$ em t= 0, e qt= qt em t=t origina:

$$Ln\ (q_e - q_t) = Ln(q_e) - k_f.t \qquad 7)$$

Após rearranjar essa equação numa forma não linear, a equação cinética de pseudo-primeira ordem torna-se:

$$q_t = q_e.[1 - \exp(-k_f.t)] \qquad 8)$$

A cinética de adsorção de pseudo-segunda ordem baseia-se em [88]:

$$\frac{dq_t}{dt} = k_s.(q_e - q_t)^2 \qquad 9)$$

Na qual $k_s$ é a constante da taxa de pseudo-segunda ordem ($g.mg^{-1}.min^{-1}$). A integração da equação (9) com as condições de contorno, $q_t = 0$ em t= 0, e qt= qt em t=t dá origem a:

$$q_t = \frac{k_s.q_e^2.t}{1+q_e.k_s.t} \qquad 10)$$

A taxa inicial de adsorção ($h_o$, expressa em $mg.g^{-1}.min^{-1}$) pode ser obtida quando t aproxima-se a zero.

$$h_o = k_s.q_e^2 \qquad 11)$$

A equação de Elovich é aplicada para cinética de quimissorção [80]. Essa equação tem sido utilizada satisfatoriamente em alguns processos de quimissorção e tem sido empregada com sucesso em processos de cinética de adsorção lenta [34]. A equação cinética é válida para sistemas nos quais a superfície do adsorvente é heterogênea e é formulada como:

$$\frac{dq_t}{dt} = \alpha.\exp(-\beta q_t) \qquad 12)$$

Integrando essa equação nas condições de contorno, qt= 0 em t=0 e qt = qt

para t= t, origina-se:

$$q_t = \frac{1}{\beta} Ln\ (t + t_o) - \frac{1}{\beta} Ln(t_o) \qquad 13)$$

Na qual $t_o$ = 1/αβ, $\alpha$ é a taxa inicial de adsorção ($mg.g^{-1}.min^{-1}$) e $\beta$ é uma constante relacionada ao grau de cobertura e à energia de ativação envolvida no processo de quimissorção ($g.mg^{-1}$).

Se t for muito maior que $t_o$, a equação cinética pode ser simplificada como:

$$qt = \frac{1}{\beta} Ln(\alpha.\beta) + \frac{1}{\beta} Ln(t) \qquad 14)$$

Apesar dos modelos cinéticos de pseudo-primeira ordem e pseudo-segunda ordem serem os modelos cinéticos de adsorção mais comumente empregados nos trabalhos de cinética de adsorção, a determinação de alguns parâmetros cinéticos, tais como as possíveis mudanças das taxas de adsorção em função da concentração inicial do adsorvato e do tempo de contato entre adsorvente e adsorvato, como também a determinação de modelos cinéticos de ordem fracionária ainda precisam ser mais bem explorados na literatura. Dessa forma, uma equação cinética alternativa de ordem fracionária foi proposta inicialmente por Lopes e colaboradores [62], na qual se fez uma adaptação à função exponencial de Avrami, utilizada para estudar cinética de decomposição térmica [89].

$$\alpha = 1 - \exp\left[-\left(k_{AV}.t\right)\right]^{n_{AV}} \qquad 15)$$

Na qual *α* é a fração de adsorção ($q_t/q_e$) no tempo t, e $k_{AV}$ é a constante cinética de Avrami ($min^{-1}$), e n a ordem fracionária do processo de adsorção que está associada às mudanças de ordem de adsorção de acordo com o tempo de contato entre o adsorvente e o adsorvato [89].

Inserindo-se *α* na equação 15, a equação cinética de adsorção de Avrami pode ser descrita como:

$$q_t = q_e.\left\{1-\exp\left[\left(k_{AV}.t\right)^{n_{AV}}\right]\right\} \quad 16)$$

No entanto, em uma reação química ou processo, os expoentes da lei da velocidade da reação não apresentam relação com os coeficientes estequiométricos da equação química. Quando isso ocorre, é uma mera coincidência. Ou seja, não existe uma forma de predizer a ordem da reação, sem a obtenção de dados experimentais de sua cinética. A fim de estabelecer uma equação de lei geral para a taxa de adsorção, o processo de adsorção na superfície do adsorvente é assumido como a etapa determinante (lenta) da taxa de adsorção. Neste caso, foca-se na concentração de adsorvato na solução e na mudança de números efetivos de sítios ativos na superfície do adsorvente durante o processo de adsorção [90].

Se a lei da velocidade de adsorção é aplicada à equação 17, a expressão da taxa inicial de adsorção de pode ser obtida [90]:

$$\frac{dq}{dt} = k_N \left(q_e - q_t\right)^n \quad 17)$$

Na qual $K_N$ é a constante da taxa de adsorção [$h^{-1}(g.mg^{-1})^{n-1}$]; $n$ é a ordem da adsorção com relação à concentração efetiva dos sítios de adsorção disponíveis na superfície do adsorvente; $q_e$ é a quantidade adsorvida no equilíbrio [$mg.g^{-1}$] e $q_t$ é a quantidade adsorvida a qualquer tempo $t$ [$mg.g^{-1}$]. A equação 17 é o resultado da aplicação da lei da taxa de reação ao processo de adsorção e pode ser utilizada sem qualquer outro pressuposto adicional. Teoricamente, o expoente $n$ na equação 17 pode ser um valor inteiro ou um número fracionário.

O número de sítios ativos ($\theta_t$) disponíveis na superfície do adsorvente pode ser definido pela equação 18.

$$\theta_t = 1 - \frac{q_t}{q_e} \quad 18)$$

A equação 19 descreve a taxa de adsorção em função da variável $\theta_t$.

$$\frac{d\theta_t}{dt} = -k.\theta_t^{\,n} \qquad 19)$$

Onde por definição *K* é:

$$k = k_N (q_e)^{n-1} \qquad 20)$$

Para um adsorvente puro $\theta_t$ = 1, tendendo a diminuir durante o processo de adsorção. Quando o processo de biossorção atinge o equilíbrio, $\theta_t$ tende a um valor fixo. Se ocorrer a saturação do biossorvente, $\theta_t$ = 0.

Integrando-se à equação 19:

$$\int_1^{\theta} \frac{d\theta_t}{\theta_t^{\,n}} = -k \int_0^t dt \qquad 21)$$

Leva-se a:

$$\frac{1}{1-n}.\left[\theta_t^{\,1-n} - 1\right] = -k.t \qquad 22)$$

Que resulta em:

$$\frac{1}{1-n}.\left[\theta_t^{\,1-n} - 1\right] = -k.t \qquad 23)$$

Aplicando-se as equações 18 e 20 na equação 23, obtém-se:

$$q_t = q_e - \frac{q_e}{\left[k_N (q_e)^{n-1}.t.(n-1)+1\right]^{1/(n-1)}} \qquad 24)$$

A equação 24 é a equação cinética de ordem geral que é válida para n ≠ 1 [90].

A possibilidade da resistência da difusão intra-partícula afetar a cinética do

processo de adsorção é geralmente avaliada pelo modelo de difusão intra-partícula [91]:

$$q_t = k_{id}.\sqrt{t} + C \qquad 25)$$

Na qual $k_{id}$ é a taxa de difusão intra-partícula ($mg.g^{-1}.min^{-0.5}$), e C é a constante relacionada com a espessura da camada de difusão ($mg.g^{-1}$).

Quando se constrói um gráfico de $q_t$ versus $\sqrt{t}$, espera-se um comportamento linear. Entretanto, às vezes, o processo é regido por múltiplas retas, indicando que a cinética de adsorção apresenta múltiplas taxas de adsorção [91].

### 3.7.4. FATORES QUE INFLUENCIAM O PROCESSO DE ADSORÇÃO

#### *3.7.4.1. Propriedades Morfológicas*

O fator determinante para um processo de adsorção eficiente é a escolha adequada de um adsorvente. Para isso, deve-se levar em consideração a capacidade de adsorção e seletividade do adsorvente, bem como a sua disponibilidade e o seu custo.

As propriedades texturais dos adsorventes tais como: área superficial, área específica, volume de poros e tamanho dos poros ou distribuição de volume de poros são fatores extremamente importantes no processo de adsorção, uma vez que esse é um fenômeno de superfície [73].

A eficiência da adsorção depende do tamanho dos poros do adsorvente, pois o adsorvato pode ser retido somente na superfície do adsorvente ou pode também se difundir pelos poros do adsorvente (difusão intra-partícula). Nesse segundo mecanismo, o tamanho dos poros do adsorvente está diretamente relacionado com a velocidade que as espécies se difundem e ainda, com a quantidade que pode ser adsorvida nos poros do material [73].

De acordo com a IUPAC, a porosidade total pode ser classificada de acordo com o diâmetro dos poros, sendo estes: microporos, mesoporos e macroporos. Os microporos apresentam diâmetros inferiores a 2 nm, os mesoporos possuem diâmetro entre 2 e 50 nm, e os macroporos representam os poros com diâmetros superiores a 50 nm [93].

Tem sido observado que o tamanho de poros que fornece a maior

capacidade de adsorção está relacionado com as dimensões da molécula do adsorvato, ou seja, a adsorção de pequenas moléculas está arrolada à fração microporosa, e a adsorção de grandes moléculas, como as moléculas de corantes, está diretamente relacionada com o volume de mesoporos [75].

A área superficial específica é frequentemente maior para materiais microporosos. Portanto, quanto menor a granulometria do adsorvente e mais poroso for o material, maior será a disponibilidade de sítios para a adsorção de moléculas do adsorvato (no caso de moléculas pequenas). Para partículas maiores, a resistência de difusão é maior e parte da superfície interna da partícula não é disponibilizada para a adsorção. O acesso aos sítios de adsorção é facilitado quanto menor for a partícula do adsorvente, o que acarreta níveis mais altos de adsorção [94]. No entanto, não é só a escolha do adsorvente que interfere no processo de adsorção, pois a descoloração do efluente é resultado de dois mecanismos, a adsorção e a troca iônica (sítios com cargas no adsorvente), e é influenciada por fatores físico-químicos, tais como a acidez da solução do adsorvato (pH), a interação entre o adsorvato e o adsorvente, o tamanho de poros do adsorvente, o tempo de contato entre o adsorvente e o adsorvato, a concentração inicial de adsorvato e a temperatura [31,95].

#### *3.7.4.2. Acidez da solução de adsorvato (pH)*

O pH da solução é o fator mais importante para o processo de adsorção, particularmente, em relação à capacidade de adsorção, já que as espécies apresentarão intervalos diferentes de pH adequado à adsorção, dependendo do adsorvente utilizado [37,96].

Um parâmetro útil que indica se a superfície se tornará parcialmente carregada negativamente ou positivamente em função do pH é o potencial de carga zero ($pH_{ZPC}$), valor de pH na qual a carga líquida da superfície é zero. Um valor de pH menor que o $pH_{ZPC}$ indica que a carga superficial é positiva e, portanto, a adsorção dos ânions será favorecida. Para valores de pH superiores aos $pH_{ZPC}$, a carga superficial é negativa e a adsorção dos cátions será favorecida [91,96].

### *3.7.4.3. Concentração inicial de adsorvato.*

O aumento de concentração inicial disponibiliza uma maior quantidade do adsorvato para os sítios ativos do adsorvente, fornecendo uma importante força motriz para superar toda a resistência de transferência de massa de corante entre a fase aquosa e a fase sólida, possibilitando uma maior quantidade adsorvida (q). Entretanto, quando os sítios ativos do adsorvente forem saturados, a percentagem de remoção pode diminuir.

Dessa forma, em adsorventes com baixa capacidade de adsorção, o aumento de concentração inicial leva a um aumento da quantidade adsorvida (q) e a uma diminuição na percentagem de remoção [97,98].

### *3.7.4.4. Efeito da Temperatura na Cinética de Adsorção*

A temperatura é um parâmetro muito significativo em sistemas de adsorção, já que a velocidade de diversos processos é drasticamente afetada por suas variações. O aumento da temperatura pode provocar um aumento da energia cinética e da mobilidade das moléculas do corante e, ainda, elevar a taxa de difusão intra-partícula do adsorvato [99]. Logo, a alteração na temperatura de um processo de adsorção conduz a uma mudança na capacidade de adsorção.

Em processos de adsorção, o efeito da temperatura sobre o sistema é refletido na constante de taxa de adsorção. Ao se realizar estudos em diversas faixas de temperaturas, obtém-se o valor das respectivas constantes de velocidade que permitem calcular a energia de ativação do processo através da Eq. (26), denominada equação de Arrhenius [100,101].

$$\ln k = \ln A - \frac{E_a}{RT} \qquad 26)$$

Onde $k$ representa a constante de velocidade da reação, $A$ a constante de Arrhenius, $E_a$ a energia de ativação de Arrhenius (kJ.mol$^{-1}$) do processo de adsorção, $T$ é a temperatura absoluta (Kelvin) e $R$ é a constante universal dos gases (8,314 J.mol$^{-1}$.K$^{-1}$). Um gráfico de ln $k$ versus 1/$T$ deve mostrar uma relação linear

com coeficiente angular de $-E_a/R$, permitindo o cálculo da $E_a$ do processo [100].

Outros parâmetros de ativação, tais como a variação da entalpia de ativação ($\Delta H^*$) e a variação de entropia de ativação ($\Delta S^*$) podem ser obtidos através da equação de Eyring:

$$\ln\left(\frac{k}{T}\right) = \ln\left(\frac{k_B}{\hbar}\right) + \frac{\Delta S^*}{R} - \frac{\Delta H^*}{R} \cdot \frac{1}{T} \qquad 27)$$

Onde $K_b$ (1,381 x $10^{-23}$ J.mol$^{-1}$) e ħ (6,626 x $10^{-34}$ J.s) são as constantes de Boltzmann e Planck, respectivamente. A relação linear ln $K/T$ versus $1/T$ fornece como coeficiente angular o termo – $\Delta H^*$/R, a partir do qual a entalpia de ativação pode ser derivada. A entropia de ativação pode ser derivada a partir do coeficiente linear, representado pelo termo: ln ($K_b$/ħ) + $\Delta S^*/R$.

A partir dos parâmetros de ativação $\Delta H^*$ e $\Delta S^*$, a energia livre de ativação ($\Delta G$) pode ser calculada pela equação 28.

$$\Delta G^* = \Delta H^* - T\Delta S^* \qquad 28)$$

### *3.7.4.5. Estudo Termodinâmico*

Os parâmetros termodinâmicos relacionados com o processo de adsorção, ou seja, a variação da energia livre de adsorção ($\Delta G°_{ads}$, *KJ.mol*$^{-1}$), variação de entalpia de adsorção ($\Delta H°_{ads}$, *KJ.*mol$^{-1}$) e variação de entropia de adsorção ($\Delta S°_{ads}$, *KJ.mol*$^{-1}$*.K*$^{-1}$) são de extrema importância. O cálculo destes parâmetros permite avaliar se o processo é favorável ou não do ponto de vista termodinâmico, bem como a espontaneidade do sistema e se a adsorção ocorre com absorção ou liberação de energia. O calor de adsorção ($\Delta H°_{ads}$) pode ser obtido através da relação linearizada de van't Hoff [102]:

$$\ln K_e = \frac{-\Delta H^o_{ads}}{R} \cdot \frac{1}{T} + \frac{\Delta S^o_{ads}}{R} \qquad 29)$$

Onde $K_e$ é a constante de equilíbrio em temperaturas determinadas,

provenientes da isoterma de adsorção utilizada no ajuste dos dados experimentais de equilíbrio de adsorção. Os valores de $\Delta H°_{ads}$ e $\Delta S°_{ads}$ podem ser calculados a partir da inclinação e do coeficiente linear, respectivamente, da reta da relação ln $K_e$ versus 1/$T$.

O aumento no valor de $K_e$ com aumento da temperatura caracteriza um processo de natureza endotérmica [103]. Quando o valor da entalpia ou calor de adsorção ($\Delta H°_{ads}$) é conhecido, calcula-se a variação da entropia ($\Delta S°_{ads}$) e da energia livre ($\Delta G°_{ads}$) através das seguintes relações termodinâmicas [103]:

$$\Delta G^o_{ads} = \Delta H^o_{ads} - T\Delta S^o_{ads} \qquad 30)$$

$$\Delta G^o_{ads} = -RT\ln(K_e) \qquad 31)$$

Combinando as equações 30 e 31 tem-se :

$$\ln\left(K_e\right) = \frac{\Delta S^o_{ads}}{R} - \frac{\Delta H^o_{ads}}{R} \times \frac{1}{T} \qquad 32)$$

Valores positivos para $\Delta H°_{ads}$ indicam um processo endotérmico, que ocorre com absorção de energia. Por outro lado, valores negativos para $\Delta H°_{ads}$ denotam um processo exotérmico, ou seja, com liberação de energia. Valores negativos para $\Delta G°_{ads}$ indicam claramente que o processo é espontâneo, termodinamicamente favorável e que o adsorvato apresenta alta afinidade com o adsorvente. Por isso, valores negativos para $\Delta G°_{ads}$ implicam em uma maior força motriz do processo de adsorção, resultando em altas capacidades de adsorção. Valores negativos para $\Delta S°_{ads}$ indicam a diminuição da aleatoriedade na interface adsorvato – solução devido às intenções existentes entre adsorvente e adsorvato [102,103].

# 4. PARTE EXPERIMENTAL

## 4.1. PREPARO DAS SOLUÇÕES

As soluções estoque foram preparadas pela dissolução dos corantes em água destilada numa concentração de 5,00 $g.L^{-1}$. As soluções de trabalho foram obtidas pela diluição das soluções estoque para a concentração necessária. Para ajustar o pH, soluções de hidróxido de sódio e de ácido clorídrico, 0,10 mol $L^{-1}$, foram preparadas. O pH das soluções foi medido com um pH metro Schott Lab modelo 850. Os corantes foram utilizados sem processos de purificação adicional.

## 4.2. PREPARO DO EFLUENTE

Dois efluentes sintéticos, contendo quatro corantes reativos, um corante direto e substâncias químicas auxiliares, foram preparados em pH 2,0. A concentração de cada componente no efluente é apresentada na Tabela 5 [104,105,106].

Tabela 5 – Composição dos efluentes sintéticos.

| | | Concentração ($mg.L^{-1}$) | |
|---|---|---|---|
| | **ʎ(nm)** | **Efluente A** | **Efluente B** |
| **Corante Reativo** | | | |
| Vermelho reativo 120 | 534 | 20,0 | 60,0 |
| Laranja reativo 16 | 493 | 5,0 | 15,0 |
| Preto Reativo 5 | 598 | 5,0 | 15,0 |
| Amarelo Brilhante 3G-P | 402 | 5,0 | 15,0 |
| **Corante direto** | | | |
| Azul direto 53 | 607 | 5,0 | 15,0 |
| **Auxiliar Químico** | | | |
| $Na_2SO_4$ | | 100,00 | 100,00 |
| NaCl | | 100,00 | 100,00 |
| $Na_2CO_3$ | | 150,00 | 150,00 |
| $CH_3COONa$ | | 150,00 | 150,00 |
| $CH_3COOH$ | | 600,0 | 600,0 |
| pH | | 2,0* | 2,0* |

*O pH da solução foi ajustado com solução HCl e NaOH 0,10 $mol.L^{-1}$.

## 4.3. CORANTES UTILIZADOS

O corante Laranja Reativo 16 (RO-16) (C.I. 17757; $C_{20}H_{17}N_3O_{10}S_3Na_2$, 601,54 g $mol^{-1}$, Figura 5) foi fornecido pela Sigma-Aldrich (St. Louis, M.O. EUA) e utilizado nos experimentos, a 50% de pureza.

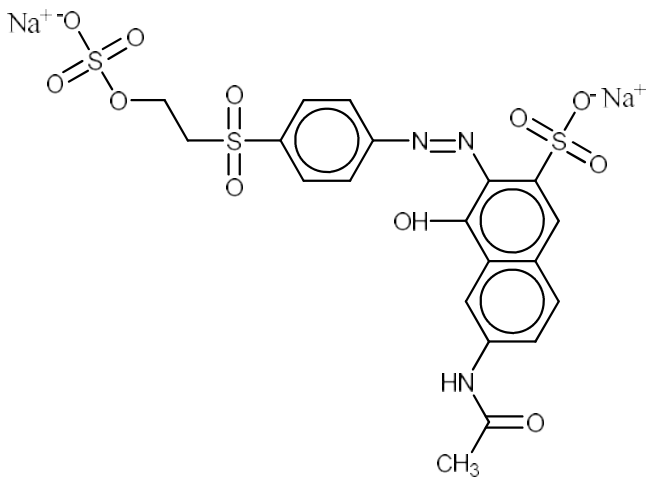

*Figura 5. Fórmula estrutural plana do corante Laranja Reativo 16 (RO-16)*

O Corante Preto Reativo 6 (RB-5) (C.I. 20505; $C_{26}H_{21}N_5O_{19}S_6Na_4$, 991,82 g $mol^{-1}$, Figura 6), foi fornecido pela Sigma-Aldrich (St. Louis, M.O. EUA) e utilizados no experimentos, a 55% de pureza.

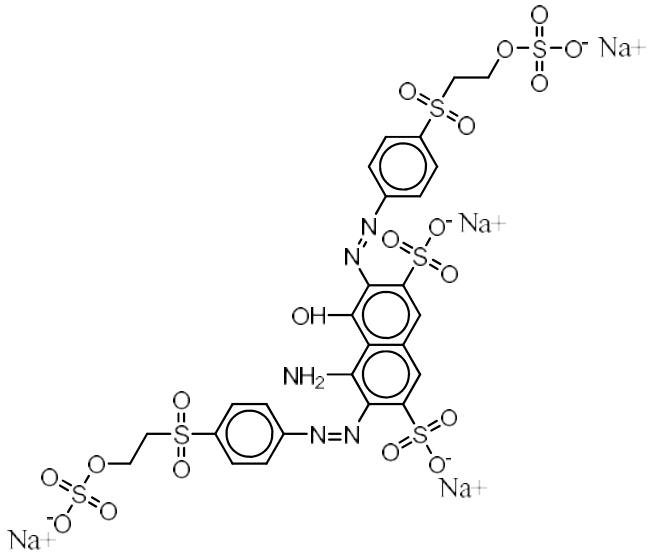

*Figura 6. Fórmula estrutural plana do corante Preto Reativo 5 (RB-5)*

O Corante Vermelho Reativo 194 (RR-194) (C.I. 18214; $C_{27}H_{18}N_7O_{16}S_5ClNa_4$; 984,21 g $mol^{-1}$, Figura 7) foi fornecido pela Bosche Científica (New Brunswick, EUA) e utilizado nos experimentos, a 80% de pureza.

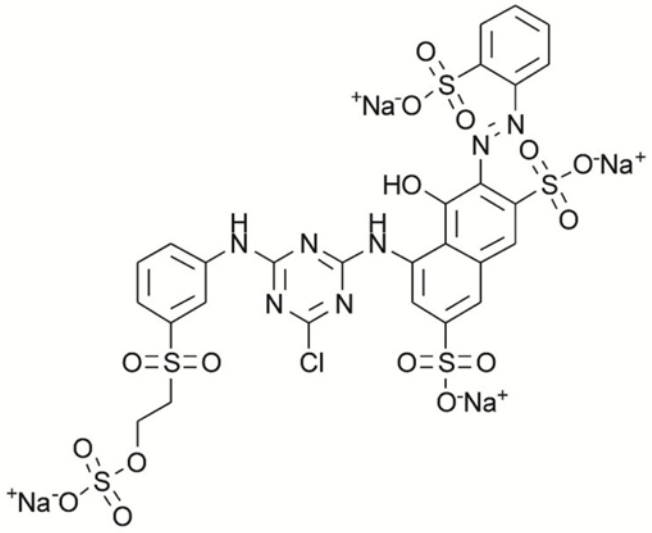

*Figura 7. Fórmula estrutural plana do corante Vermelho Reativo 194 (RR-194)*

O Corante Azul Direto 53 (DB-53) (C.I. 23860; $C_{34}H_{24}N_6O_{14}S_4Na_4$; 960,81 g $mol^{-1}$, Figura 8) foi fornecido pela Vetec (Rio de Janeiro, Brasil) e utilizados nos experimentos, a 85% de pureza.

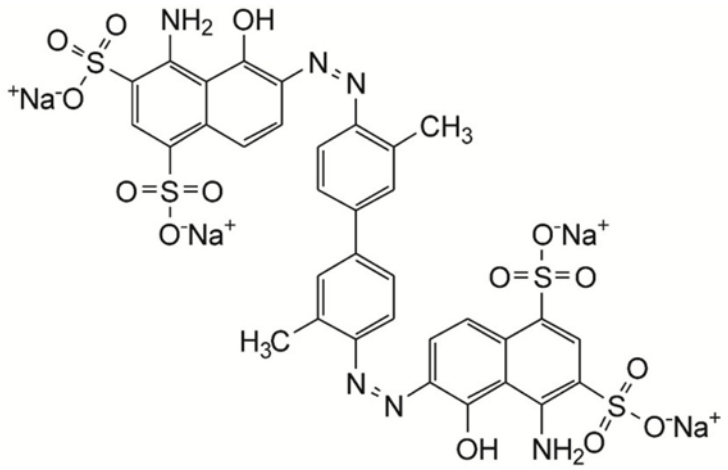

*Figura 8. Fórmula estrutural plana do corante Azul Direto 53 (DB-53)*

O Corante Vermelho Reativo 120 (RR-120) (C.I. 25810; $C_{44}H_{24}N_{14}O_{20}S_6Cl_6Na_6$; 1469,98 g $mol^{-1}$, Figura 9) foi fornecido pela Sigma-Aldrich (Switzerland) e utilizado nos experimentos, a 80% de pureza.

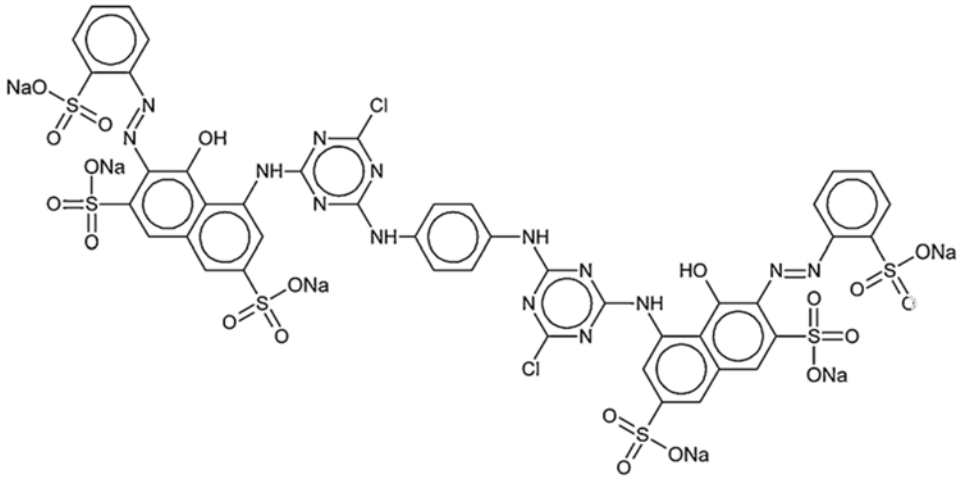

*Figura 9. Fórmula estrutural plana do corante Vermelho Reativo 120 (RR-120)*

## 4.4. PREPARO DOS ADSORVENTES

### 4.4.1. TALO DO AÇAÍ (AS) E CASCA DE CUPUAÇU (CS)

O talo do açaí foi fornecido por uma indústria de sorvetes de Belém-PA, Brasil. A casca de cupuaçu foi fornecida por uma indústria de gelatina de Belém-PA, Brasil. Ambos os materiais foram cedidos pelas indústrias por se tratarem de um material residual e foram lavados com água da torneira para remover a poeira e, posteriormente, com água deionizada. Em seguida, foram secos a 70 °C em um forno com provimento de ar por 8h. Após, foram triturados em moinho de disco e peneirados. As partículas de biossorvente com diâmetro $\leq$ 250 nm foram utilizadas.

### 4.4.2. TALO DO AÇAÍ ACIDIFICADO

A fim de aumentar a quantidade de corante adsorvida, o talo do açaí (AS) foi protonado. Para esse processo, foram adicionados 200,0 mL de HCl 3 mol.$L^{-1}$ a 5,0 g de AS. A suspensão foi deixada em agitação por 24 horas a 70°C. Posteriormente, o adsorvente foi filtrado e a fase sólida lavada com água até que o pH da água de lavagem estivesse em torno de 5,5. O material foi seco a 70°C em um forno com provimento de ar por 8 h, produzindo o talo do açaí

acidificado, denominado AAS.

### 4.4.3. MICROALGA VERDE-AZULADA *S. PLATENSIS* (SP).

O cultivo da microalga ocorreu sob condições não controladas no sul do Brasil sendo dividido em três etapas. Inicialmente, a cepa *Strain LEB-52* foi colocada em Erlenmeyers em meio 20% Zarrouk, [107] cuja composição é apresentada na tabela 6. Após o período de adaptação de cerca de um dia, o conteúdo dos Erlenmeyers foi transposto para foto-biorreatores abertos de 4L, onde permaneceu por aproximadamente 15 dias, até que a concentração de alga chegasse a 0,15 $g.L^{-1}$. Para última etapa do cultivo, o conteúdo do reator de 4L foi transposto para um foto-biorreator de 450 L. Nesse reator a microalga foi cultivada por um período de 30 a 45 dias ou até que a concentração da microalga fosse igual a 1,5 $g.L^{-1}$. Após essa etapa, a biomassa foi recuperada por filtração, lavada com água destilada e prensada para alcançar o teor de umidade de 76%. A biomassa úmida foi seca em tabuleiros perfurados que utilizam fluxo de ar perpendicular sob as seguintes condições: temperatura do ar de 60°C, velocidade de 1,5 $m.s^{-1}$, umidade relativa entre 7 e 10% e capacidade de carga do tabuleiro de 4 $Kg.m^2$. A biomassa seca foi moída em um moinho de disco e peneirada. As partículas com diâmetro entre 68 e 75 µm foram utilizadas [47].

Tabela 6 - Composição do meio Zarrouk.

| | Concentração $g.L^{-1}$ |
|---|---|
| $NaHCO_3$ | 16,8 |
| $NaNO_3$ | 2,5 |
| $K_2HPO_4$ | 0,5 |
| $K_2SO_4$ | 1,0 |
| NaCl | 1,0 |
| $MgSO_4.7H_2O$ | 0,2 |
| $CaCl_2$ | 0,04 |
| $FeSO_4.7H_2O$ | 0,01 |
| EDTA | 0,08 |
| Micronutrientes | - |

### 4.4.4. CARVÃO ATIVO (AC)

O carvão ativo comercial utilizado para comparação com a microalga verde azulada *S. platensis* apresentava partículas com diâmetro inferior a 90 μm e foi fornecido pela Merck.

## 4.5. CARACTERIZAÇÃO DOS ADSORVENTES

### 4.5.1. ANÁLISE ESTRUTURAL.

Para identificar os sítios ativos dos adsorventes, as amostras foram caracterizadas por espectroscopia vibracional na região do infravermelho. Para caracterizar a casca do cupuaçu, o talo do açaí e o talo do açaí acidificado foi utilizado um espectrômetro vibracional Shimadzu modelo 8300 (Kyoto, Japão). A caracterização do carvão ativo e da microalga verde azulada S. platensis foi realizada em um espectrômetro Varian, modelo 640-IR, utilizando-se o método KBr. Os espectros foram obtidos com resolução de 4 $cm^{-1}$, com 100 varreduras cumulativas [108].

### 4.5.2. ANÁLISE TEXTURAL

A área superficial específica dos adsorventes foi determinada pela técnica de multipontos BET (Brunauer, Emmett e Teller) [108], utilizando uma aparelhagem volumétrica apropriada para nitrogênio líquido a 77 K. As isotermas de adsorção e dessorção de nitrogênio foram empregadas para se obter a distribuição do tamanho de poros a 77 K (ponto de ebulição do nitrogênio líquido), usando o método de BJH (Barret, Joyner, e Halenda) [108,109].

As amostras foram pré-tratadas a 473 K durante 24 h em atmosfera de nitrogênio, a fim de eliminar a umidade absorvida na superfície da amostra sólida. Os adsorventes foram então submetidos a 298 K num vácuo, atingindo uma pressão residual de $10^{-4}$ Pa.

Para caracterização dos adsorventes CS, AS e AAS, um analisador de adsorção volumétrica, ASAP 2020, fornecido pela Micromeritrics, foi utilizado. Já para os adsorventes AC e SP foi utilizado um analisador de adsorção volumétrica, Nova 1000, fornecido pela Quantachrome Instruments [109,110].

### 4.5.3 ANÁLISE MORFOLOGÍCA

Os adsorventes foram analisados por microscopia de varredura eletrônica (MEV) utilizando um microscópio eletrônico marca Jeol, modelo JSM 6060, com uma tensão de 5 a 20 KV e amplificações das imagens variando de 500 a 10.000 vezes [110].

### 4.5.4 POTENCIAL DE CARGA ZERO.

Para a determinação do potencial de carga zero ($pH_{pzc}$) dos adsorventes, foram adicionados 20,00 mL de solução de NaCl 0,050 mol.$L^{-1}$ com pH inicial ($pH_i$) previamente ajustado (o $pH_i$ foi ajustado de 2 a 10 pela adição de HCl 0,1 mol.$L^{-1}$ ou NaOH) a vários frascos, cilíndricos, com volume de 50,0 mL. Os valores do $pH_i$ das soluções foram medidos sem que a solução tivesse contato com o adsorvente. Em cada um dos frascos foram acrescentados 50,0 mg dos adsorventes e,

imediatamente, os mesmos foram tampados. As suspensões foram deixadas sob agitação constante em um agitador Tecnal, modelo TE-240, a 150 rpm e 298 K, por 48 horas, para que atingissem o equilíbrio. As suspensões foram, então, centrifugadas a 3600 rpm por 10 minutos e os valores de pH final das soluções ($pH_f$) sobrenadantes foram registrados. O valor de $pH_{pzc}$ é o ponto em que a curva de $\Delta$pH ($pH_f - pH_i$) em função do $pH_i$ cruza a linha de zero [24].

## 4.6. ESTUDOS DE ADSORÇÃO

Os estudos de adsorção foram realizados em triplicata. Para esses experimentos, foram pesados de 20,0 a 200,0 mg de adsorvente em tubos Falcon de 50,0 mL contendo 20,0 mL de solução do corante (10,00 $mg.L^{-1}$ a 1200,0 $mg.L^{-1}$). Os tubos foram deixados sob agitação por um período adequado de tempo (de 5 minutos a 24 horas), sob temperaturas que variaram de 298 K e 323 K. O pH das soluções de corante variaram de 2,0 a 10,0.

Posteriormente, as amostras foram centrifugadas a 3600 rpm em uma centrífuga Fanem Baby I, por 10 minutos, e alíquotas de 1 mL a 10 mL do sobrenadante foram devidamente diluídas em balão volumétrico. A concentração final do corante remanescente na solução, após a adsorção, foi determinada por espectrofotometria de absorção molecular na região do visível, utilizando um espectrofotômetro UV-Vis T90+ fornecido pela PG Instruments, utilizando-se cubetas de vidro óptico.

Foram feitas medições de absorbância no comprimento de onda máximo dos corantes RB-5, RO-16, RR-194 e DB-53, RR-120 em 590nm, 493 nm, 505 nm, 607 e 534 nm, respectivamente.

A quantidade do corante adsorvido e a porcentagem de remoção de corante pelos adsorventes foram calculadas mediante aplicação das Equações 33 e 34, respectivamente:

$$q = \frac{(C_o - C_f)}{m}.V \qquad 33)$$

$$\%\text{Remoção}=100.\frac{(C_o-C_f)}{C_o} \quad 34)$$

Onde q é a quantidade de corante adsorvido pelos adsorventes ($mg.g^{-1}$); $C_o$ é a concentração inicial da solução de corante em contato com o adsorvente ($mg.L^{-1}$); $C_f$ é a concentração do corante ($mg.L^{-1}$) após o processo de adsorção; V é o volume de solução de corante (L) em contato com o adsorvente e m é a massa (g) do adsorvente.

## 4.7. ESTUDOS DE DESSORÇÃO

Para os experimentos de dessorção 50,0 $mg.L^{-1}$ de corante RR-120 foi agitado com 50,0 mg de SP ou AC ou durante 1 h. Após o processo de adsorção, os adsorventes foram filtrados em membranas de acetato de celulose 0,2 μm, e lavados com água para remoção do corante não adsorvido. Para dessorção do corante RR-120, os adsorventes carregados foram agitados em 20,0 mL de solução adequada durante um período de tempo que variou de 15 a 60 minutos. As soluções utilizadas foram: NaCl (0,05 a 0,50 $mol.L^{-1}$), NaOH (0,05 a 0,50 $mol.L^{-1}$) ou uma mistura de NaCl (0,05 a 0,50 $mol.L^{-1}$) + NaOH 0,10 $mol.L^{-1}$. O corante dessorvido foi separado e quantificado como no processo de adsorção.

## 4.8. AVALIAÇÃO ESTATÍSTICA DOS PARÂMETROS CINÉTICOS E DAS ISOTERMAS DE ADSORÇÃO

Para estabelecer precisão, confiabilidade e reprodutibilidade dos dados coletados, todas as medidas de adsorção em batelada foram realizadas em triplicata. Todos os corantes foram armazenados em frascos de vidro, que foram limpos por imersão em $HNO_3$ 1,4 $mol.L^{-1}$ por 24h, lavados cinco vezes com água deionizada, secos e armazenados em um local adequado.

Para a calibração analítica, as soluções padrão com concentrações variando entre 5,00 e 150,0 $mg.L^{-1}$ dos corantes que serão empregados, juntamente com um branco de água padrão com pH ajustado em 2,0. A calibração analítica linear das curvas foi fornecida pelo *software* UVWin do T90 + espectrofotômetro PG

Instruments.

Os modelos cinéticos e de equilíbrio foram ajustados empregando um método não-linear, com interações sucessivas, calculadas pelo método de Levenberg-Marquardt. Também foram calculadas, a partir do *software* Microcal Origin 7.0, as interações não-lineares pelo método Simplex. Além disso, os modelos também foram avaliados pelo coeficiente de determinação ($R^2$), coeficiente de determinação ajustado ($R^2_{adj}$), bem como por uma função objetiva ($F_{error}$), que mede as diferenças na quantidade de corante adsorvido pelo adsorvente previsto pelos modelos e a quantidade de corante adsorvido, medido experimentalmente. $R^2$, $R^2_{adj}$ e $F_{error}$ são representados, nas equações. 36, 37 e 38, respectivamente:

$$R^2 = \left( \frac{\sum_i^n \left( q_{i,exp} - \overline{q}_{i,exp} \right)^2 - \sum_i^n \left( q_{i,exp} - q_{i,model} \right)^2}{\sum_i^n \left( q_{i,exp} - \overline{q}_{i,exp} \right)^2} \right) \qquad 36)$$

$$R^2_{adj} = 1 - \left( 1 - R^2 \right) . \left( \frac{n-1}{n-p} \right) \qquad 37)$$

$$F_{error} = \sqrt{\left( \frac{1}{n-p} \right) . \sum_i^n \left( q_{i,exp} - q_{i,model} \right)^2} \qquad 38)$$

Onde $q_{i,model}$ representa a capacidade de adsorção do adsorvato pelo adsorvente fornecida pelo modelo pré-definido e ajustado, $q_{i,exp}$ é a capacidade de adsorção experimental, $p$ é o número de parâmetros do modelo e $n$ é o número de pontos experimentais realizados e $\overline{q}_{exp}$ representa a média de todos os valores de $q_{i,exp}$. [80].

# 5. CONCLUSÃO

A capacidade máxima de adsorção de RB-5 e RO-16 foi de 52,3 e 61,3 $mg.g^{-1}$, respectivamente, utilizando AS como biossorvente e 72,3 e 156 $mg.g^{-1}$, respectivamente, utilizando AAS como biossorvente.

A capacidade máxima de adsorção de RR-194 e DB-53 foi de 64,1 e 37,5 $mg.g^{-1}$, respectivamente, utilizando CS como biossorvente.

A capacidade máxima de adsorção de RR-120 foi de 482,2 e 267,2 $mg.g^{-1}$ utilizando SP e AC como adsorvente, respectivamente.

O talo do açaí na forma natural (AS) e acidificada (AAS) e a casca do cupuaçu (CS) podem ser considerados excelentes biossorvente, para remover os corantes têxteis Preto Reativo 5 (RB-5), Laranja Reativo 16 (RO-16), Vermelho Reativo 194 (RR-194) e Azul Direto 53 (DB-53) de soluções aquosas.

A microalga verde azulada *S. platensis* se mostrou uma ótima alternativa para a remoção do corante Vermelho Reativo 120 (RR-120) de efluente sintético. Além de apresentar alta eficiência de remoção, 97,1%, os estudos de dessorção utilizando solução 0,50 $mol.L^{-1}$ de NaOH demonstraram que a microalga pode ser reutilizada com mínima redução da eficiência de remoção do corante RR-120, diferentemente do carvão ativo, que, apesar de apresentar uma boa eficiência de remoção, apresentou um índice de dessorção baixo, de cerca de 13%, impossibilitando sua reutilização como adsorvente.

Os biossorventes foram caracterizados por espectroscopia FTIR, MEV e curvas de adsorção e dessorção de nitrogênio. Foi demonstrado que a posição dos grupos OH de fenóis e álcoois e os grupos carboxilatos no espectro foi deslocada para menores números de ondas após o contato com os corantes, indicando que esses grupos devem participar do mecanismo de biossorção.

O modelo de ordem fracionária de Avrami foi o que melhor se ajustou aos resultados obtidos para os biossorventes CS, AS E AAS. Para o biossorvente SP, o modelo de pseudo-primeira ordem foi o que obteve um melhor ajuste. O modelo de difusão intra-partícula sugere que a biossorção ocorre em várias etapas.

O equilíbrio foi atingido após 10 e 4 h de contato entre RB-5 e RO-16 e os biossorventes AS e AAS, respectivamente. O menor tempo de contato para AAS foi atribuído aos macroporos gerados na fibra após o tratamento ácido.

O tempo de equilíbrio para os corantes RR-194 e DB-53 foi de 8 e 18 h, respectivamente, utilizando CS como biossorvente. O maior tempo de contato de DB-53 foi atribuído a maior resistência à transferência de massa.

O equilíbrio para remoção do corante RR-120 foi atingido após 2h para ambos os adsorventes. O tempo de contato fixado para o biossorvente SP é para o carvão ativo foi de 3h, a fim de garantir o equilíbrio para concentrações superiores de adsorvato.

O modelo de isoterma de Sips foi o que melhor se ajustou para os sistemas de adsorção utilizando CS, AS e AAS como biossorvente. Para o carvão ativo e para o biossorvente SP, o modelo de Liu foi o que obteve um melhor ajuste.

# 6. BIBLIOGRAFIA


1. Disponível em: http://www.qmc.ufsc.br/qmcweb/artigos/dye/corantes.html, acessado em setembro de 2012.
2. Disponível em: http://www.abiquim.org.br, acessado em setembro de 2012.
3. Brasil. CNNPA. Resolução nº 44, do dia 25 de novembro de 1977. Disponível em: http://www.anvisa.gov.br/legis/resol/44_77.htm, acessado em setembro de 2012.
4. Brasil. Anvisa. Resolução nº 79, do dia 28 de agosto de 2000, anexo III. Apresenta a listagem de corantes utilizados nos cosméticos. Disponível em: http://www.anvisa.gov.br/cosmeticos/legis/especifica_registro.htm, acessado em setembro de 2012.
5. Calvete, T. **Casca de Pinhão – in Natura e Carvão Ativo – Adsorventes para Remoção de Corantes em Efluentes Aquosos**. Porto Alegre: Universidade Federal do Rio Grande do Sul, 2011.
6. Zanoni, M.; Carneiro, P. *Ciência Hoje.* **2001**, 29, 61.
7. BRASIL. CONAMA. Resolução nº 357, de 17 de março de 2005. Estabelece as condições e padrões de lançamento de efluentes. Disponível em: http://www.mma.gov.br/port/conama/legiabre.cfm?codlegi=459, acessado em setembro de 2012.
8. BRASIL. CONAMA. Resolução n° 397, de 03 de abril de 2008. Estabelece as condições e padrões de lançamento de efluentes. Disponível em: http://www.mma.gov.br/port/conama/legiabre.cfm?codlegi=563, acessado em setembro de 2012.
9. Ali, N.; Hameedb, A.; Ahmedb, S.; *J. Hazard. Mater*. **2009**, 164, 322.
10. Pavan, F.A., Dias, S.L.P., Lima, E.C., Benvenutti, E.V. *Dyes Pigm.* **2008**, 76, 64.
11. Vanhulle, S.; Trovaslet, M.; Enaud, E.; Lucas, M.; Taghavi, S.; Van der Lelie, D.; Van Aken, B.; Foret, M.; Onderwater, R.; Wesenberg, D.; Agathos, S.; Scheneider,Y.; Corbisier, A.; *Environ. Sci. Technol*. **2008**, 42, 584.
12. Paulino, A.; Guilherme, M.; Reis, A.; Campese, G.; Muniz, E.; Nozaki, J.; J. *Colloid Interface Sci.* **2006**, 301, 55.

13. Kunz, A.; Zamora, P.; Moraes, S.; Durán, N.; *Quim. Nova*. **2002**, 25, 78.
14. Goodell, B.; Qian, Y.; Jellison, J.; Richard. M.; *Water Environ. Res.* **2004**, 76, 2703.
15. Forgacs, E., Cseháti, T., Oros, G. *Environment International.* **2004**; 30, 953.
16. Lin, J., Zhang, X., Li, Z., Lei, L. *Bioresour. Technol.* **2010**, 101, 34.
17. Kammradt, P.; **Remoção de Cor de Efluentes de Tinturarias Industriais Através de Processo de Oxidação Avançada**. Curitiba: Universidade Federal do Paraná, 2004.
18. Moghaddam, S.S., Moghaddam, M.R.A., Arami, M. *J. Hazard. Mater.* **2010**, 175, 651.
19. Fanchiang, J.M., Tseng, D.H. *Chemosphere.* **2009**, 77, 214.
20. Elmorsi, T.M., Riyad, Y.M., Mohamed, Z.H., El-Bary, H.M.H.A. *J. Hazard. Mater.* **2010**, 174, 352.
21. Gül, Ş.; Yıldırım, Ö.Ö. *Chem. Eng. J.* **2009**, 155, 684.
22. Huitle, C.A.M., Brillas, E. *Appl. Catal., B.* **2009**, 87, 105.
23. Lau, W.J., Ismail, A.F. *Desalination.* **2009**, 245, 321.
24. Calvete, T, Lima, E.C., Cardoso, N.F., Dias, S.L.P., Pavan, F.A. *Chem. Eng. J.* **2009**, 155, 627.
25. Royer, B., Cardoso, N.F., Lima, E.C., Ruiz, V.S.O., Macedo, T.R., Airoldi, C. *J. Colloid Interface Sci.* **2009**, 336, 398.
26. Royer, B., Cardoso, N.F., Lima, E.C., Vaghetti, J.C.P., Simon, N.M., Calvete, T., Veses, R.C. *J. Hazard. Mater.* **2009**, 164, 1213.
27. Jesus, A.; **Utilização de humina como um material alternativo na adsorção/dessorção de corantes reativos**. São Cristóvão: Universidade Federal de Sergipe, 2010.
28. Ip, A.; Barford, J.; McKay, G. *J. Colloid Interface Sci.* **2009**, 337, 32.
29. Khaled, A., El-Nemr, A., El-Sikaily, A., Abdelwahab, *J. Hazard. Mater.* **2009**, 165, 100.
30. Nunes, A.A., Franca, A.S., Oliveira, L.S., *Bioresour. Technol.* **2009**, 100, 1786.
31. Gupta, V.K., Suhas, I. *J. Environ Manage.* **2009**, 90, 2313.
32. El-Mouzdahir, Y., Elmchaouri, A., Mahboub, R., Gil, A., Korili, S.A. *Desalination* **2010**, 250, 335.

33. Alpat, S.K., Özbayrak, Ö., Alpat, Ş., Akçay, H. *J. Hazard. Mater.* **2008**, 151, 213.
34. Lima, E.C., Royer, B., Vaghetti, J.C.P., Simon, N.M., da Cunha, B.M., Pavan, F.A., Benvenutti, E.V., Veses, R.C., Airoldi, C. *J. Hazard. Mater.* **2008**, 155, 536.
35. Pavan, F.A., Lima, E.C., Dias, S.L.P., Mazzocato, A.C. *J. Hazard. Mater.* **2008**, 150, 703.
36. Pavan, F.A., Gushikem, Y., Mazzocato, A.S., Dias, S.L.P., Lima, E.C. *Dyes Pigm.* **2007**, 72, 256.
37. Brito, S.M.O., Andrade, H.M.C., Soares, L.F., de Azevedo, R.P. *J. Hazard. Mater.* **2010**, 174, 84.
38. Ahmad, R. *J. Hazard. Mater.* **2009**: 171, 767.
39. Weng, C.H.; Lin, Y.T., Tzeng, T.W. *J. Hazard. Mater.* **2009**, 170, 417.
40. Vieira, A.P., Santana, S.A.A., Bezerra, C.W.B., Silva, H.A.S., Chaves, J.A.P., de Melo, J.C.P., da Silva-Filho, E.C., Airoldi C. *J. Hazard. Mater.* **2009**, 166, 1272.
41. Hameed, B.H., *J. Hazard. Mater.* **2009**, 166, 233.
42. Uddin, M.T., Islam, M.A., Mahmud, S., Rukanuzzaman, M. *J. Hazard. Mater.* **2009**, 164, 53.
43. Tunç, Ö., Tanacı, H., Aksu, Z. *J. Hazard. Mater.* **2009**, 163, 187.
44. Vijayaraghavan, K., Yun, Y.S. *Biotechnol Adv.* **2008**, 26, 266.
45. Cardoso, N. F.; Lima, E. C.; Pinto, I. S.; Amavisca, C. V.; Royer, B.; Pinto, R. B.; Alencar, W. S.; Pereira, S. F. P. *J. Environ Manage.* **2011**, 92, 1237.
46. Cardoso, N. F.; Lima, E. C.; Calvete, T.; Pinto, I. S.; Amavisca, C. V.; Fernandes, T. H. M.; Pinto, R. B.; Alencar, W. S. *J. Chem. Eng. Data.* **2011**, 56, 1857.
47. Cardoso, N. F.; Lima, E. C.; Royer, B.; Bach, M. V.; Dotto, G. L.; Pinto, L. A. A.; Calvete, T.; *J. Hazard. Mater.* **2012**, no prelo.
48. Dotto, G. L.; Lima, E. C.; Pinto, L. A. *Bioresour. Technol.* **2012**, 103, 123.
49. Oliveira, D.;. **Corantes como importante classe de contaminantes ambientais – um estudo de caso**. São Paulo: Universidade de São Paulo, 2005.

50. Revista Eletrônica do departamento de Química da UFSC, disponível na internet: http:// www.qmc.ufsc.br/qmcweb/artigos/dye/corantes.html, acessado em setembro de 2012.
51. Guarantini, C.; Zanoni, M.; *Quim. Nova*. **2000**, 23, 71.
52. Index Colour (Society of Dyers and Colourists and American Association of Textile Chemists and Colourists), **2012**)
53. Asku,Z. , *Process Biochemistry*, **2005**, 40, 997-1026.
54. Matyjas, E.; Rybicki, E.; *Autex Research Journal*. **2003,** 3, 90-95.
55. Santana, C.; **Estudo da Degradação de Corante Textil em Matrizes Aquosas Por Meio dos Processos Oxidativos Avançados $O_3/H_2O_2$/UV e Foto-Fenton.** São Paulo: Universidade de São Paulo, 2010.
56. Coates, E. *J. Soc. Dyers and Colourists*, **1969,** 355.
57. Walker, G. M. e Weatherley, L. R. *Chem. Eng. J.* **2001,** 83, 201.
58. Dakiky, M. e Nemcova, I. *Dyes Pigm.* **1999,** 40, 141.
59. Wang, S.; Li, H.; *Dyes Pigm*. **2007**, 72, 308.
60. Harrelkas, F.; Azizi, A.; Yaacoubi, A.; Benhammou, A.; Pons, M.; *Desalination. Water Treat.* **2009**, 235, 330.
61. Vaghela, S.; Jethva, A.; Mehta, B.; Dave,S.; Adimurthy, S.; Ramachandraiah, G.; *Environ. Sci. Technol*. **2005**, 39, 2848.
62. Demirbas, A.; *J. Hazard. Mater*. **2009**, 157, 220.
63. Cardoso, N.; **Remoção do Corante Azul de Metileno de Efluentes Aquosos Utilizando Casca de Pinhão *in Natura* e Carbonizada como Adsorvente.** Porto Alegre: Universidade Federal do Rio Grande do Sul, 2010.
64. Padmesh, T.; Vijayaraghavan K.; Sekaran G.; Velan M.; *J. Hazard. Mater.* **2005**, 125, 121.
65. Molinari, R.; Argurio, P.; Poerio, T.; *Desalination.* **2004**, *162*, 217.
66. Bertazzoli, R.; Pelegrini, R.; *Quim. Nova.* **2002**, *25*, 477.
67. Tseng, R.L.; Tseng, S.K.; Wu, F.; *Colloids Surf. A.* **2006**, *279*, 69.
68. Riga, A.; Soutsasb, K.; Ntampegliotisa, K.; Karayannisa, V.; Papapolymeroua, G. *Desalination*. **2007**, 211, 72.
69. De Boer, J. H. *The dynamical character of adsorption. 2º* Ed. Clarenadon Press, Oxford, 1968.
70. Dąbrowski, A. *Adv. Colloid. Interface Sci.* **2001**, 93, 135.

71. Ruthven, D. M. *Principles of adsorption and adsorption processes*. John Wiley & Sons, Inc. New York, 1984.
72. Geim, A. K., Kim, P. Sci. Am. **2008,** 298, 68.
73. Machado, F. M. **Nanotubos de Carbono como Nanoadsorventes na Remoção de Corantes Sintéticos de Soluções Aquosas: Um Estudo Experimental e Teórico.** Porto Alegre: Universidade Federal do Rio Grande do Sul, 2012.
74. McCabe, W. L., Smith, J. C., Harriot, P. *Unit operations of chemical engineering*. 4º Ed. McGraw-Hill International Editions, New York, 1985.
75. Kruppa, N. E.; Cannon, F. S. *J. Am. Water Association.* **1996,** 88, 94.
76. Weber-Jr, W.J., Morris, J.C. *J. Sanit. Eng. Div. Am. Soc. Civil Eng.* **1963**, 89, 31.
77. Luo, X., Zhang, L. *J. Hazard. Mater.* **2009,** 171, 340
78. Crini, G., Peindy, H. N. *Dyes Pigm.* **2006,** *70*, 204.
79. Yang, R.T. *Gas separation by adsorption processes*. Butterworths, London, 1987.
80. Vaghetti, J.C.P., Lima, E.C., Royer, B., Cardoso, N.F., Martins, B., Calvete, T. *Sep. Sci. Technol.* **2009**, 44, 615.
81. Langmuir, I. The adsorption of gases on plane surfaces of glass, mica and platinum. *J. A. Chem. Soc.* **1918**, 40, 1361.
82. Freundlich, H.M.F. *Z. Phys. Chem.* **1906**, 57A, 385.
83. Sips, R. *J. Chem. Phys.* **1948**, 16, 490.
84. Redlich, O., Peterson, D.L. *J. Phys. Chem.* **1959**, 63, 1024.
85. Y. Liu, H. Xu, S.F. Yang, J.H. Tay, *J. Biotechnol.* **2003**, 102, 233.
86. Sun, G.; Xiangjing, X. U.; *Eng. Res*. **1997**, 36, 808.
87. Largegren, S. *Kungliga Suensk Vetenskapsakademiens Handlingar*. **1898**, 241,1.
88. Ho, Y.S, Mckay, G.M. *Process Biochem.* **1999**, 34, 451.
89. Lopes, E.C.N., dos Anjos, F.S.C., Vieira, E.F.S., Cestari, A.R. *J. Colloid Interface Sci.* **2003**, 263, 542.
90. Shawabkeh, R. A.; Tutunji, M. F. *Clay. Appl. Clay Sci.* **2003**, 24, 111.
91. Mishra, A. K., Arockiadoss, T., Ramaprabhu, S. *Chem. Eng. J.* **2010,** 162, 1026.
92. Demirbas, E.; Kobya, M.; Sulak, M.; *Bioresour. Technol.* **2008**, 99, 5368.

93. Dąbrowski, A. *Adv. Colloid Interface Sci.* **2001***,* 93,135.

94. Bhatnagar, A., Jain, A. K. *J. Colloid Interface Sci.***2005,** 281, 49.

95. Pavan, F.; Lima, E.; Dias, S.; Mazzocato, A.; *J. Hazard. Mater*. **2008**, 150, 703.

96. Calvete, T; Lima, E. C.; Cardoso, N. F.; Vaghetti, J. C. P.; Dias, S. L. P.; Pavan, F.A. *J. Environ. Manage.* **2010**, 91, 1695.

97. Amin, N.; *J. Hazard. Mater.* **2009***,*165, 52.

98. Vasques, A.; Guelli, S.; Valleb, J.; Souza, A.; *J Chem Technol Biotechnol,* **2009**; 84, 1146.

99. Robinson, T., Chandran, B., Nigam, P. *Bioresour. Technol.* **2002,** 85,119.

100. Özcan, A. S., Özcan, A. *J. Colloid Interface Sci.* **2004,** 276, 39.

101. Netpradit, S., Thiravetyan, P., Towprayoon, S. *J. Colloid Interface Sci.* **2004,** 270, 255.

102. Dai, M. *J. Colloid Interface Sci*, ***1998,*** 198, 6.

103. Chao, L., Lu, Z., Li, A., Liu, W., Jiang, Z., Chen, J., *Sep. Purif. Technol.* **2005,** 44, 91.

104. Machado, F.M.; Bergmann, C.P.; Fernandes, T.H.M.; Lima, E.C.; Royer, B.; Calvete, T.; Fagan, S.B.; *J. Hazard. Mater.* **2011,** 192, 1122.

105. Hessel, C.; Allegre, C.; Maisseu, M.; Charbit, F.; Moulin, P. *J. Environ. Manage.* **2007,** 83, 171.

106. Alencar, W.S.; Lima, E.C.; Royer, B.; dos Santos, B.D.; Calvete, T.; da Silva, E.A. Alves, C.N. *Sep. Sci. Technol*. **2012,** 47, 513.

107. Zarrouk, C**; Contribuition to the cyabophyceae study: influence various physical and chimical factors on growth and photosynthesis of *Spirulina máxima (Setch et Gardner) Geitler* extract.** France, University of Paris, 966.

108. Arenas, L.T., Vaghetti, J.C.P., Moro, C.C., Lima, E.C., Benvenutti, E.V., Costa, T.M.H. *Mater. Lett.* **2004**, 58, 895.

109. Arenas, L.T., Lima, E.C., dos Santos-Jr, A.A., Vaghetti, J.C.P., Costa, T.M.H., Benvenutti, E.V. *Colloids Surf., A .* **2007**, 297, 240.

110. Jacques, R.C., Lima, E.C., Dias, S.L.P., Mazzocato, A.C., Pavan, F.A. *Sep. Purif. Technol.* **2007**, 57: 193-198.

# Anexo 1

Journal of Environmental Management 92 (2011) 1237–1247

Contents lists available at ScienceDirect

Journal of Environmental Management

journal homepage: www.elsevier.com/locate/jenvman

# Application of cupuassu shell as biosorbent for the removal of textile dyes from aqueous solution

Natali F. Cardoso [a], Eder C. Lima [a,*], Isis S. Pinto [a], Camila V. Amavisca [a], Betina Royer [a], Rodrigo B. Pinto [a], Wagner S. Alencar [b], Simone F.P. Pereira [b]

[a] Institute of Chemistry, Federal University of Rio Grande do Sul, UFRGS, Av. Bento Gonçalves 9500, Caixa Postal 15003, CEP 91501-970, Porto Alegre, RS, Brazil
[b] Institute of Exact and Natural Sciences, Federal University of Para, UFPA, Belem, PA, Brazil

ARTICLE INFO

*Article history:*
Received 11 July 2010
Received in revised form
15 November 2010
Accepted 12 December 2010
Available online 31 December 2010

*Keywords:*
Biosorption
Cupuassu shell
Textile dyes
Nonlinear isotherm fitting
Adsorption kinetics

ABSTRACT

The cupuassu shell (Theobroma grandiflorum) which is a food residue was used in its natural form as biosorbent for the removal of C.I. Reactive Red 194 and C.I. Direct Blue 53 dyes from aqueous solutions. This biosorbent was characterized by infrared spectroscopy, scanning electron microscopy, and nitrogen adsorption/desorption curves. The effects of pH, biosorbent dosage and shaking time on biosorption capacities were studied. In acidic pH region (pH 2.0) the biosorption of the dyes were favorable. The contact time required to obtain the equilibrium was 8 and 18 h at 298 K, for Reactive Red 194 and Direct Blue 53, respectively. The Avrami fractionary-order kinetic model provided the best fit to experimental data compared with pseudo-first-order, pseudo-second-order and chemisorption kinetic adsorption models. The equilibrium data were fitted to Langmuir, Freundlich, Sips and Radke–Prausnitz isotherm models. For both dyes the equilibrium data were best fitted to the Sips isotherm model.



## 1. Introduction

Dyes are one of the most hazardous chemical compound class found in industrial effluents which need to be treated since their presence in water bodies reduces light penetration, precluding the photosynthesis of aqueous flora (Pavan et al., 2008; Royer et al., 2009a, 2009b, 2010a). They are also aesthetically objectionable for drinking and other purposes. Dyes can also cause allergy, dermatitis, skin irritation and also provoke cancer and mutation in humans (Brookstein, 2009; de Lima et al., 2007; Rosenkranz et al., 2007).

Dyes are a kind of organic compound with a complex aromatic molecular structure that can bring bright and firm color to other materials. However, the complex aromatic molecular structures of dyes make them more stable and more difficult to biodegrade (Calvete et al., 2010; Royer et al., 2010b). The most efficient method for the removal of synthetic dyes from aqueous effluents is the adsorption procedure (Al-Degs et al., 2008; Cestari et al., 2009; Mittal et al., 2010; Rosa et al., 2008). This process transfers the dyes from the water effluent to a solid phase thereby keeping the effluent volume to a minimum (Al-Degs et al., 2008; Calvete et al., 2010). Subsequently, the adsorbent can be regenerated or stored in a dry place without direct contact with the environment (Calvete et al., 2009, 2010).

Activated carbon is the most employed adsorbent for dye removal from aqueous solution because of its excellent adsorption properties (Calvete et al., 2009, 2010; Órfão et al., 2006; Olivares-Marín et al., 2009). However, the extensive use of activated carbon for dye removal from industrial effluents is expensive, limiting its large application for wastewater treatment (Crini, 2006; Gupta and Suhas, 2009). Therefore, there is a growing interest in finding alternative low cost adsorbents for dye removal from aqueous solution. Among these alternative adsorbents, it can be cited: hazelnut shell, saw dust, walnut, saw dust cherry, saw dust oak, saw dust pitch pine, saw dust pine, cane pitch, soy meal hull, banana pitch (Gupta and Suhas, 2009); sugar cane bagasse, cotton waste, chitin and chitosan, peat, microorganisms such as fungus and yeasts (Crini, 2006); maize cob (Crini, 2006; Gupta and Suhas, 2009); Brazilian pine-fruit shell (Lima et al., 2008; Royer et al., 2009b, 2010c); mandarin peel, yellow passion fruit peel (Pavan et al., 2007); tree leaves (Deniz and Saygideger, 2010); wood shavings (Janoš et al., 2009); coffee bean (Baek et al., 2010); babassu (Vieira et al., 2009); marine algae (Bekçi et al., 2009) etc.

Cupuassu (*Theobroma grandiflorum*), is a tropical rainforest tree related to cacao (Gondim et al., 2001), native in the Brazilian Amazon. Cupuassu trees usually range from 5 to 15 m in height (Gondim et al., 2001), and cupuassu fruits are oblong, brown, and

* Corresponding author. Tel.: +55 (51) 3308 7175; fax: +55 (51) 3308 7304.
*E-mail addresses:* eder.lima@ufrgs.br, profederlima@gmail.com (E.C. Lima).

0301-4797/$ – see front matter © 2010 Elsevier Ltd. All rights reserved.
doi:10.1016/j.jenvman.2010.12.010

fuzzy. They are 20 cm long, 1–2 kg in weight, and covered with a thick (4–7 mm) hard exocarp (Gondim et al., 2001). The pulp is greatly appreciated for its pleasant acidic taste, being consumed fresh or processed, mainly as juice, ice cream, candy and jellies. In addition, the seeds can be used to make chocolate. The annual production of cupuassu in the Brazilian Amazon is about 5200 tonnes (Gondim et al., 2001). About 42% of weight of cupuassu is its shell, which is a waste material that presents no aggregate economic value (Gondim et al., 2001). The disposal of large amounts of cupuassu shell (CS) directly in the soil and/or in natural waters may contaminate the environment in an uncontrolled way because the decomposition of this waste material leads to the generation of various chemical compounds and microorganisms. In this context, combining the need to reduce costs with commercial adsorbents and by using CS as biosorbent for the removal of dyes from industrial effluents, it is a good economical and environmental advantage to in developing countries such as Brazil.

The present work aimed to use CS in natural form as biosorbent for the successful removal of C.I. Direct Blue 53 (DB-53) and C.I. Reactive Red 194 (RR-194) dyes from aqueous solutions. These dyes are largely used for textile dying in the Brazilian cloth industries.

## 2. Materials and methods

### 2.1. Solutions and reagents

De-ionized water was used throughout the experiments for solution preparations.

The textile dyes, C.I. Reactive Red 194 (RR-194; C.I. 18214; CAS 23354-52-1; $C_{27}H_{18}N_7O_{16}S_5ClNa_4$; 984.21 g mol$^{-1}$) was furnished by Bosche Scientific (New Brunswick, USA) at 80% of purity and C.I. Direct Blue 53 (DB-53; C.I. 23860; CAS 314-13-6; $C_{34}H_{24}N_6O_{14}S_4Na_4$; 960.81 g mol$^{-1}$) was furnished by Vetec (Rio de Janeiro, Brazil) at 85% of purity (see Supplementary Fig. 1). The dyes were used without further purification. It should be pointed out that no color changes of the dyes were observed when these were immersed in aqueous solution ranging from pH 2.0 to 9.0. The RR-194 dye has three sulfonate groups and one sulfato-ethyl-sulfone group, and the DB-53 has four sulfonate groups. These groups present negative charges even in highly acidic solutions due to their pKa values lower than zero (Lima et al., 2008). The stock solution was prepared by dissolving the dyes in distilled water to the concentration of 5.00 g L$^{-1}$. Working solutions were obtained by diluting the dye stock solutions to the required concentrations. To adjust the pH solutions, 0.10 mol L$^{-1}$ sodium hydroxide or hydrochloric acid solutions were used. The pH of the solutions was measured using a Schott Lab 850 set pHmeter.

### 2.2. Adsorbent preparation and characterization

CS was furnished by jelly industry in Belém-PA, Brazil, as a residual material. CS was washed with tap water to remove dust and with de-ionized water. Then, it was dried at 343 K in an air-supplied oven for 8 h. After that, CS was grounded in a disk-mill and subsequently sieved. The part of biosorbent which presented diameter of particles $\leq$ 250 μm was used.

The CS biosorbent was characterized by FTIR using a Shimadzu FTIR, model 8300 (Kyoto, Japan). The spectra were obtained with a resolution of 4 cm$^{-1}$, with 100 cumulative scans.

The surface analyses and porosity were carried out with a volumetric adsorption analyzer, ASAP 2020, from Micromeritrics, at 77 K (boiling point of nitrogen). The samples were pre-treated at 373 K for 24 h under a nitrogen atmosphere in order to eliminate the moisture adsorbed on the solid sample surface. After, the samples were submitted to 298 K in vacuum, reaching the residual pressure of $10^{-4}$ Pa. For area and pore calculations, the DBET and BJH (Arenas et al., 2007; Jacques et al., 2007) methods were used.

The biosorbent sample was also analyzed by scanning electron microscopy (SEM) in Jeol microscope, model JSM 6060, using an acceleration voltage of 20 kV and magnification ranging from 100 to 5000 fold (Vaghetti et al., 2008).

The point of zero charge ($pH_{pzc}$) of the adsorbent was determined by adding 20.00 mL of 0.050 mol L$^{-1}$ NaCl to several Erlenmeyer flasks. A range of initial pH ($pH_i$) values of the NaCl solutions were adjusted from 2.0 to 10.0 by adding 0.1 mol L$^{-1}$ of HCl and NaOH. The total volume of the solution in each flask was brought to exactly 30.0 mL by further addition of 0.050 mol L$^{-1}$ NaCl solution. The $pH_i$ values of the solutions were then accurately noted and 50.0 mg of CS was added to each flask, which was securely capped immediately. The suspensions were shaken in a shaker at 298 K and allowed to equilibrate for 48 h. The suspensions were then centrifuged at 3600 rpm for 10 min and the final pH ($pH_f$) values of the supernatant liquid were recorded. The value of $pH_{pzc}$ is the point where the curve of $\Delta pH$ ($pH_f - pH_i$) versus $pH_i$ crosses the line equal to zero (Calvete et al., 2009).

### 2.3. Biosorption studies

The biosorption studies for evaluation of the CS biosorbent for the removal of the RR-194 and DB-53 dyes from aqueous solutions were carried out in triplicate using the batch contact biosorption method. For these experiments, fixed amounts of biosorbent (20.0–200.0 mg) were placed in 50.0 mL cylindrical high-density polystyrene flasks (height 117 mm and diameter 30 mm) containing 20.0 mL of dye solutions (10.00–250.0 mg L$^{-1}$), which were agitated for a suitable time (0.25–48 h) at 298 K. Blanks without adsorbents were carried out in order to verify the possibility of the dye being adsorbed at the flask. It was not observed any adsorption of the dye at the high-density polystyrene flask after 48 h of contact. The pH of the dye solutions ranged from 2.0 to 9.0. Subsequently, in order to separate the biosorbents from the aqueous solutions, the flasks were centrifuged at 3600 rpm for 10 min, and aliquots of 1–10 mL of supernatant were properly diluted with water.

The final concentrations of the dyes remained in the solution were determined by visible spectrophotometry by visible spectrophotometry using a T90+ UV–VIS spectrophotometer furnished by PG Instruments (London-England) provided with optical quartz cells. Absorbance measurements were made at the maximum wavelength of RR-194 and DB-53 which were 505 and 607 nm.

The amount of dyes uptaken and the percentage of removal of the dyes by the biosorbent were calculated by applying the Eqs. (1) and (2), respectively:

$$q = \frac{\left(C_o - C_f\right)}{X} \quad (1)$$

$$\%\text{Removal} = 100 \cdot \frac{\left(C_o - C_f\right)}{C_o} \quad (2)$$

where $q$ is the amount of dyes taken up by the biosorbent (mg g$^{-1}$); $C_o$ is the initial dye concentration put in contact with the adsorbent (mg L$^{-1}$), $C_f$ is the dye concentration (mg L$^{-1}$) after the batch adsorption procedure, and X is biosorbent dosage (g L$^{-1}$).

### 2.4. Kinetic and equilibrium models

Avrami fractionary-order (Lopes et al., 2003), pseudo-first-order (Largegren, 1898), pseudo-second-order (Blanachard et al., 1984), Elovich-chemisorption (Vaghetti et al., 2009) and intra-particle

**Table 1**
Kinetic adsorption models.

| Kinetic model | Nonlinear equation |
|---|---|
| Fractionary-order | $q_t = q_e \cdot \{1 - \exp[-(k_{AV} \cdot t)]^{n_{AV}}\}$ |
| Pseudo-first order | $q_t = q_e \cdot [1 - \exp(-k_f \cdot t)]$ |
| Pseudo-second-order | $q_t = \frac{k_s \cdot q_e^2 \cdot t}{1 + q_e \cdot k_s \cdot t}$ <br> $h_o = k_s \cdot q_e^2$ <br> initial sorption rate |
| Chemisorption | $q_t = \frac{1}{\beta}(\alpha \cdot \beta) + \frac{1}{\beta}(t)$ |
| Intra-particle diffusion | $q_t = k_{id} \cdot \sqrt{t} + C$ |

diffusion model (Weber and Morris, 1963.) kinetic equations are given in Table 1.

Langmuir (Langmuir, 1918), Freundlich (Freundlich, 1906), Sips (Sips, 1948) and Radke–Prausnitz (Radke and Prausnitz, 1972.) isotherm equations are given in Table 2.

### 2.5. Quality assurance and statistical evaluation of the kinetic and isotherm parameters

To establish the accuracy, reliability and reproducibility of the collected data, all the batch adsorption measurements were performed in triplicate. Blanks were run in parallel and they were corrected when necessary (Vaghetti et al., 2008).

All dye solutions were stored in glass flasks, which were cleaned by soaking in 1.4 mol $L^{-1}$ $HNO_3$ for 24 h (Lima et al., 2002), rinsing five times with de-ionized water, dried, and stored in a flow hood.

For analytical calibration, standard solutions with concentrations ranging from 5.00 to 50.0 mg $L^{-1}$ of RR-194 and DB-53 dyes were employed, running against a blank solution of water adjusted in a suitable pH. The linear analytical calibrations of the curves were furnished by the software UVWin of the T90 + PG Instruments spectrophotometer. The detection limits of the method, obtained with signal/noise ratio of 3 (Lima et al., 1998), were 0.12 and 0.16 mg $L^{-1}$, for RR-194 and DB-53, respectively. All the analytical measurements were performed in triplicate, and the precision of the standards was better than 3% ($n = 3$). For checking the accuracy of the RR-194 and DB-53 dye sample solutions during the spectrophotometric measurements, standards containing dyes at 20.00 mg $L^{-1}$ were employed as quality control at each five determinations (Lima et al., 2003).

The kinetic and equilibrium models were fitted by employing a nonlinear method, with successive interactions calculated by the method of Levenberg–Marquardt and also interactions calculated by the Simplex method, using the nonlinear fitting facilities of the software Microcal Origin 7.0. In addition, the models were also evaluated by adjusted determination factor ($R^2_{adj}$), as well as by an error function ($F_{error}$) (Lima et al., 2007), which measures the differences in the amount of dye taken up by the adsorbent predicted by the models and the actual $q$ measured experimentally. $R^2_{adj}$ and $F_{error}$ are given below, respectively:

**Table 2**
Isotherm models.

| Isotherm model | Equation |
|---|---|
| Langmuir | $q_e = \frac{Q_{max} \cdot K_L \cdot C_e}{1 + K_L \cdot C_e}$ |
| Freundlich | $q_e = K_F \cdot C_e^{1/n_F}$ |
| Sips | $q_e = \frac{Q_{max} \cdot (K_S \cdot C_e)^{1/n_S}}{1 + (K_S \cdot C_e)^{1/n_S}}$ |
| Radke–Prausnitz | $q_e = \frac{Q_{max} \cdot K_{RP} \cdot C_e}{(1 + K_{RP} \cdot C_e)^{1/n_{RP}}}$ |

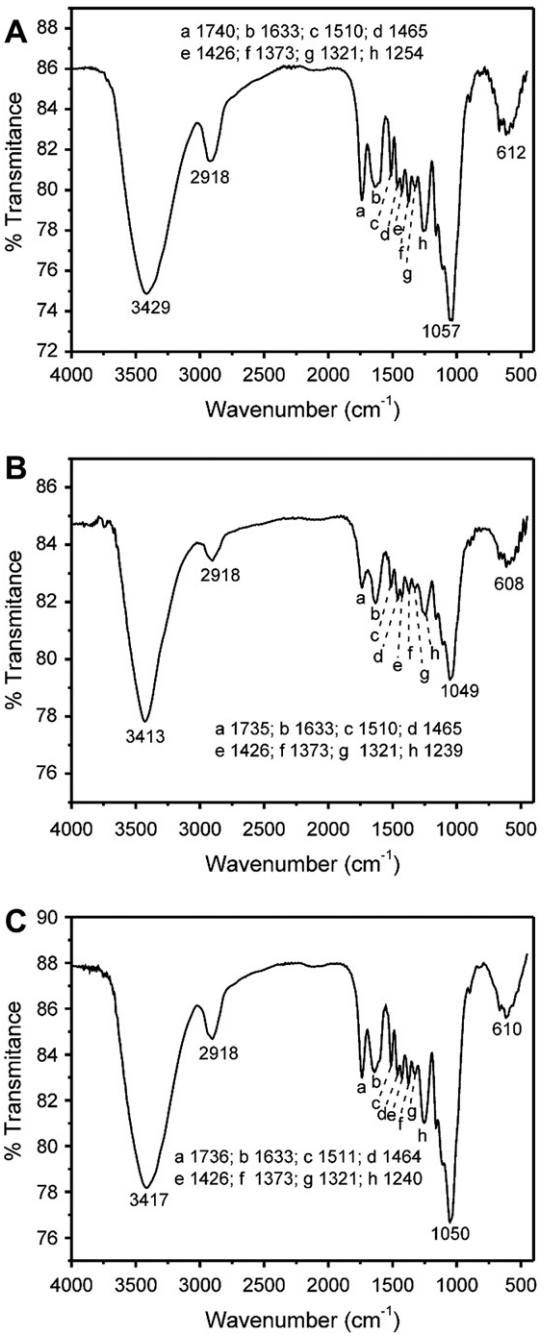


**Fig. 1.** FTIR vibrational spectra. A) CS before the adsorption; B) CS + RR-194 after the adsorption; C) CS + DB-53 after the adsorption. The number indicated for the bands correspond to wavenumbers that are expressed in $cm^{-1}$.

$$R^2_{adj} = 1 - \left( \frac{\sum_i^n \left(q_{i,exp} - q_{model}\right)^2}{\sum_i^n \left(q_{i,exp} - \overline{q}_{exp}\right)^2} \right) \cdot \left( \frac{n-1}{n-p} \right) \quad (3)$$

$$F_{error} = \sqrt{\left( \frac{1}{n-p} \right) \cdot \sum_i^n \left(q_{i,exp} - q_{imodel}\right)^2} \quad (4)$$

where $q_{i,model}$ is the value of $q$ predicted by the fitted model, $q_{i,exp.}$ is the value of $q$ measured experimentally, $\overline{q}_{exp}$ is the average of $q$

experimentally measured, $n$ is the number of experiments performed, and $p$ is the number of parameter of the fitted model.

## 3. Results and discussion

### 3.1. Characterization of biosorbents

FTIR technique was used to examine the surface groups of CS biosorbent and to identify the groups responsible for the dyes adsorption. Infrared spectra of the adsorbent and dye-loaded adsorbent samples, before and after the adsorption process, were recorded in the range 4000–400 $cm^{-1}$. Fig. 1A–C shows the FTIR vibrational spectra of the CS before the adsorption (CS; Fig. 1A) and loaded with the RR-194 dye (CS + RR-194; Fig. 1B) and with DB-53 (CS + DB-53, Fig. 1C). The intense absorption bands at 3429, 3413, and 3417 $cm^{-1}$ are assigned to O–H bond stretching for CS, CS + RR-194 and CS + DB-53, respectively (Smith, 1999; Vaghetti et al., 2009; Lima et al., 2008). The $CH_2$ stretching band at 2918 $cm^{-1}$ is assigned to asymmetric stretching of $CH_2$ groups (Smith, 1999; Vaghetti et al., 2008; Lima et al., 2008) which present the same wavenumber before and after the adsorption with two different dyes, indicating that this group did not participate in the biosorption process. Bands at 1740, 1735 and 1736 $cm^{-1}$, for CS, CS + RR-194 and CS + DB-53, respectively are assigned to carbonyl groups of carboxylic acid (Smith, 1999; Vaghetti et al., 2009). Several bands in the range of 1633-1321 are assigned to ring modes of the aromatic rings (Smith, 1999). The wavenumbers of these bands were practically the same before and after the biosorption using RR-194 and DB-53 dyes, indicating that aromatic groups do not participate on the biosorption mechanism. A sharp band at 1254, 1239 and 1240 $cm^{-1}$ as well as the intense bands at 1057, 1049 and 1050 $cm^{-1}$ are assigned to C–O stretch of phenolic compounds found in lignin (Smith, 1999; Vaghetti et al., 2009) and C–O stretching vibration of alcohols (Smith, 1999), for CS, CS + RR-194 and CS + DB-53, respectively. The FTIR results indicate that the interaction of RR-194 and DB-53 dyes with the CS biosorbent should occur with the O–H bonds of phenols and alcohols present in the lignin structure as well as the interactions with the carboxylate group because these groups suffered a shift to lower wavenumbers after the biosorption procedure. Similar results were previously observed for adsorption of dyes on fly ash (Kara et al., 2007) and activated carbon adsorbent (Calvete et al., 2010).

The textural properties of CS obtained by nitrogen adsorption/desorption curves were: superficial area ($S_{BET}$) 1.2 $m^2\ g^{-1}$; average pore diameter (BJH) 20.02 nm; and average pore volume 0.0073 $cm^3\ g^{-1}$. The superficial area of agricultural residues is usually a low value (Kumari et al., 2006; Yurtsever and Sengil, 2009). On the other hand, the average pore diameter of CS biomaterial is relatively large, even when compared with activated carbons (Calvete et al., 2009; 2010) or silicates (Royer et al., 2010a, 2010b). The maximum diagonal lengths of the RR-194 and DB-53 (see supplementary Fig. 2. The dimensions of the chemical moleculae were calculated using ChemBio 3D® Ultra version 11.0.) are 2.05 and 1.47 nm, respectively. The ratios of average pore diameter of the biosorbent to the maximum diagonal length of each dye are 9.77 and 13.62, for RR-194 and DB-53, respectively. Therefore, the mesopores of CS could accommodate up to 9 and 13 molecules of RR-194 and DB-53, respectively. This number of molecules, which could be accommodated in each pore of the biosorbent, is considered large when compared with other adsorbents reported in the literature (Calvete et al., 2009, 2010; Lima et al., 2008; Royer et al., 2009b).

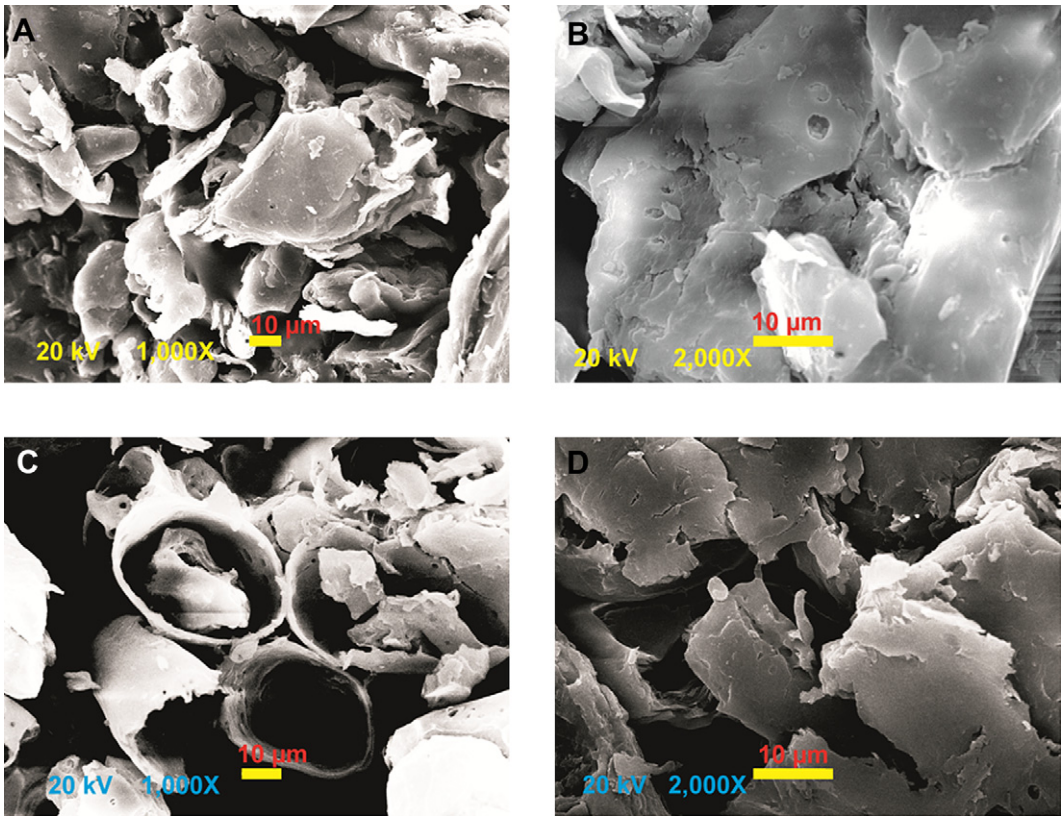


**Fig. 2.** SEM of CS. A) without contact with dye solution, magnification 1,000×; B) without contact with dye solution, magnification 2,000×; C) after contact with RR-194 dye solution (pH 2.0) for 12 h, magnification 1000×; D) after contact with RR-194 dye solution (pH 2.0) for 12 h, magnification 2000×.

Scanning electron microscopies (SEM) of the biosorbent in natural form without contact with dye solution (Fig. 2A and B) and after contact with RR-194 dye solution at pH 2.0 (Fig. 2C and D) are shown in Fig. 2. As can be seen, CS biosorbent without contact with dye solution is a more compact fibrous material presenting some macroporous (porous with diameter $>$ 50 nm; see Fig. 2A and B). On the other hand, after the CS biosorbent being submitted to an RR-194 dye solution at pH 2.0, the cavities of the fibrous materials were expanded, which should allow the diffusion of dye molecules through the macroporous of the CS biosorbent. Similar results were also obtained with DB-53 after the contact with CS biosorbent (data not shown). It is important to focus that using SEM technique it is not possible to verify the presence of dye on the biosorbent surface, since the scale of the micrograph is micrometers and the dimension of the dyes are in nanometer scale. The changes provoked at cupuassu shell (cavities) should be attributed to the acidic solution at pH 2.0.

Taking into account that CS biosorbent presents a low superficial area ($S_{BET}$) and some macroporous (see Fig. 2), it could be inferred that CS predominates a mixture of mesoporous (porous with diameter ranging from 2 to 50 nm, see textural results described above) and macroporous (porous with diameter $>$ 50 nm). On the other hand, the number of microporous (porous with a diameter $<$ 2 nm) should be a minimum (Gay et al., 2010; Jacques et al., 2007). Usually, the microporous structure is responsible for higher superficial area ($S_{BET}$) of the materials (Gay et al., 2010; Kumari et al., 2006; Yurtsever and Sengil, 2009), since the nitrogen probe molecule utilized in the measurements is retained basically at the microporous structure (Arenas et al., 2007; Jacques et al., 2007). This explains the low superficial area ($S_{BET}$) of CS biosorbent.

### 3.2. Effects of acidity on adsorption

One of the most important factors in adsorption studies is the effect of the acidity of the medium (Lima et al., 2007, 2008; Royer et al., 2009a, 2009b). Different species may present divergent ranges of suitable pH depending on which adsorbent is used. Effects of initial pH on percentage of removal of RR-194 and DB-53 dyes using CS biosorbent were evaluated within the pH range between 2 and 9 (Fig. 3A and B, respectively). For both dyes, the percentage of dye removal was remarkably decreased from pH 2.0, attaining practically less than 1% of dye removal at pH 6.5. Similar behavior for dye removal utilizing lignocellulosic adsorbents was also observed (Akar et al., 2008; Deniz and Saygideger, 2010).

The $pH_{PZC}$ value determined for CS is 5.92. For pH values lower than $pH_{pzc}$, the adsorbent presents a positive surface charge (Calvete et al., 2009; Lima et al., 2008). The dissolved RR-194 and DB-53 dyes are negatively charged in water solutions. The adsorption of these dyes takes place when the biosorbent presents a positive surface charge. For CS, the electrostatic interaction occurs for pH $<$ 5.92. However, the lower the pH value from the $pH_{pzc}$, the more positive the surface of the biosorbent (Calvete et al., 2009).

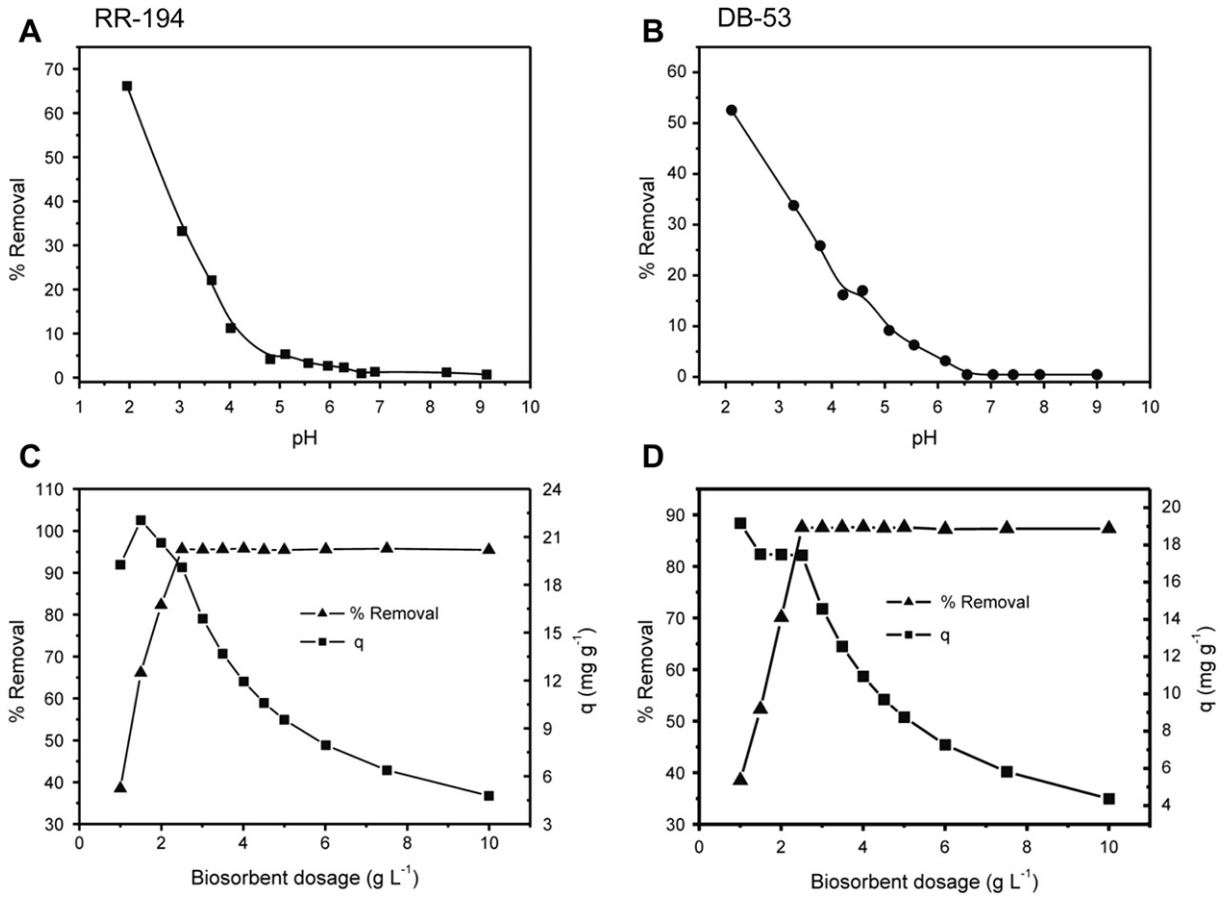


**Fig. 3.** Optimization of biosorption conditions. Effect of pH on the biosorption of RR-194 (A) and DB-53 (B). Effect of the biosorbent dosage on the percentage of removal and in the amount adsorbed of RR-194 (C) and DB-53 (D). Conditions: A) and B) $C_o$ = 50.0 mg $L^{-1}$ and mass of biosorbent of 30.0 mg for both dyes. C) and D) $C_o$ = 50.0 mg $L^{-1}$, pH 2.0 for both dyes. The temperature was fixed at 298 K.

This behavior explains the high sorption capacity of CS for both RR-194 and DB-53 at pH 2. In order to continue the biosorption studies, the initial pH was fixed at 2.0.

### 3.3. Adsorbent dosage

The study of biosorbent dosages for the removal of RR-194 and DB-53 dyes from aqueous solution was carried out using biosorbent dosages ranging from 1.0 to 10.0 g $L^{-1}$ and fixing the initial dye concentration at 50.0 mg $L^{-1}$. For both dyes, the highest amount of dye removal was attained for biosorbent doses of at least 2.5 g $L^{-1}$ (Fig. 3C and D, for RR-194 and DB-53, respectively). For biosorbent dosages higher than this value, the removal of the dyes remained almost constant. Increases in the percentage of the dye removal with biosorbent dosages could be attributed to increases in the biosorbent surface areas, augmenting the number of adsorption sites available for adsorption, as already reported in several papers (Lima et al., 2008; Royer et al., 2009b, 2010b; Vaghetti et al., 2008, 2009). On the other hand, the increase in the biosorbent doses promotes a remarkable decrease in the amount of dye uptake per gram of adsorbent ($q$), (Fig. 3C and D), an effect that can be mathematically explained by combining the Eqs. (1) and (2):

$$q = \frac{\%\text{Removal} \cdot C_o}{100 \cdot X} \quad (5)$$

As observed in the Eq. (5), the amount of dye uptaken ($q$) and the biosorbent dosage (X) is inversely proportional. For a fixed dye percentage removal (after doses of 2.5 g $L^{-1}$), the increase of biosorbent doses leads to a decrease in $q$ values, since the initial dye concentration ($C_o$) is always fixed. These results clearly indicate that the biosorbent dosages must be fixed at 2.5 g $L^{-1}$, which is the biosorbent dosage that corresponds to the minimum amount of adsorbent that leads to constant dye removal. Biosorbent dosages were therefore fixed at 2.5 g $L^{-1}$ for both dyes.

### 3.4. Kinetic studies

Adsorption kinetic studies are important in the treatment of aqueous effluents because they provide valuable information on the mechanism of the adsorption process (Calvete et al., 2009, 2010; Vaghetti et al., 2009).

In attempting to describe the biosorption kinetics of RR-194 and DB-53 dyes by CS biosorbent, four diffusion kinetic models were tested, as shown in Fig. 4A and B (RR-194); 4C, 4F (DB-53). The kinetic parameters for the kinetic models are listed in Table 3. Based on the $F_{error}$ values, it was observed that the Avrami model provides the best fit to the data for using RR-194 and DB-53 dye, because its $F_{error}$ values were at least 3.18 and 3.11 times lower, for RR-194 and DB-53, respectively than the values obtained for pseudo-first-order, pseudo-second-order and Elovich-chemisorption kinetic models. The lower the error function, the lower the difference of the $q$ calculated by the model from the experimentally measured $q$ (Lima et al., 2007, 2008; Calvete et al., 2009, 2010). It should be pointed out that the $F_{error}$ utilized in this work takes into account the number of the fitted parameter (p term of Eq. (4)), since it is reported in the literature (Gunay, 2007) that depending on the number of parameters one nonlinear equation presents, it has the best fitting of the results (Gunay, 2007). For this reason, the number of fitted parameter should be considered in the calculation of $F_{error}$. Also, it was verified that the $q_e$ values found in the fractionary-order were closer to the experimental $q_e$ values, when compared with all other kinetic models. These results indicate that the fractionary-order kinetic model should explain the adsorption process of RR-194 and DB-53 using CS biosorbent.

The Avrami kinetic equation has been successfully employed to explain several kinetic processes of different adsorbents and adsorbates (Calvete et al., 2009, 2010; Cestari et al., 2005; Lopes et al., 2003; Lima et al., 2008; Royer et al., 2009a, 2009b, 2010a, 2010b; Vaghetti et al., 2009). The Avrami exponent ($n_{AV}$) is a fractionary number related with the possible changes of the adsorption mechanism that takes place during the adsorption process (Calvete et al., 2009, 2010; Lima et al., 2008). Instead of following only an integer-kinetic order, the mechanism adsorption could follow multiple kinetic orders that are changed during the contact of the adsorbate with the adsorbent (Calvete et al., 2009, 2010; Lima et al., 2008). The $n_{AV}$ exponent is a resultant of the multiple kinetic order of the adsorption procedure.

Since kinetic results fit very well to the fractionary kinetic model (Avrami model) for the RR-194 and DB-53 dyes using CS as biosorbent (Table 3 and Fig. 4), the intra-particle diffusion model (Vaghetti et al., 2009) was used to verify the influence of mass transfer resistance on the binding of RR-194 and DB-53 dyes to the biosorbent (Table 3 and Fig. 4C,D,G and H). The intra-particle diffusion constant, $k_{id}$ (mg $g^{-1}$ $h^{-0.5}$), can be obtained from the slope of the plot of $q_t$ (uptaken at any time, mg $g^{-1}$) versus the square root of time. Fig. 4C and D (RR-194); 4G, 4H (DB-53) shows the plots of $q_t$ versus $t^{1/2}$, with multi-linearity for the RR-194 and DB-53 dyes using CS biosorbent. These results imply that the adsorption processes involve more than one single kinetic stage (or adsorption rate) (Vaghetti et al., 2009). For the DB-53 dye, the adsorption process exhibits three stages, which can be attributed to each linear portion of the Fig. 4G and H. The first linear portion was attributed to the diffusional process of the dye to the CS biosorbent surface (Vaghetti et al., 2009); hence, it was the fastest sorption stage. The second portion, ascribed to intra-particle diffusion, was a delayed process. The third stage may be regarded as the diffusion through smaller pores, which is followed by the establishment of equilibrium. For RR-194 dye, the adsorption process exhibits only two stages, being the first linear part attributed to intra-particle diffusion, and the second stage the diffusion through smaller pores, which is followed by the establishment of equilibrium (Vaghetti et al., 2009).

It was observed in Fig. 4 that the minimum contact time of RR-194 and DB-53 with the CS biosorbent to reach equilibrium was about 8 and 18 h, respectively. This great difference in the minimum contact time to reach the equilibrium is associated with the difference in the mechanism of adsorption. The Avrami constant rate ($k_{AV}$) for RR-194 was 29.4% higher than the $k_{AV}$ for DB-53 dye, which implies that the diffusion from the film could not explain completely the remarkable differences on the kinetics of adsorption of RR-194 in relation to DB-53. On the other hand, the intra-particle diffusion constant ($k_{id}$) for RR-194 was more than 9-fold higher than the $k_{id}$ for DB-53, indicating that the resistance to the mass transfer is much lower for RR-194 dye. This could explain the difference of 10 h to reach the equilibrium for RR-194 in relation to DB-53. Probably DB-53 molecules should be more aggregated, forming dimers in aqueous solution, which would increase the resistance to the mass transfer inside the porous of CS biosorbent (Murakami, 2002).

In order to continue this work, the contact time between the biosorbent and biosorbates was fixed at 10.0 and 20.0 h using RR-194 and DB-53 dyes as biosorbates, respectively and CS as biosorbent to guarantee that for both dyes the equilibrium would be attained even in higher biosorbate concentrations.

### 3.5. Equilibrium studies and mechanism of adsorption

An adsorption isotherm describes the relationship between the amount of adsorbate taken up by the adsorbent ($q_e$) and the

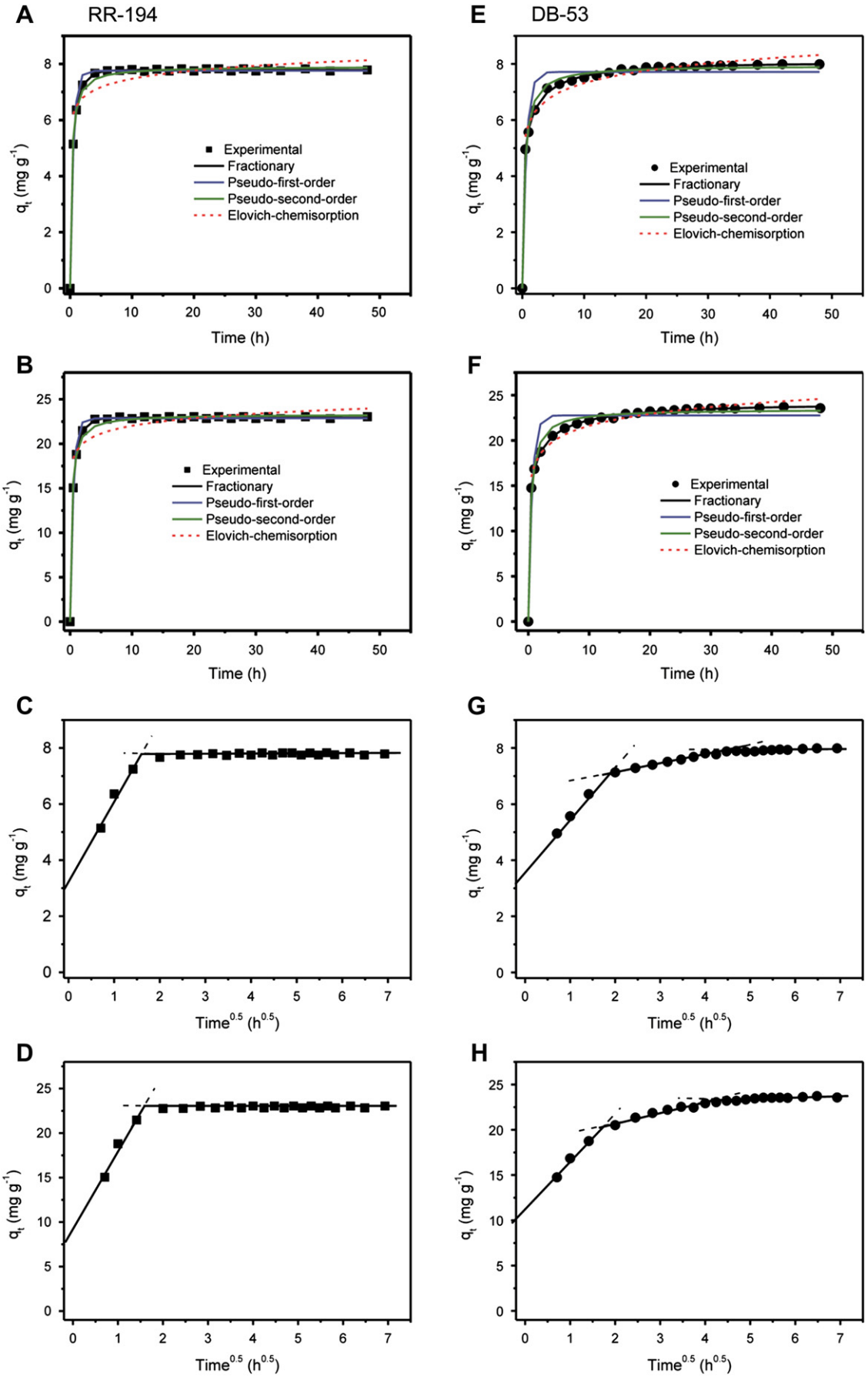


**Fig. 4.** Kinetic biosorption curves. A) RR-194, $C_o$ 20.0 mg $L^{-1}$; B) RR-194, $C_o$ 60.0 mg $L^{-1}$; C) RR-194, $C_o$ 20.0 mg $L^{-1}$; D) RR-194, $C_o$ 60.0 mg $L^{-1}$; E) DB-53, $C_o$ 20.0 mg $L^{-1}$; F) DB-53, $C_o$ 60.0 mg $L^{-1}$; G) DB-53, $C_o$ 20.0 mg $L^{-1}$; H) DB-53, $C_o$ 60.0 mg $L^{-1}$. Conditions: pH was fixed at 2.0; the biosorbent dosage was fixed at 2.5 g $L^{-1}$; and the temperature was fixed at 298 K.

**Table 3**
Kinetic parameters for RR-194 and DB-53 removal using CS as biosorbent. Conditions: temperature was fixed at 298 K; pH 2.0 biosorbent dosage of 2.5 g $L^{-1}$.

| | RR-194 | | DB-53 | |
|---|---|---|---|---|
| | 20.0 mg $L^{-1}$ | 60.0 mg $L^{-1}$ | 20.0 mg $L^{-1}$ | 60.0 mg $L^{-1}$ |
| Fractionary-order | | | | |
| $k_{AV}$ ($h^{-1}$) | 2.25 | 2.20 | 1.71 | 1.73 |
| $q_e$ (mg $g^{-1}$) | 7.79 | 22.9 | 8.04 | 24.1 |
| $n_{AV}$ | 0.652 | 0.685 | 0.367 | 0.334 |
| $R^2_{adj}$ | 0.9996 | 0.9995 | 0.9991 | 0.9997 |
| $F_{error}$ | 0.0312 | 0.0977 | 0.0513 | 0.0866 |
| Pseudo-first order | | | | |
| $k_f$ ($h^{-1}$) | 1.96 | 1.95 | 1.52 | 1.58 |
| $q_e$ (mg $g^{-1}$) | 7.76 | 22.9 | 7.71 | 22.8 |
| $R^2_{adj}$ | 0.9940 | 0.9951 | 0.9502 | 0.9438 |
| $F_{error}$ | 0.129 | 0.343 | 0.384 | 1.202 |
| Pseudo-second order | | | | |
| $k_s$ (g $mg^{-1}$ $h^{-1}$) | 0.518 | 0.176 | 0.331 | 0.115 |
| $q_e$ (mg $g^{-1}$) | 7.91 | 23.3 | 7.95 | 23.5 |
| $h_o$ (mg $g^{-1}$ $h^{-1}$) | 32.4 | 95.4 | 20.9 | 63.1 |
| $R^2_{adj}$ | 0.9965 | 0.9954 | 0.9914 | 0.9886 |
| $F_{error}$ | 0.0992 | 0.332 | 0.160 | 0.541 |
| Chemisorption | | | | |
| $\alpha$ (mg $g^{-1}$ $h^{-1}$) | $2.16 \times 10^6$ | $7.03 \times 10^6$ | $6.06 \times 10^3$ | $1.78 \times 10^4$ |
| $\beta$ (g $mg^{-1}$) | 2.38 | 0.811 | 1.57 | 0.530 |
| $R^2_{adj}$ | 0.9538 | 0.9509 | 0.9840 | 0.9889 |
| $F_{error}$ | 0.358 | 1.09 | 0.217 | 0.535 |
| Intra-particle diffusion | | | | |
| $k_{id}$ (mg $g^{-1}$ $h^{-0.5}$) | 2.92[a] | 8.90[a] | 0.271[b] | 0.962[b] |

[a] First stage.
[b] Second stage.

adsorbate concentration remaining in the solution after the system attained the equilibrium ($C_e$). There are several equations to analyze experimental adsorption equilibrium data. The equation parameters of these equilibrium models often provide some insight into the adsorption mechanism, the surface properties and affinity of the adsorbent. In this work, the Langmuir, the Freundlich, the Sips and the Radke–Prausnitz isotherm models were tested.

The isotherms of adsorption of RR-194 and DB-53 were carried out at 298 K on the CS biosorbent, using the best experimental conditions described previously (Table 4 and Fig. 5). Based on the $F_{error}$, the Sips model is the best isotherm model for both dyes. The Sips model showed in Table 4 presents the lowest $F_{error}$ values, which means that the $q$ fit by this isotherm model was close to the $q$ measured experimentally when compared with other isotherm models. For RR-194 the Langmuir and the Freundlich isotherm models were not suitably fitted, presenting $F_{error}$ values ranging from 3.37 to 26.0-fold higher than the $F_{error}$ values obtained by the Sips isotherm model. For DB-53, the Langmuir, the Freundlich and the Radke-Praunsnitz presented $F_{error}$ values ranging from 12.1 to 41.1-fold higher than the $F_{error}$ values obtained by the Sips isotherm model. Therefore, all these models mentioned above for RR-194 and DB-53 dyes, using CS as biosorbent, have no physical value. Only for RR-194, the Radke–Prausnitz presented a $F_{error}$ value 1.58-fold higher than the $F_{error}$ value obtained by the Sips isotherm model. Taking into account that the Sips isotherm model presented the lowest $F_{error}$ value for both dyes, this isotherm model was chosen as the best for describing the equilibrium of adsorption of RR-194 and DB-53

**Table 4**
Isotherm parameters for RR-194 and DB-53 biosorption, using CS as biosorbent. Conditions: temperature was fixed at 298 K; contact time was fixed at 10 and 20 h for RR-194 and DB-53, respectively; pH was fixed at 2.0; biosorbent dosage was fixed at 2.5 g $L^{-1}$.

| | RR-194 | DB-53 |
|---|---|---|
| Langmuir | | |
| $Q_{max}$ (mg $g^{-1}$) | 66.0 | 38.8 |
| $K_L$ (L $mg^{-1}$) | 0.203 | 1.66 |
| $R^2_{adj}$ | 0.9978 | 0.9475 |
| $F_{error}$ | 0.735 | 1.99 |
| Freudlich | | |
| $K_F$ ($mg \cdot g^{-1} \cdot (mg \cdot L^{-1})^{-1/n_F}$) | 23.1 | 24.8 |
| $n_F$ | 4.15 | 8.54 |
| $R^2_{adj}$ | 0.8669 | 06480 |
| $F_{error}$ | 5.67 | 5.15 |
| Sips | | |
| $Q_{max}$ (mg $g^{-1}$) | 64.1 | 37.5 |
| $K_S$ (L $mg^{-1}$) | 0.214 | 1.56 |
| $n_S$ | 0.890 | 0.549 |
| $R^2_{adj}$ | 0.9998 | 0.9998 |
| $F_{error}$ | 0.218 | 0.125 |
| Radke–Prausnitz | | |
| $Q_{max}$ (mg $g^{-1}$) | 75.4 | 48.5 |
| $K_{RP}$ (L $g^{-1}$) | 0.165 | 1.10 |
| $n_{RP}$ | 0.952 | 0.943 |
| $R^2_{adj}$ | 0.9995 | 0.9696 |
| $F_{error}$ | 0.345 | 1.51 |

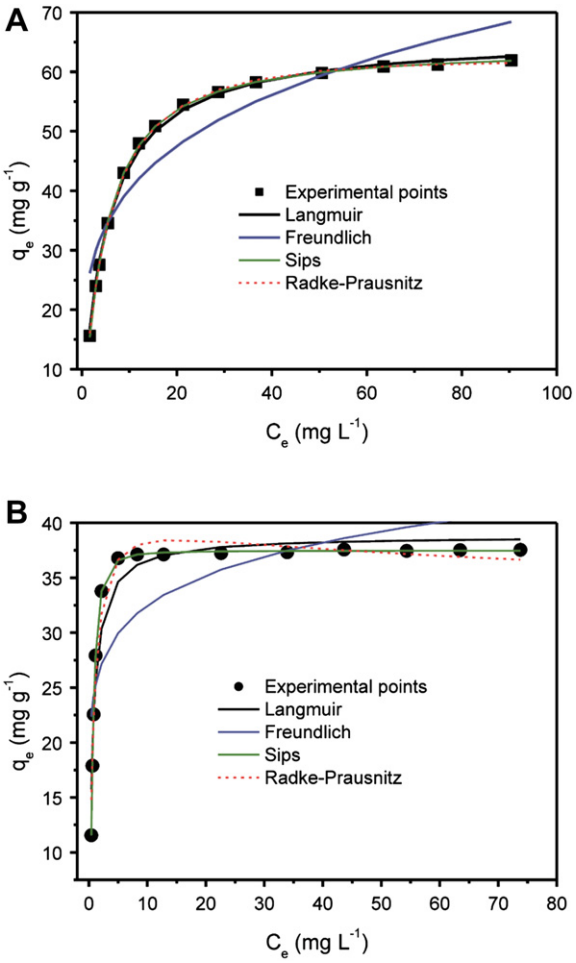


**Fig. 5.** Isotherm curves. A) RR-194; B) DB-53. Conditions: pH was fixed at 2.0; the biosorbent dosage was fixed at 2.5 g $L^{-1}$; and the temperature was fixed at 298 K. The contact time were fixed at 10 and 20 h for RR-194 and DB-53, respectively.

using CS as biosorbent. Therefore, based on the Sips isotherm model, the maximum amounts of RR-194 and DB-53 uptaken were 64.1 and 37.5 mg $g^{-1}$ for both dyes, respectively. These values indicate that CS is a fair good biosorbent for the removal of these dyes from aqueous solutions.

It should be highlighted that the maximum amount adsorbed of RR-194 by CS biosorbent was 70.9% higher than the value obtained for the adsorption of DB-53. Considering that the kinetics of adsorption of RR-194 was faster than the kinetics of adsorption of DB-53 as well as considering the pH studies showed above, it is possible to propose a mechanism of adsorption for RR-194 and DB-53, which is depicted in Fig. 6. In the first step, the CS is immersed in a solution with pH 2.0, being the functional groups (OH, carboxylates, please see Fig. 1) of the biosorbent protonated (see Fig. 3A and B). This step is fast for both dyes. The second step is the separation of the agglomerates of dyes in the aqueous solution. Dyes are in an organized state in the aqueous solution, besides being hydrated (Murakami, 2002). These self-associations of dyes in aqueous solutions should be dissociated before these dyes being adsorbed. Furthermore, the dyes should be dehydrated before being adsorbed. For RR-194 dye, this step is relatively fast. On the other hand, this stage is relatively slower for DB-53 (Murakami, 2002). This explains the differences of the minimum contact time for RR-194 and DB-53 to attain the equilibrium (see section 3.4). The third stage is the electrostatic attraction of the negatively charged dyes by the positively surface charged CS biosorbent at pH 2 (see Fig. 1). This stage should be the rate controlling step for RR-194. For DB-53, this is also the rate controlling step, however, the stage 2 presents some significance to overall mechanism of adsorption.

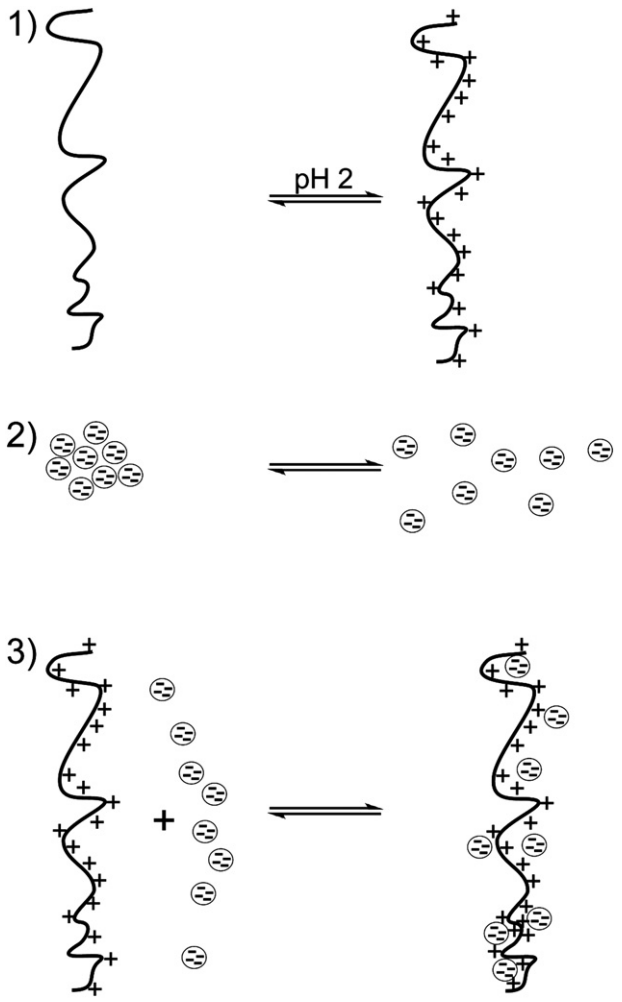


**Fig. 6.** Mechanism of biosorption of RR-194 and DB-53 dyes by the CS biosorbent. The circle stands for the dyes with four negative charges.

## 4. Conclusion

The cupuassu shell (CS; *T. grandiflorum*) is a good alternative biosorbent to remove C.I. Reactive Red 194 (RR-194) and C.I. Direct Blue 53 (DB-53) textile dyes from aqueous solutions. The CS was characterized by FTIR spectroscopy, SEM and nitrogen adsorption/desorption curves. It was demonstrated that the OH groups of phenols and alcohols and the carboxylate groups presented shift to lower wavenumber after contact with both dyes, indicating that these groups should participate of the biosorption mechanism.Both dyes interact with the biosorbent at the solid/liquid interface when suspended in water. The best conditions were established with respect to pH and contact time to saturate the available sites located on the adsorbent surface. Five kinetic models were used to adjust the adsorption and the best fit was the Avrami (fractionary-order) kinetic model. However, the intra-particle diffusion model gave multiple linear regions, which suggested that the biosorption may also be followed by multiple adsorption rates. The equilibration time for RR-194 and DB-53 dye were obtained after 8 and 18 h, respectively of contact between the dyes and the biosorbent. The equilibrium isotherm of these dyes was obtained, being these data better fitted to the Sips isotherm model. The maximum adsorption capacities were 64.1 and 37.5 mg $g^{-1}$ for RR-194 and DB-53, respectively, using CS biosorbent.

## Acknowledgements

The authors are grateful to Conselho Nacional de Desenvolvimento Científico e Tecnológico (CNPq), to Coordenação de Aperfeiçoamento de Pessoal de Nível Superior (CAPES), and to Fundação de Amparo à Pesquisa do Estado do Rio Grande do Sul (FAPERGS) for financial supports and fellowships. We are also grateful to Centro de Microscopia Eletrônica (CME-UFRGS) for the use of the SEM microscope.

## Nomenclature

| | |
|---|---|
| C | constant related with the thickness of boundary layer (mg $g^{-1}$). |
| $C_e$ | dye concentration at the equilibrium (mg $L^{-1}$). |
| $C_f$ | dye concentration at ending of the adsorption (mg $L^{-1}$). |
| $C_o$ | initial dye concentration put in contact with the adsorbent (mg $L^{-1}$). |
| $h_o$ | the initial sorption rate (mg $g^{-1}$ $h^{-1}$) of pseudo-second order equation. |
| $k_{AV}$ | is the Avrami kinetic constant $[(h^{-1})^{-n_{AV}}]$ |
| $K_F$ | the Freundlich equilibrium constant $[mg \cdot g^{-1} \cdot (mg \cdot L^{-1})^{-1/n_F}]$ |
| $k_f$ | the pseudo-first order rate constant ($h^{-1}$). |
| $k_{id}$ | the intra-particle diffusion rate constant (mg $g^{-1}$ $h^{-0.5}$). |
| $K_L$ | the Langmuir equilibrium constant (L $mg^{-1}$). |
| $K_{RP}$ | the Radke–Prausnitz equilibrium constant (L $mg^{-1}$) |
| $K_S$ | the Sips equilibrium constant (L $mg^{-1}$) |
| $k_s$ | the pseudo-second order rate constant (g $mg^{-1}$ $h^{-1}$). |
| $n_{AV}$ | is a fractionary reaction order (Avrami) which can be related, to the adsorption mechanism |
| $n_F$ | dimensionless exponent of the Freundlich equation |

$n_{RP}$ dimensionless exponent of the Radke–Prausnitz equation
$n_S$ dimensionless exponent of the Sips equation
$q$ amount adsorbed of the dye by the adsorbent (mg $g^{-1}$).
$q_e$ amount adsorbate adsorbed at the equilibrium (mg $g^{-1}$).
$Q_{max}$ the maximum adsorption capacity of the adsorbent (mg $g^{-1}$).
$q_t$ amount of adsorbate adsorbed at time (mg $g^{-1}$).
$t$ time of contact ($h$).
X biosorbent dosage (g $L^{-1}$).

*Greek letters*

$\alpha$ the initial adsorption rate (mg $g^{-1}$ $h^{-1}$) of the Elovich Equation
$\beta$ Elovich constant related to the extent of surface coverage and also to the activation energy involved in chemisorption (g $mg^{-1}$).

## Appendix. Supplementary material

Supplementary data related to this article can be found online at doi:10.1016/j.jenvman.2010.12.010.

## References


Akar, T., Ozcan, A.S., Tunali, S., Ozcan, A., 2008. Biosorption of a textile dye (Acid Blue 40) by cone biomass of Thuja orientalis: Estimation of equilibrium, thermodynamic and kinetic parameters. Bioresour. Technol. 99, 3057–3065.

Al-Degs, Y.S., El-Barghouthi, M.I., El-Sheikh, A.H., Walker, G.M., 2008. Effect of solution pH, ionic strength, and temperature on adsorption behavior of reactive dyes on activated carbon. Dyes Pigm. 77, 16–23.

Arenas, L.T., Lima, E.C., dos Santos Jr., A.A., Vaghetti, J.C.P., Costa, T.M.H., Benvenutti, E.V., 2007. Use of statistical design of experiments to evaluate the sorption capacity of 1,4-diazoniabicycle[2.2.2]octane/silica chloride for Cr(VI) adsorption. Colloids Surf. A 297, 240–248.

Baek, M.H., Ijagbemi, C.O., Se-Jin, O., Kim, D.S., 2010. Removal of Malachite green from aqueous solution using degreased coffee bean. J. Hazard. Mater. 176, 820–828.

Bekçi, Z., Seki, Y., Cavas, L., 2009. Removal of malachite green by using an invasive marine alga *Caulerpa racemosa* var. *cylindracea*. J. Hazard. Mater. 161, 1454–1460.

Blanachard, G., Maunaye, M., Martin, G., 1984. Removal of heavy metals from waters by means of natural zeolites. Water Res. 18, 1501–1507.

Brookstein, D.S., 2009. Factors associated with textile pattern dermatitis caused by contact allergy to dyes, finishes, foams, and preservatives. Dermatol. Clin. 27, 309–322.

Calvete, T., Lima, E.C., Cardoso, N.F., Dias, S.L.P., Pavan, F.A., 2009. Application of carbon adsorbents prepared from the Brazilian-pine fruit shell for removal of Procion Red MX 3B from aqueous solution - Kinetic, equilibrium, and thermodynamic studies. Chem. Eng. J. 155, 627–636.

Calvete, T., Lima, E.C., Cardoso, N.F., Vaghetti, J.C.P., Dias, S.L.P., Pavan, F.A., 2010. Application of carbon adsorbents prepared from Brazilian-pine fruit shell for the removal of reactive orange 16 from aqueous solution: kinetic, equilibrium, and thermodynamic studies. J. Environ. Manage. 91, 1695–1706.

Cestari, A.R., Vieira, E.F.S., Pinto, A.A., Lopes, E.C.N., 2005. Multistep adsorption of anionic dyes on silica/chitosan hybrid 1. Comparative kinetic data from liquid- and solid-phase models. J. Colloid Interface Sci. 292, 363–372.

Cestari, A.R., Vieira, E.F.S., Vieira, G.S., da Costa, L.P., Tavares, A.M.G., Loh, W., Airoldi, C., 2009. The removal of reactive dyes from aqueous solutions using chemically modified mesoporous silica in the presence of anionic surfactant-The temperature dependence and a thermodynamic multivariate analysis. J. Hazard. Mater. 161, 307–316.

Crini, G., 2006. Non-conventional low-cost adsorbents for dye removal: a review. Bioresou. Technol. 97, 1061–1085.

de Lima, R.O.A., Bazo, A.P., Salvadori, D.M.F., Rech, C.M., Oliveira, D.P., Umbuzeiro, G.A., 2007. Mutagenic and carcinogenic potential of a textile azo dye processing plant effluent that impacts a drinking water source. Mutat. Res. Genet. Toxicol. Environ. Mutagen 626, 53–60.

Deniz, F., Saygideger, S.D., 2010. Equilibrium, kinetic and thermodynamic studies of Acid Orange 52 dye biosorption by Paulownia tomentosa Steud. Leaf powder as a low-cost natural biosorbent. Bioresou. Technol. 101, 5137–5143.

Freundlich, H.M.F., 1906. Über die adsorption in lösungen. Z. Phys. Chem. 57A, 385–470.

Gay, D.S.F., Fernandes, T.H.M., Amavisca, C.V., Cardoso, N.F., Benvenutti, E.V., Costa, T.M.H., Lima, E.C., 2010. Silica grafted with a silsesquioxane containing the positively charged 1,4-diazoniabicyclo[2.2.2]octane group used as adsorbent for anionic dye removal. Desalination 258, 128–135.

Gondim, T.M.S., Thamazini, M.J., Calvacante, M.J.B., de Souza, J.M.L., 2001. Aspectos da produção de cupuaçu. Embrapa, Rio Branco-AC.

Gunay, A., 2007. Application of nonlinear regression analysis for ammonium exchange by natural (Bigadiç) clinoptilolite. J. Hazard. Mater. 148, 708–713.

Gupta, V.K., Suhas, I.A., 2009. Application of low-cost adsorbents for dye removal – A review. J. Environ. Manage. 90, 2313–2342.

Jacques, R.A., Bernardi, R., Caovila, M., Lima, E.C., Pavan, F.A., Vaghetti, J.C.P., Airoldi, C., 2007. Removal of Cu(II), Fe(III) and Cr(III) from aqueous solution by aniline grafted silica gel. Sep. Sci. Technol. 42, 591–609.

Janoš, P., Coskun, S., Pilařová, V., Rejnek, J., 2009. Removal of basic (Methylene Blue) and acid (Egacid Orange) dyes from waters by sorption on chemically treated wood shavings. Bioresour. Technol. 100, 1450–1453.

Kara, S., Aydiner, C., Demirbas, E., Kobya, M., Dizge, N., 2007. Modeling the effects of adsorbent dose and particle size on the adsorption of reactive textile dyes by fly ash. Desalination 212, 282–293.

Kumari, P., Sharma, P., Srivastava, S., Srivastava, M.M., 2006. Biosorption studies on shelled Moringa oleifera Lamarck seed powder: removal and recovery of arsenic from aqueous system. Int. J. Miner. Process 78, 131–139.

Langmuir, I., 1918. The adsorption of gases on plane surfaces of glass, mica and platinum. J. Am. Chem. Soc. 40, 1361–1403.

Largegren, S., 1898. About the theory of so-called adsorption of soluble substances. Kungliga Suensk Vetenskapsakademiens Handlingar 241, 1–39.

Lima, E.C., Fenga, P.G., Romero, J.R., de Giovani, W.F., 1998. Electrochemical behaviour of $[Ru(4,4'\text{-}Me_2bpy)_2(PPh_3)(H_2O)](ClO_4)_2$ in homogeneous solution and incorporated into carbon paste electrodes. Application to oxidation of benzylic compounds. Polyhedron 17, 313–318.

Lima, E.C., Barbosa- Jr., F., Krug, F.J., Tavares, A., 2002. Copper determination in biological materials by ETAAS using W-Rh permanent modifier. Talanta 57, 177–186.

Lima, E.C., Brasil, J.L., Santos, A.H.D.P., 2003. Evaluation of Rh, Ir, Ru, W-Rh, W-Ir, and W-Ru as permanent modifiers for the determination of lead in ashes, coals, sediments, sludges, soils, and freshwaters by electrothermal atomic absorption spectrometry. Anal. Chim. Acta 484, 233–242.

Lima, E.C., Royer, B., Vaghetti, J.C.P., Brasil, J.L., Simon, N.M., dos Santos Jr., A.A., Pavan, F.A., Dias, S.L.P., Benvenutti, E.V., da Silva, E.A., 2007. Adsorption of Cu(II) on Araucaria angustifolia wastes: determination of the optimal conditions by statistic design of experiments. J. Hazard. Mater. 140, 211–220.

Lima, E.C., Royer, B., Vaghetti, J.C.P., Simon, N.M., da Cunha, B.M., Pavan, F.A., Benvenutti, E.V., Veses, R.C., Airoldi, C., 2008. Application of Brazilian-pine fruit coat as a biosorbent to removal of reactive red 194 textile dye from aqueous solution, kinetics and equilibrium study. J. Hazard. Mater. 155, 536–550.

Lopes, E.C.N., dos Anjos, F.S.C., Vieira, E.F.S., Cestari, A.R., 2003. An alternative Avrami equation to evaluate kinetic parameters of the interaction of Hg(II) with thin chitosan membranes. J. Colloid Interface Sci. 263, 542–547.

Mittal, A., Mittal, J., Malviya, A., Kaur, D., Gupta, V.K., 2010. Adsorption of hazardous dye crystal violet from wastewater by waste materials. J. Colloid Interface Sci. 343, 463–473.

Murakami, K., 2002. Thermodynamic and kinetic aspects of self-association of dyes in aqueous solution. Dyes Pigm. 53, 31–43.

Olivares-Marín, M., Del-Prete, V., Garcia-Moruno, E., Fernández-González, C., Macías-García, A., Gómez-Serrano, V., 2009. The development of an activated carbon from cherry stones and its use in the removal of ochratoxin A from red wine. Food Control 20, 298–303.

Órfão, J.J.M., Silva, A.I.M., Pereira, J.C.V., Barata, S.A., Fonseca, I.M., Faria, P.C.C., Pereira, M.F.R., 2006. Adsorption of a reactive dye on chemically modified activated carbons-Influence of pH. J. Colloid Interface Sci. 296, 480–489.

Pavan, F.A., Gushikem, Y., Mazzocato, A.S., Dias, S.L.P., Lima, E.C., 2007. Statistical design of experiments as a tool for optimizing the batch conditions to methylene blue biosorption on yellow passion fruit and mandarin peels. Dyes Pigm. 72, 256–266.

Pavan, F.A., Dias, S.L.P., Lima, E.C., Benvenutti, E.V., 2008. Removal of congo red from aqueous solution by anilinepropylsilica xerogel. Dyes Pigm. 76, 64–69.

Radke, C.J., Prausnitz, J.M., 1972. Adsorption of organic solutes from dilute aqueous solution on activated carbon. Ind. Eng. Chem. Fundam. 11, 445–451.

Rosa, S., Laranjeira, M.C.M., Riela, H.G., Fávere, V.T., 2008. Cross-linked quaternary chitosan as an adsorbent for the removal of the reactive dye from aqueous solutions. J. Hazard. Mater. 155, 253–260.

Rosenkranz, H.S., Cunningham, S.L., Mermelstein, R., Cunningham, A.R., 2007. The challenge of testing chemicals for potential carcinogenicity using multiple short-term assays: an analysis of a proposed test battery for hair dyes. Mutat. Res. Genet. Toxicol. Environ. Mutagen 633, 55–66.

Royer, B., Cardoso, N.F., Lima, E.C., Ruiz, V.S.O., Macedo, T.R., Airoldi, C., 2009a. Organofunctionalized kenyaite for dye removal from aqueous solution. J. Colloid Interface Sci. 336, 398–405.

Royer, B., Cardoso, N.F., Lima, E.C., Vaghetti, J.C.P., Simon, N.M., Calvete, T., Veses, R.C., 2009b. Applications of Brazilian-pine fruit shell in natural and carbonized forms as adsorbents to removal of methylene blue from aqueous solutions - Kinetic and equilibrium study. J. Hazard. Mater. 164, 1213–1222.

Royer, B., Cardoso, N.F., Lima, E.C., Macedo, T.R., Airoldi, C., 2010a. A useful organofunctionalized layered silicate for textile dye removal. J. Hazard. Mater. 181, 366–374.

Royer, B., Cardoso, N.F., Lima, E.C., Macedo, T.R., Airoldi, C., 2010b. Sodic and acidic crystalline lamellar magadiite adsorbents for removal of methylene blue from aqueous solutions. Kinetic and equilibrium studies. Sep. Sci. Technol. 45, 129–141.

Royer, B., Lima, E.C., Cardoso, N.F., Calvete, T., Bruns, R.E., 2010c. Statistical design of experiments for optimization of batch adsorption conditions for removal of reactive red 194 textile dye from aqueous effluents. Chem. Eng. Commun. 197, 775–790.

Sips, R., 1948. On the structure of a catalyst surface. J. Chem. Phys. 16, 490–495.

Smith, B., 1999. Infrared Spectral Interpretation – A Systematic Approach. CRC Press, Boca Raton.

Vaghetti, J.C.P., Lima, E.C., Royer, B., Brasil, J.L., da Cunha, B.M., Simon, N.M., Cardoso, N.F., Noreña, C.P.Z., 2008. Application of Brazilian-pine fruit coat as a biosorbent to removal of Cr(VI) from aqueous solution. Kinetics and equilibrium study. Biochem. Eng. J. 42, 67–76.

Vaghetti, J.C.P., Lima, E.C., Royer, B., da Cunha, B.M., Cardoso, N.F., Brasil, J.L., Dias, S.L.P., 2009. Pecan nutshell as biosorbent to remove Cu(II), Mn(II) and Pb (II) from aqueous solutions. J. Hazard. Mater. 162, 270–280.

Vieira, A.P., Santana, S.A.A., Bezerra, C.W.B., Silva, H.A.S., Chaves, J.A.P., de Melo, J.C.P., Silva-Filho, E.C., Airoldi, C., 2009. Kinetics and thermodynamics of textile dye adsorption from aqueous solutions using babassu coconut mesocarp. J. Hazard. Mater. 166, 1272–1278.

Weber Jr., W.J., Morris, J.C., 1963. Kinetics of adsorption on carbon from solution. J. Sanit. Eng. Div. Am. Soc. Civil Eng. 89, 31–59.

Yurtsever, M., Sengil, I.A., 2009. Biosorption of Pb(II) ions by modified quebracho tannin resin. J. Hazard. Mater. 163, 58–64.

# Anexo 2

JOURNAL OF CHEMICAL & ENGINEERING DATA

ARTICLE

pubs.acs.org/jced

# Application of Aqai Stalks As Biosorbents for the Removal of the Dyes Reactive Black 5 and Reactive Orange 16 from Aqueous Solution

Natali F. Cardoso, Eder C. Lima,* Tatiana Calvete, Isis S. Pinto, Camila V. Amavisca, Thais H. M. Fernandes, Rodrigo B. Pinto, and Wagner S. Alencar

Institute of Chemistry, Federal University of Rio Grande do Sul, UFRGS, Av. Bento Gonçalves 9500, Postal Box 15003, 91501-970 Porto Alegre, RS, Brazil

Supporting Information

**ABSTRACT:** The aqai palm stalk (*Euterpe oleracea*) is a food residue used in its natural form (AS) and also protonated (AAS) as biosorbents for the removal of the textile dyes C.I. Reactive Black 5 and C.I. Reactive Orange 16 from aqueous solutions. This biosorbent was characterized by infrared spectroscopy, scanning electron microscopy, and nitrogen adsorption/desorption curves. The effects of pH, biosorbent dosage, and shaking time on the biosorption capacities were studied. In the acidic pH region (pH 2.0), the biosorption of the dyes was favorable. The contact time to obtain the equilibrium at 298 K was fixed at (10 and 4) h for the AS and AAS biosorbents, respectively, using both dyes. The Avrami fractionary-order kinetic model provided the best fit to the experimental data compared with the pseudofirst-order and pseudosecond-order kinetic adsorption models. The equilibrium data were fitted to the Langmuir, Freundlich, and Sips isotherm models. For both dyes the equilibrium data were best fitted to the Sips isotherm model.

## INTRODUCTION

Dyes are one of the most hazardous chemical compound classes found in industrial effluents which need to be treated since their presence in water bodies reduces light penetration, precluding the photosynthesis of aqueous flora.[1,2] They are also aesthetically objectionable for drinking and other purposes.[3] Dyes can also cause allergy, dermatitis, and skin irritation[4] and also provoke cancer and cell mutations in humans.[5,6]

There are some methods that are used for treating waters containing dyes, such as, coagulation and flocculation,[7] degradation by visible light assisted by photocatalytic ozonation,[8] photocatalytic oxidation,[9] oxidative decomposition using the Fenton process,[10] catalytic wet air oxidation,[11] electrochemical degradation,[12] biological treatment with microorganisms.[13] However, all these processes lead to the formation of other byproducts that require continuous monitoring and identification, besides of most of them are expensive for treatment on a large scale.[14] One of the most employed methods for the removal of synthetic dyes from aqueous effluents is the adsorption procedure.[15,16] This process transfers the dyes from the water effluent to a solid phase, decreasing remarkably the dye bioavailability to live organisms. The decontaminated effluent could then be released to the environment or the water could be reutilized in the industrial process. Subsequently, the adsorbent can be regenerated or stored in a dry place without direct contact with the environment.[15,16]

Activated carbon is the most employed adsorbent for dye removal from aqueous solution because of its excellent adsorption properties.[17−19] However, the extensive use of activated carbon for dye removal from industrial effluents is expensive, limiting its large application for wastewater treatment.[20,21] Therefore, there is growing interest in finding alternative low cost adsorbents for dye removal from aqueous solution. These alternative adsorbents, include: helzenet shell,[21] saw dust wallnut,[21] saw dust cherry,[21] saw dust oak,[21] saw dust pitch pine,[21] saw dust pine,[21] cane pitch,[21] soy meal hull,[21] banana pitch,[21] sugar cane bagasse,[20] cotton waste,[20] chitin and chitosan,[20] peat,[20] microorganisms such as fungus and yeasts,[20] maize cob,[20,21] and Brazilian pine-fruit shell.[15,22,23]

Aqai palm (*Euterpe oleracea*) is native to the Brazilian Amazon; however, it has already been cultivated in the United States.[24] The palms of *E. oleracea* are multistemmed, monoecious, and may reach heights of > 25 m. The fruit, a small, round, black-purple drupe about 25 mm in circumference, is produced in branched panicles of (500 to 900) fruits.[25,26] Aqai pulp is utilized in the manufacture of a variety of foods and beverages.[25,26] The Brazilian annual production of aqai is about 160 000 tons.[27] About 20% of the weight of the aqai is the stalk (AS) that held its fruits, which is a waste material that presents no aggregate economic value.[27]

The disposal of large amounts of AS directly in the soil and/or in natural waters may contaminate the environment in an uncontrolled way because the decomposition of this waste material leads to the generation of various chemical compounds and microorganisms. In this context, combining the need to reduce costs with commercial adsorbents and by using AS as a biosorbent for the removal of dyes from industrial effluents, is a good economical and environmental advantage to developing countries such as Brazil.

The present work aimed to use aqai stalk in natural (AS) and protonated (AAS) forms as biosorbents for the successful removal

**Received:** August 21, 2010
**Accepted:** February 25, 2011
**Published:** March 14, 2011

of the dyes C.I. Reactive Black 5 (RB-5) and C.I. Reactive Orange 16 (RO-16) from aqueous solutions. These dyes are largely used for textile dying in the Brazilian cloth industries.

## MATERIALS AND METHODS

**Solutions and Reagents.** Deionized water was used throughout the experiments for solution preparations.

The textile dyes, C.I. Reactive Black 5 (C.I. 20505; CAS 12225-25-1; $C_{26}H_{21}N_5O_{19}S_6Na_4$, 991.82 $g\cdot mol^{-1}$, $\lambda_{max}$ = 590 nm, see Supporting Information, Figure 1) at 55% purity and C.I. Reactive Orange 16 (C.I. 17757; CAS 20262-58-2; $C_{20}H_{17}N_3O_{11}S_3Na_2$, 617.54 $g\cdot mol^{-1}$, $\lambda_{max}$ = 493 nm, see Supporting Information, Figure 1) at 50 % purity, both were furnished by Sigma-Aldrich (St. Louis, MO). The dyes were used without further purification. The RB-5 dye has two sulfonate groups and two sulfato-ethyl-sulfone groups, and the RO-16 has one sulfato-ethyl-sulfone group and one sulfonate group. These groups present negative charges even in highly acidic solutions due to their p$K_a$ values that are lower than zero.[18,22] A stock solution was prepared by dissolving the dyes in distilled water to the concentration of 5.00 $g\cdot L^{-1}$. Working solutions were obtained by diluting the dye stock solutions to the required concentrations. To adjust the pH solutions, 0.10 $mol\cdot L^{-1}$ sodium hydroxide or hydrochloric acid solutions were used. The pH of the solutions was measured using a Schott Lab 850 set pH meter.

**Adsorbent Preparation and Characterization.** AS was furnished by the ice cream industry in Belém-PA, Brazil, as a residual material. AS was washed with tap water to remove dust and with deionized water. Then, it was dried at 70 °C in an air-supplied oven for 8 h. After that, AS was grounded in a disk-mill and subsequently sieved. The part of the biosorbent which presented a diameter of particles ≤ 250 $\mu$m was used. This unmodified aqai stalk was assigned as AS.

In order to increase the amount adsorbed of RB-5 and RO-16 dyes by the AS biosorbent the biomaterial was protonated as described below.[22] An amount of 5.0 g of AS was added to 200.0 mL of 3 $mol\cdot L^{-1}$ of HCl, and the slurry was magnetically stirred for 24 h at 70 °C. Subsequently, the slurry was filtered in a sintered glass funnel, and the solid phase was thoroughly washed with water, until the filtrate reached the pH of distilled water. Subsequently, the material was dried at 70 °C in an air supplied oven for 8 h, yielding the acidified aqai stalk (AAS).

The AS and AAS biosorbents were characterized by FTIR using a Shimadzu FTIR, model 8300 (Kyoto, Japan). The spectra were obtained with a resolution of 4 $cm^{-1}$, with 100 cumulative scans.[28]

The surface analyses and porosity were carried out with a volumetric adsorption analyzer, ASAP 2020, from Micrometrics, at 77 K (boiling point of nitrogen). The samples were pretreated at 373 K for 24 h under a nitrogen atmosphere in order to eliminate the moisture adsorbed on the solid sample surface. After, the samples were submitted to 298 K in a vacuum, reaching the residual pressure of $10^{-4}$ Pa. For area and pore size distribution calculations, the BET and BJH methods were used.[29,30]

The AS and AAS biosorbent samples were also analyzed by scanning electron microscopy (SEM) in a Jeol microscope, model JSM 6060, using an acceleration voltage of 20 kV and magnification ranging from 100 to 5000 fold.[31]

**Biosorption Studies.** The biosorption studies for evaluation of the AS and AAS biosorbents for the removal of the RB-5 and RO-16 dyes from aqueous solutions were carried out in triplicate using the batch contact biosorption method. For these experiments, fixed amounts of biosorbent [(20.0 to 200.0) mg] were placed in 50 mL cylindrical high-density polystyrene flasks (117 mm height and 30 mm diameter) containing 20.0 mL of dye solutions [(10.00 to 300.0) $mg\cdot L^{-1}$], which were agitated for a suitable time [(0.5 to 48) h] at 298 K. The pH of the dye solutions ranged from 2.0 to 10.0. Subsequently, in order to separate the biosorbents from the aqueous solutions, the flasks were centrifuged at 3600 rpm for 10 min, and aliquots of (1 to 10) mL of supernatant were properly diluted with water.

**Table 1. Kinetic Adsorption Models**

| kinetic model | equation |
|---|---|
| fractionary-order | $q_t = q_e\{1 - \exp[-(k_{AV}t)]^{nAV}\}$ |
| | $h_o = k_s q_e$ |
| | initial sorption rate |
| pseudofirst order | $q_t = q_e[1 - \exp(-k_f t)]$ |
| | $h_o = k_s q_e$ |
| | initial sorption rate |
| pseudosecond order | $q_t = (k_s q_e^2 t)/(1 + q_e k_s t)$ |
| | $h_o = k_s q_e^2$ |
| | initial sorption rate |
| intraparticle diffusion | $q_t = k_{id}(t)^{1/2} + C$ |

**Table 2. Equilibrium Models**

| isotherm model | equation |
|---|---|
| Langmuir | $q_e = (Q_{max}K_L C_e)/(1 + K_L C_e)$ |
| Freundlich | $q_e = K_F C_e^{1/nF}$ |
| Sips | $q_e = (Q_{max}(K_S C_e)^{1/ns})/(1 + (K_S C_e)^{1/ns})$ |

The final concentrations of the dyes remaining in the solution were determined by visible spectrophotometry using a T90+ UV−vis spectrophotometer furnished by PG Instruments (London-England) provided with quartz optical cells. Absorbance measurements were made at the maximum wavelength of RB-5 and RO-16 which were (590 and 493) nm, respectively.

The amount of dyes adsorbed and the percentage of removal of the dyes by the biosorbent were calculated by applying the eqs 1 and 2, respectively:

$$q = \frac{(C_o - C_f)}{X} \quad (1)$$

$$\%\ \text{removal} = 100\cdot\frac{(C_o - C_f)}{C_o} \quad (2)$$

where $q$ is the amount of dyes adsorbed by the biosorbent ($mg\cdot g^{-1}$), $C_o$ is the initial dye concentration put in contact with the adsorbent ($mg\cdot L^{-1}$), $C_f$ is the dye concentration ($mg\cdot L^{-1}$) after the batch adsorption procedure, and $X$ is biosorbent dosage ($g\cdot L^{-1}$).

**Kinetic and Equilibrium Models.** The Avrami fractionary-order,[32] pseudofirst-order,[33] pseudosecond-order,[34] and intraparticle diffusion model[35] kinetic equations are given in Table 1.

The Langmuir,[36] Freundlich,[37] and Sips[38] isotherm equations are given in Table 2.

**Quality Assurance and Statistical Evaluation of the Kinetic and Isotherm Parameters.** To establish the accuracy, reliability,

Table 3. FTIR Bands ($cm^{-1}$) of the Adsorbents AS and AAS before and after the Adsorption of RB-5 and RO-16 Dyes

| wavenumber ($cm^{-1}$) | | | | | | |
|---|---|---|---|---|---|---|
| AS | AS+RB-5 | AS+RO-16 | AAS | AAS+RB-5 | AAS+RO-16 | assignments |
| 3433 | 3427 | 3426 | 3431 | 3425 | 3419 | O−H bond stretching[44,45] |
| 1735 | 1730 | 1730 | 1734 | 1730 | 1730 | stretching of carbonyl groups of carboxylic acid[45] |
| 1252 | 1245 | 1246 | 1252 | 1241 | 1241 | C−O stretch of phenolic compounds found in lignin[44,45] |
| 1045 | 1033 | 1030 | 1057 | 1044 | 1046 | C−O stretch of phenolic compounds found in lignin[44,45] |

and reproducibility of the collected data, all of the batch adsorption measurements were performed in triplicate. Blanks were run in parallel and they were corrected when necessary.[39]

All dye solutions were stored in glass flasks, which were cleaned by soaking in 1.4 $mol \cdot L^{-1}$ $HNO_3$ for 24 h,[40] rinsing five times with deionized water, dried, and stored in a flow hood.

For analytical calibration, standard solutions with concentrations ranging from (5.00 to 50.0) $mg \cdot L^{-1}$ of the dyes were employed, running against a blank solution of water adjusted to pH 2.0. The linear analytical calibration of the curve was furnished by the UVWin software of the T90+ PG Instruments spectrophotometer. The detection limits of the method, obtained with a signal/noise ratio of 3,[41] were (0.18 and 0.11) $mg \cdot L^{-1}$, for RB-5 and RO-16, respectively. All of the analytical measurements were performed in triplicate, and the precision of the standards was better than 3 % ($n = 3$). For checking the accuracy of the RB-5 and RO-16 dye sample solutions during the spectrophotometric measurements, standards containing dyes at 5.00 $mg \cdot L^{-1}$ were employed as a quality control every five determinations.[42]

The kinetic and equilibrium models were fitted by employing a nonlinear method, with successive interactions calculated by the method of Levenberg−Marquardt and also interactions calculated by the Simplex method, using the nonlinear fitting facilities of the software Microcal Origin 7.0. In addition, the models were also evaluated by adjusted determination factor ($R_{adj}^2$), as well as by an error function ($F_{error}$),[43] which measures the differences in the amount of dye taken up by the adsorbent predicted by the models and the actual $q$ measured experimentally. $R_{adj}^2$ and $F_{error}$ are given below, in eqs 3 and 4, respectively

$$R_{adj}^2 = 1 - \left( \frac{\sum_i^n (q_{i,exp} - q_{i,model})^2}{\sum_i^n (q_{i,exp} - \overline{q}_{i,exp})^2} \right) \left( \frac{n-1}{n-p} \right) \quad (3)$$

$$F_{error} = \sqrt{\left( \frac{1}{n-p} \right) \sum_i^n (q_{i,exp} - q_{i,model})^2} \quad (4)$$

where $q_{i,model}$ is each value of $q$ predicted by the fitted model, $q_{i,exp}$ is each value of $q$ measured experimentally, $\overline{q}_{exp}$ is the average of $q$ experimentally measured, $n$ is the number of experiments performed, and $p$ is the number of parameters of the fitted model.[43]

## RESULTS AND DISCUSSION

**Characterization of Biosorbents.** The FTIR technique was used to examine the surface groups of the AS and AAS biosorbents and to identify the groups responsible for the dyes adsorption. Infrared spectra of the adsorbents and dye-loaded adsorbent samples, before and after the adsorption process, were recorded in the range (4000 to 400) $cm^{-1}$ (see the Supporting Information, Figure 2A-F). Table 3 presents the significant changes of FTIR vibrational spectra of AS and AAS adsorbents before the adsorption and loaded with the RB-5 and RO-16 dyes after the adsorption. The FTIR band assignments are based on the literature.[44,45] As previously observed for an activated carbon[18,19] and a fly ash adsorbent[46] after the adsorption procedure, the functional groups that interact with the dye suffered a shift to lower wavenumbers when the adsorbate withdrew electrons of the adsorbent group. These FTIR results indicate that the interaction of RB-5 and RO-16 dyes with the AS and AAS biosorbents should occur with the O−H bonds of phenols and alcohols present in the lignin structure as well as interactions with the carboxylate group because these groups suffered a shift to lower wavenumbers after the biosorption procedure.

The textural properties of AS and AAS obtained by nitrogen adsorption/desorption curves were: superficial area ($S_{BET}$) (1.6 and 2.0) $m^2 \cdot g^{-1}$; average pore diameter (BJH) (10.77 and 11.80) nm; and total pore volume (0.0050 and 0.0077) $cm^3 \cdot g^{-1}$ for AS and AAS, respectively. The superficial area of agricultural residues is usually a low value.[47,48] On the other hand, the average pore diameter of AS and AAS biomaterials are relatively large, even when compared with activated carbons[17,18] or silicates.[2,3,16] The maximum diagonal lengths of the RB-5 and RO-16 (see the Supporting Information, Figure 1) are (2.55 and 1.68) nm, respectively. The ratios of average pore diameter of the biosorbents to the maximum diagonal length of each dye are 4.22 (ØAS/ØRB-5); 4.63 (ØAAS/ØRB-5); 6.41 (ØAS/ØRO-16); and 7.02 (ØAAS/ØRO-16). Therefore, the mesopores of the biosorbents could accommodate up to 4 molecules of RB-5 for AS and AAS and up to 6 molecules of RO-16 for AS and up to 7 molecules of RO-16 for AAS. This number of molecules, which could be accommodated in each pore of the biosorbent, is considered large when compared with other adsorbents reported in the literature.[17,18]

Scanning electron microscope (SEM) analysis results of the AS and AAS biosorbents without contact with the dye solution (Figure 1A,C for AS and AAS, respectively) and after contact with the RO-16 dye solution at pH 2.0 (Figure 1B,D for AS and AAS, respectively) are shown in Figure 1. As can be seen, for the AS biosorbent without contact with the dye solution is a more compact fibrous material (see Figure 1A). On the other hand, after the AS biosorbent has been in contact with an RO-16 dye solution at pH 2.0 for 4 h, some cavities of the fibrous materials appeared, which should allow the diffusion of dye molecules through the macropore (pore with Ø > 50 nm)[29,30] of the AS biosorbent. For the AAS biosorbent, the material already presents several macropore structures (see Figure 1C) and after the contact with RO-16 dye solution at pH 2.0 for 8 h, no significant differences were observed. Therefore, the acid

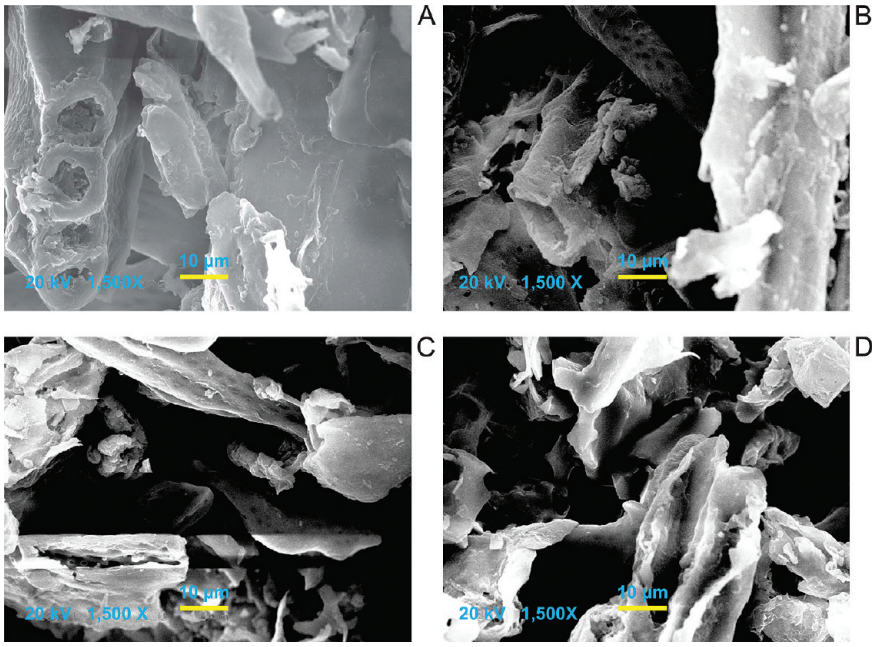


**Figure 1.** SEM of (A) AS without contact with dye solution, (B) AS after contact with RO-16 dye solution, (C) AAS without contact with dye solution, and (D) AAS after contact with RO-16 dye solution. Magnification 1500×; accelerating voltage 20 kV.

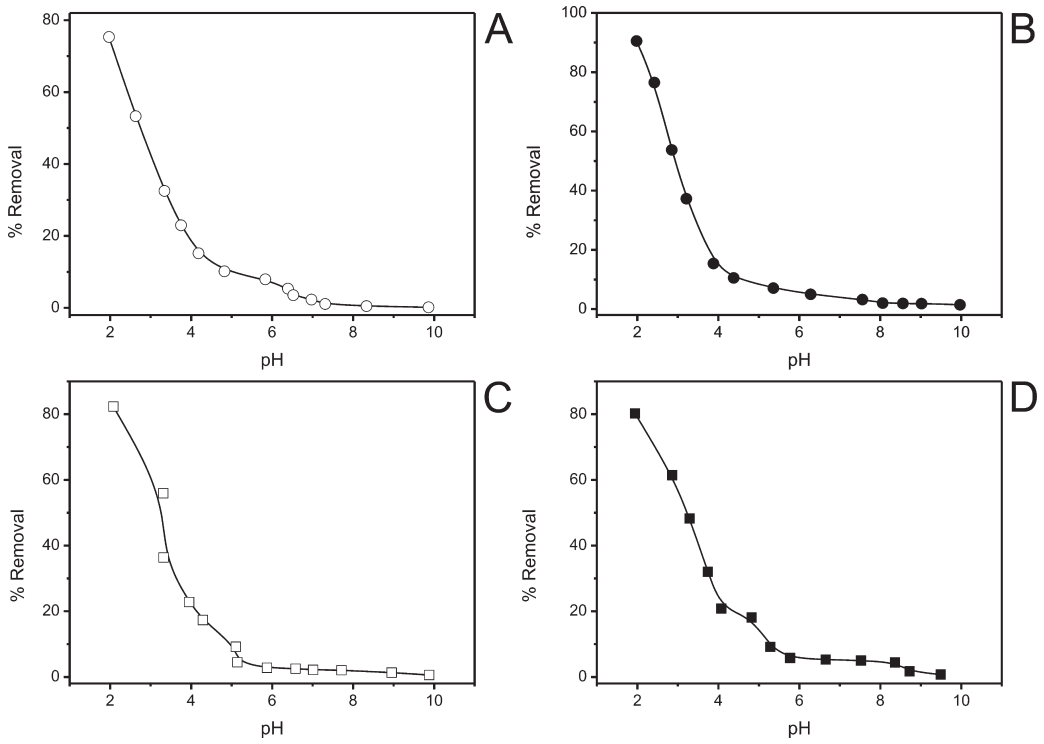


**Figure 2.** Effect of pH on the biosorption of (A) RB-5 on AS biosorbent, (B) RB-5 on AAS biosorbent, (C) RO-16 on AS biosorbent, and (D) RO-16 on AAS biosorbent. Conditions: $C_o$= 40.0 mg·$L^{-1}$ of dye solution and mass of biosorbent of 30.0 mg for both dyes. The temperature was fixed at 298 K.

treatment of aqai fiber with 3.0 mol·$L^{-1}$ HCl generated several macropores on the biomaterial fiber, which allowed the diffusion of the dyes by the pore of the biosorbent. By these results it is expected that the AAS biosorbent should present higher sorption capacity than the AS biosorbent, as already reported in the literature.[30] The macropores facilitate the diffusion of the dye molecules inside the fiber pores of the biosorbents (increasing the intraparticle diffusion). As the adsorbate diffuses through the pores of the biosorbent, the dye could be adsorbed at the internal sites of the biomaterial. On the other


dx.doi.org/10.1021/je100866c |J. Chem. Eng. Data 2011, 56, 1857–1868

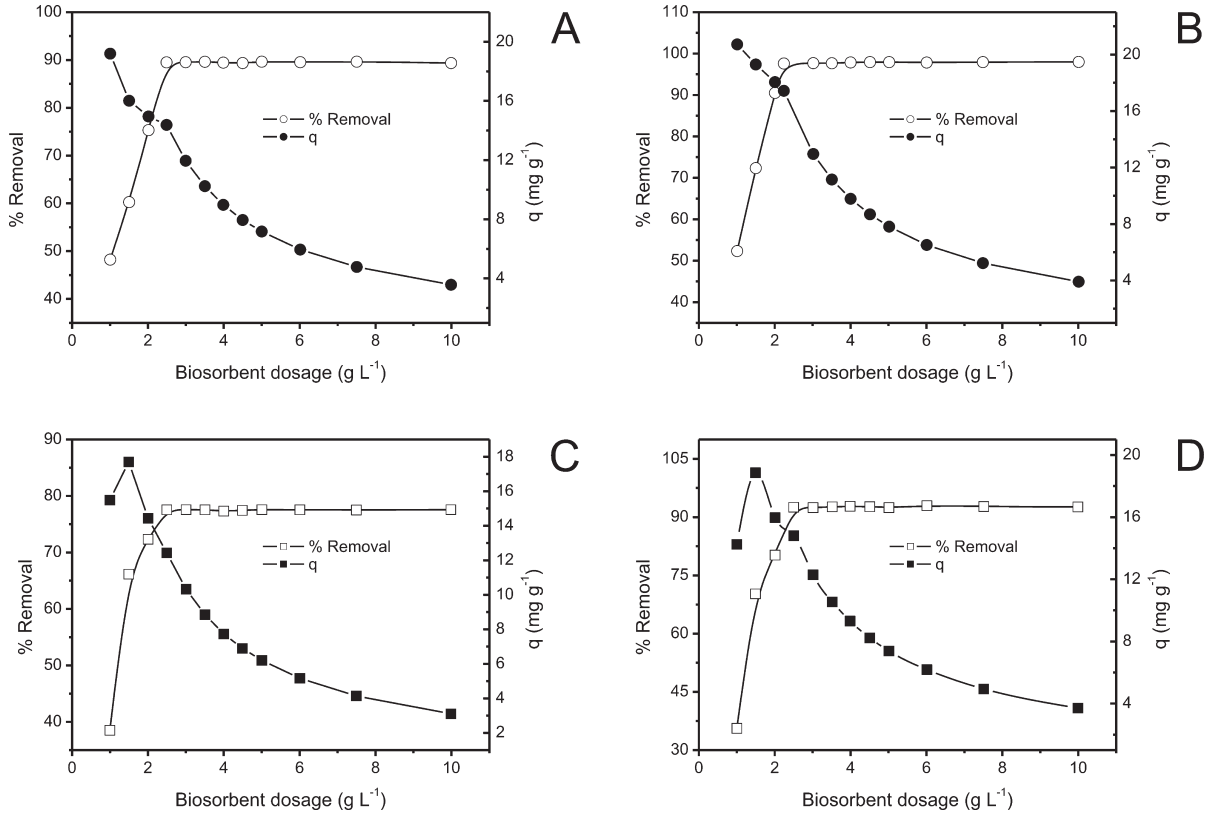


**Figure 3.** Effect of biosorbent dosage on the percentage of dye removal and amount of dye adsorbed. (A) RB-5 adsorbed on AS, (B) RB-5 adsorbed on AAS, (C) RO-16 adsorbed on AS, and (D) RO-16 adsorbed on AAS. Conditions: initial pH 2.0; $C_o$= 40.0 mg·L$^{-1}$; $T$ = 298 K, time of contact 12 h.

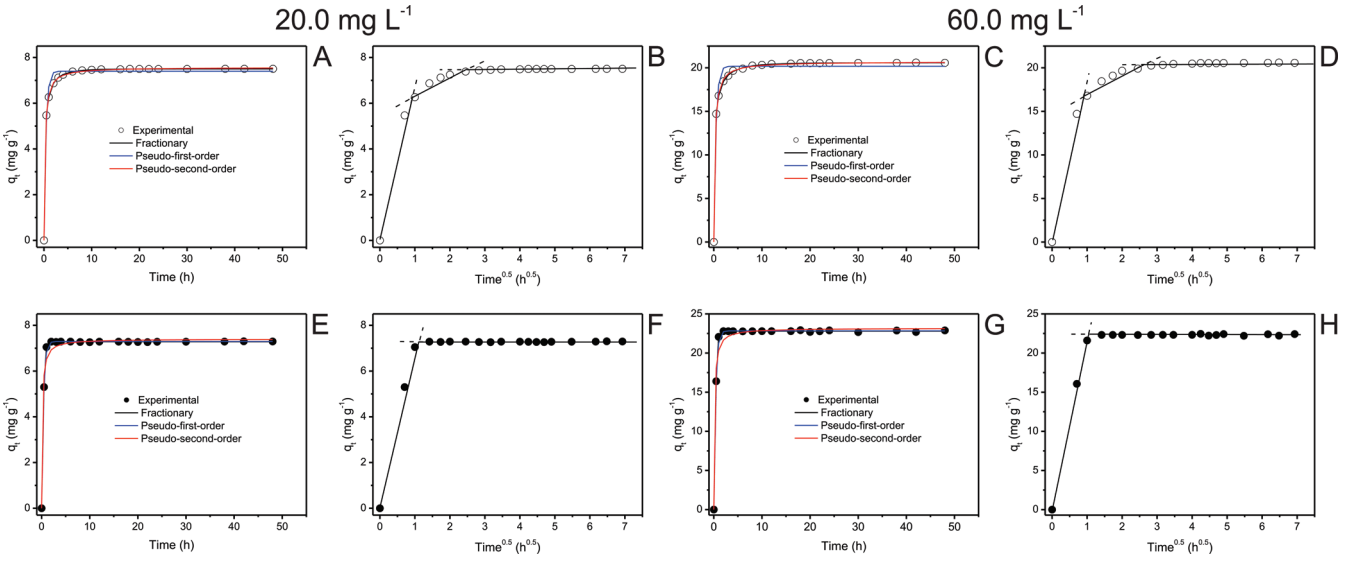


**Figure 4.** Kinetic biosorption curves of RB-5 dye. (A) Biosorbent AS; $C_o$ 20.0 mg·L$^{-1}$; (B) intraparticle diffusion; biosorbent AS; $C_o$ 20.0 mg·L$^{-1}$; (C) biosorbent AS; $C_o$ 60.0 mg·L$^{-1}$; (D) intraparticle diffusion; biosorbent AS; $C_o$ 60.0 mg·L$^{-1}$; (E) biosorbent AAS; $C_o$ 20.0 mg·L$^{-1}$; (F) intraparticle diffusion; biosorbent AAS; $C_o$ 20.0 mg·L$^{-1}$; (G) biosorbent AAS; $C_o$ 60.0 mg·L$^{-1}$; (H) intraparticle diffusion; biosorbent AAS; $C_o$ 60.0 mg·L$^{-1}$. Conditions: pH was fixed at 2.0; the biosorbent dosage was fixed at 2.5 g·L$^{-1}$; and the temperature was fixed at 298 K.

hand, the biosorbent with a lower number of macropore structures, the adsorption is limited to the external surface of the biosorbent, decreasing the total amount adsorbed.[30] Similar results were also obtained with RB-5 after the contact with AS and AAS biosorbents (data not shown).

Taking into account that AS and AAS biosorbents present low superficial areas ($S_{BET}$) and some macropores (see Figure 1), it could be inferred that AS and AAS predominate a mixture of mesopores (pores with diameters ranging from (2 to 50) nm, see textural results described above) and


dx.doi.org/10.1021/je100866c |J. Chem. Eng. Data 2011, 56, 1857–1868

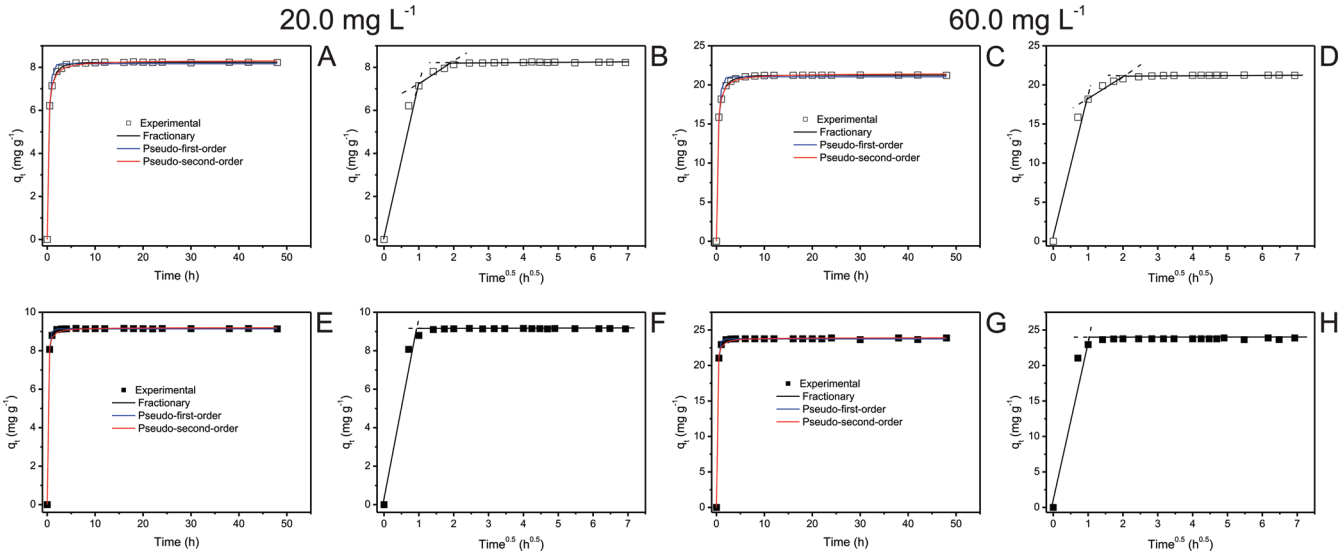


**Figure 5.** Kinetic biosorption curves of RO-16 dye. (A) Biosorbent AS; $C_o$ 20.0 mg·L$^{-1}$; (B) intraparticle diffusion; biosorbent AS; $C_o$ 20.0 mg·L$^{-1}$; (C) biosorbent AS; $C_o$ 60.0 mg·L$^{-1}$; (D) intraparticle diffusion; biosorbent AS; $C_o$ 60.0 mg·L$^{-1}$; (E) biosorbent AAS; $C_o$ 20.0 mg·L$^{-1}$; (F) intraparticle diffusion; biosorbent AAS; $C_o$ 20.0 mg·L$^{-1}$; (G) biosorbent AAS; $C_o$ 60.0 mg·L$^{-1}$; (H) intraparticle diffusion; biosorbent AAS; $C_o$ 60.0 mg·L$^{-1}$. Conditions: pH was fixed at 2.0; the biosorbent dosage was fixed at 2.5 g·L$^{-1}$; and the temperature was fixed at 298 K.

**Table 4. Kinetic Parameters for RB-5 and RO-16 Removal Using AS and AAS as Biosorbents**[a]

| | AS | | | | AAS | | | |
|---|---|---|---|---|---|---|---|---|
| | RB-5 | | RO-16 | | RB-5 | | RO-16 | |
| | 20 mg·L$^{-1}$ | 60 mg·L$^{-1}$ | 20 mg·L$^{-1}$ | 60 mg·L$^{-1}$ | 20 mg·L$^{-1}$ | 60 mg·L$^{-1}$ | 20 mg L$^{-1}$ | 60 mg L$^{-1}$ |
| | | | | Fractionary-Order | | | | |
| $k_{AV}$ (h$^{-1}$) | 3.57 | 3.44 | 3.84 | 3.79 | 2.41 | 2.36 | 6.84 | 6.72 |
| $q_e$ (mg·g$^{-1}$) | 7.50 | 20.6 | 8.23 | 21.2 | 7.28 | 22.3 | 9.15 | 23.8 |
| $n_{AV}$ | 0.461 | 0.422 | 0.523 | 0.498 | 1.40 | 1.44 | 0.618 | 0.637 |
| $h_o$ (mg·g$^{-1}$·h$^{-1}$) | 26.8 | 70.9 | 31.6 | 80.5 | 17.6 | 52.8 | 62.5 | 159.8 |
| $R_{adj}^2$ | 1.000 | 0.9999 | 0.9999 | 1.000 | 1.000 | 0.9998 | 1.000 | 0.9999 |
| $F_{error}$ | 0.00459 | 0.0414 | 0.0188 | 0.0132 | 0.00972 | 0.0686 | 0.00786 | 0.0649 |
| | | | | Pseudofirst-Order | | | | |
| $k_f$ (h$^{-1}$) | 2.37 | 2.26 | 2.61 | 2.53 | 2.72 | 2.67 | 4.21 | 4.27 |
| $q_e$ (mg·g$^{-1}$) | 7.40 | 20.2 | 8.17 | 21.0 | 7.29 | 22.4 | 9.13 | 23.7 |
| $h_o$ (mg·g$^{-1}$·h$^{-1}$) | 17.6 | 45.6 | 21.3 | 53.3 | 19.9 | 59.8 | 38.5 | 101 |
| $R_{adj}^2$ | 0.9861 | 0.9799 | 0.9928 | 0.9908 | 0.9985 | 0.9981 | 0.9994 | 0.9994 |
| $F_{error}$ | 0.205 | 0.677 | 0.1615 | 0.4715 | 0.0663 | 0.231 | 0.0524 | 0.135 |
| | | | | Pseudosecond-Order | | | | |
| $k_s$ (g·mg$^{-1}$·h$^{-1}$) | 0.674 | 0.222 | 0.741 | 0.270 | 0.992 | 0.313 | 1.79 | 0.715 |
| $q_e$ (mg·g$^{-1}$) | 7.57 | 20.7 | 8.33 | 21.5 | 7.40 | 22.7 | 9.21 | 23.9 |
| $h_o$ (mg·g$^{-1}$·h$^{-1}$) | 38.6 | 95.3 | 51.4 | 124 | 54.3 | 161 | 152 | 409 |
| $R_{adj}^2$ | 0.9997 | 0.9993 | 0.9989 | 0.9994 | 0.9839 | 0.9826 | 0.9988 | 0.9986 |
| $F_{error}$ | 0.0327 | 0.124 | 0.0631 | 0.1233 | 0.216 | 0.691 | 0.0741 | 0.200 |
| | | | | Intraparticle Diffusion | | | | |
| $k_{id}$ (mg·g$^{-1}$·h$^{-0.5}$) | 0.751[c] | 2.13[c] | 0.965[c] | 2.60[c] | 7.13[b] | 21.8[b] | 9.28[b] | 24.2[b] |

[a] Conditions: temperature was fixed at 298 K; pH 2.0 biosorbent dosage of 2.5 g·L$^{-1}$. [b] First stage. [c] Second stage.

macropores (pores with diameters > 50 nm). On the other hand, the number of micropores (pores with a diameter < 2 nm) should be a minimum.[28−30] Usually, the micropore structure is responsible for higher superficial area ($S_{BET}$) of the materials,[30,47,48] since the nitrogen probe molecule utilized in the measurements is retained basically at the micropore structure.[28−30]


dx.doi.org/10.1021/je100866c |J. Chem. Eng. Data 2011, 56, 1857–1868

**Table 5. Isotherm Parameters for RB-5 and RO-16 Biosorption, Using AS and AAS as Biosorbents**[a]

| | AS | | AAS | |
|---|---|---|---|---|
| | RB-5 | RO-16 | RB-5 | RO-16 |
| | Langmuir | | | |
| $Q_{max}$ ($mg \cdot g^{-1}$) | 47.6 | 35.8 | 55.3 | 62.9 |
| $K_L$ ($L \cdot mg^{-1}$) | 0.0870 | 0.0513 | 0.219 | 0.0618 |
| $R_{adj}^2$ | 0.9933 | 0.9830 | 0.9407 | 0.9707 |
| $F_{error}$ | 0.968 | 1.13 | 3.08 | 2.87 |
| | Freudlich | | | |
| $K_F$ ($mg \cdot g^{-1} \cdot (mg \cdot L^{-1})^{-1/n_F}$) | 11.8 | 4.97 | 21.5 | 10.3 |
| $n_F$ | 3.59 | 2.42 | 4.90 | 2.63 |
| $R_{adj}^2$ | 0.9465 | 0.9937 | 0.9713 | 0.9971 |
| $F_{error}$ | 2.74 | 0.687 | 2.15 | 0.900 |
| | Sips | | | |
| $Q_{max}$ ($mg \cdot g^{-1}$) | 52.3 | 61.3 | 72.3 | 156 |
| $K_S$ ($L \cdot mg^{-1}$) | 0.0684 | 0.0115 | 0.0957 | 0.00345 |
| $n_S$ | 1.28 | 1.63 | 2.06 | 2.02 |
| $R_{adj}^2$ | 0.9999 | 0.9998 | 0.9998 | 0.9995 |
| $F_{error}$ | 0.0903 | 0.114 | 0.169 | 0.376 |

[a] Conditions: temperature was fixed at 298 K; contact time was fixed at (10 and 4) h for AS and AAS, respectively; pH was fixed at 2.0; biosorbent dosage was fixed at 2.5 $g \cdot L^{-1}$.

This explains the low superficial areas ($S_{BET}$) of the AS and AAS biosorbents.

**Effects of Acidity on Adsorption.** One of the most important factors in adsorption studies is the effect of the acidity of the medium.[1,2,19,22] Different species may present divergent ranges of suitable pH depending on which adsorbent is used. Effects of initial pH on removal percentage of RB-5 and RO-16 dyes using AS and AAS biosorbents were evaluated within the pH range between (2 and 10) (Figure 2A–D). For both dyes, the percentage of dye removal decreased remarkably from pH 2.0, attaining practically less than 3.2 % and 5.0 % of dye removal at pH 7.5 for AS and AAS, respectively. Similar behavior for dye removal utilizing lignocellulose adsorbents has also been observed.[22,49]

The dissolved RB-5 and RO-16 dyes are negatively charged in water solutions, because they present sulfonate and sulfato-ethyl-sulfone groups.[18,22] The adsorption of these dyes takes place when the biosorbent presents a positive surface charge. At pH 2.0, these lignocellulosic materials presents positive surface charge.[22,49] This behavior explains the high sorption capacity of AS and AAS biosorbents for both RB-5 and RO-16 at pH 2. In order to continue the biosorption studies, the initial pH was fixed at 2.0 for both biosorbents.

**Adsorbent Dosage.** The study of biosorbent dosages for the removal of RB-5 and RO-16 dyes from aqueous solution was carried out using biosorbent dosages ranging from (1.0 to 10.0) g $L^{-1}$ of AS and AAS, and fixing the initial dye concentration at 40.0 mg $L^{-1}$ and using a time of contact between the adsorbents and adsorbates of 12 h. For both dyes and biosorbents, the highest amount of dye removal was attained for biosorbent doses of at least 2.5 $g \cdot L^{-1}$ (Figure 3A,B for RB-5 and Figure 3C,D for RO-16). For biosorbent dosages higher than this value, the percentage of dye removal remained almost constant. Increases in the percentage of the dye removal with biosorbent dosages up to 2.5 $g \cdot L^{-1}$ could be attributed to increases in the biosorbent surface areas, augmenting the number of adsorption sites available for adsorption, as already reported in several papers.[2,3,15,16,19,31,35,40] On the other hand, the increase in the biosorbent doses promotes a remarkable decrease in the amount of dye uptake per gram of adsorbent ($q$; Figure 3).

An effect that can be mathematically explained by combining eqs 1 and 2

$$q = \frac{\%\ \text{removal}\ C_o}{100X} \tag{5}$$

As observed from eq 5, the amount of dye uptake ($q$) and the biosorbent dosage ($X$) are inversely proportional. For a fixed dye percentage removal, the increase of adsorbent dosage leads to a decrease in $q$ values, since the volume ($V$) and initial dye concentrations ($C_o$) are always fixed. These values clearly indicate that the biosorbent dosage must be fixed at 2.5 $g \cdot L^{-1}$, which is the biosorbent dosage that corresponds to the minimum amount of adsorbent that leads to constant dye removal.[1,50]

**Kinetic Studies.** Adsorption kinetic studies are important in the treatment of aqueous effluents because they provide valuable information on the mechanism of the adsorption process.[31,35]

In attempting to describe the biosorption kinetics of RB-5 and RO-16 dyes by using the AS and AAS biosorbents, four kinetic models were tested, as shown in Figures 4 and 5 for RB-5 and RO-16, respectively. The kinetic parameters for the kinetic models are listed in Table 4. The pseudosecond-order kinetic model presented $F_{error}$ values ranging from 3.00 to 22.3 (RB-5) and from 3.08 to 9.43 (RO-16) times higher the values obtained for the Avrami-fractionary kinetic adsorption model, using both biosorbents. Also, for the pseudofirst-order model, the $F_{error}$ values ranged from 3.36 to 44.7 (RB-5) and from 2.07 to 35.7 (RO-16) times higher than the $F_{error}$ values obtained for the Avrami-fractionary kinetic adsorption model using both biosorbents. The lower the error function, the lower the difference of the $q$ calculated by the model from the experimentally measured $q$.[1,18,19,44] It should be pointed out that the $F_{error}$ utilized in this work takes into account the number of fitted parameters ($p$ term of eq 4), since it is reported in the literature[51] that depending on the number of parameters a nonlinear equation presents, it has the best fitting of the results. For this reason, the number of fitted parameter should be considered in the calculation of $F_{error}$. Also, it was verified that the $q_e$ values found in the fractionary-order were closer to the experimental $q_e$ values, when compared with all other kinetic models. These results indicate that the Avrami fractionary-order kinetic model should explain the adsorption process of RB-5 and RO-16 dyes using the AS and AAS biosorbents.

The Avrami kinetic equation has been successfully employed to explain several kinetic processes of different adsorbents and adsorbates.[1−3,16−19,23,30−32,44,52−57] The Avrami exponent ($n_{AV}$) is a fractionary number related with the possible changes of the adsorption mechanism that takes place during the adsorption process.[30−32] Instead of following only an integer-kinetic order, the mechanism adsorption could follow multiple kinetic orders that are changed during the contact of the adsorbate with the adsorbent.[30−32] The $n_{AV}$ exponent is a result of the multiple kinetic order of the adsorption procedure.[1−3]

Since kinetic results fit very well to the Avrami-fractionary kinetic model for the RB-5 and RO-16 dyes using AS and AAS as biosorbents (Table 4 and Figures 4 and 5), the intraparticle diffusion model[36] was used to verify the influence of mass transfer resistance on the binding of RB-5 and RO-16 dyes to the

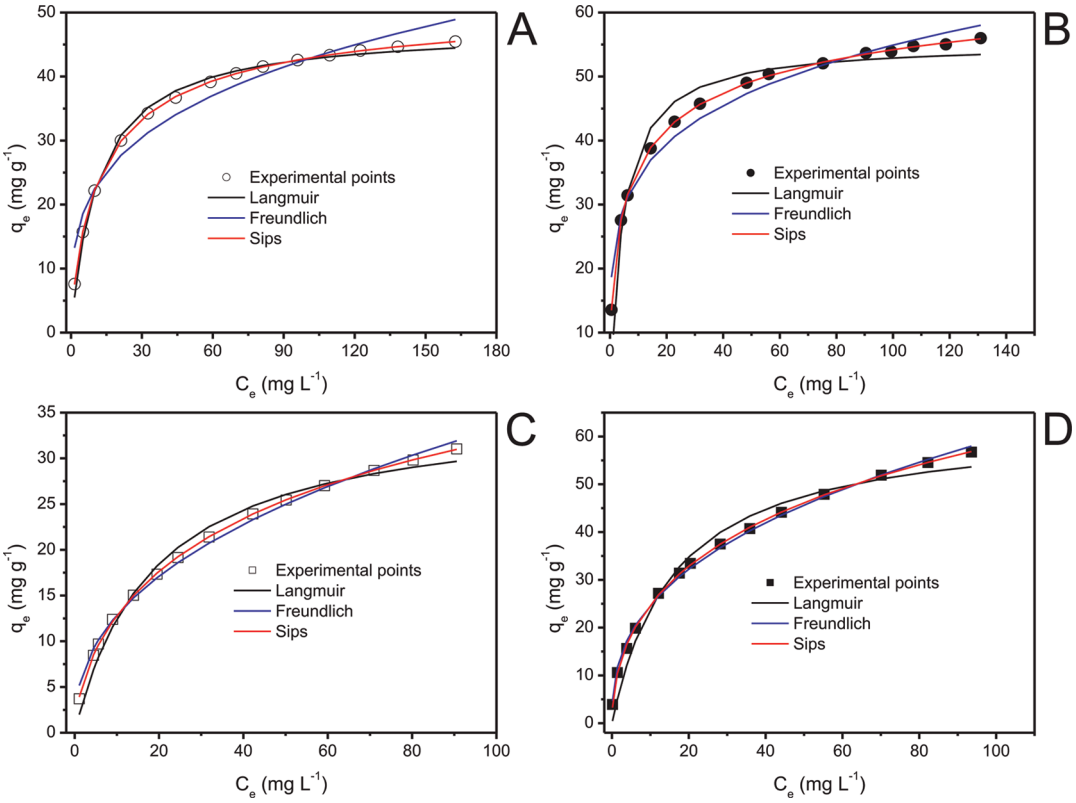


**Figure 6.** Isotherm curves. (A) RB-5 on AS biosorbent; (B) RB-5 on AAS biosorbent; (C) RO-16 on AS biosorbent; (D) RO-16 on AAS biosorbent. Conditions: pH was fixed at 2.0; the biosorbent dosage was fixed at 2.5 g·L$^{-1}$; and the temperature was fixed at 298 K. The contact time were fixed at (10 and 4) h for AS and AAS, respectively.

biosorbent (Table 4 and Figure 4B,D,F,H and 5B,D,F,H). The intraparticle diffusion constant, $k_{id}$ (mg·g$^{-1}$·h$^{-0.5}$), can be obtained from the slope of the plot of $q_t$ (uptaken at any time, mg·g$^{-1}$) versus the square root of time. These figures show the plots of $q_t$ versus $t^{1/2}$, with multilinearity for the RB-5 and RO-16 dyes using the AS and AAS biosorbents. These results imply that the adsorption processes involve more than one single kinetic stage (or adsorption rate).[35] For the AS biosorbent, the adsorption process exhibits three stages, which can be attributed to each linear portion of the figure (Figures 4B,D and 5B,D). The first linear portion was attributed to the diffusional process of the dye to the CS biosorbent surface;[35] hence, it was the fastest sorption stage. The second portion, ascribed to intraparticle diffusion, was a delayed process. The third stage may be regarded as the diffusion through smaller pores, which is followed by the establishment of equilibrium. For the AAS biosorbent, the adsorption process exhibits only two stages, being the first linear part attributed to intraparticle diffusion, and the second stage the diffusion through smaller pores, which is followed by the establishment of equilibrium.[35]

It was observed in Figures 4 and 5 that the minimum contact time of RB-5 and RO-16 dyes with the AS biosorbent to reach equilibrium was about (8 and 6) h, respectively. For the AAS biosorbent the minimum contact time to attain equilibrium was 2 h for both dyes. This great difference in the minimum contact time to reach equilibrium is associated with the difference in the mechanism of adsorption. These results imply that the diffusion of the dyes from the film could not explain completely the remarkable differences on the kinetics of adsorption of the dyes. As observed in Figures 4 and 5, for the AS biosorbent, three regions were observed in the intraparticle diffusion kinetic graph, on the other hand for the AAS biosorbent, only two linear regions were presented. For the AS biosorbent the film and intraparticle diffusion are rate controlling steps. On the other hand, for the AAS biosorbent, only the intraparticle diffusion is a rate controlling step. This could be confirmed by the intraparticle diffusion constants ($k_{id}$). The $k_{id}$ for RB-5 and RO-16 were at least 9.5 and 9.6 times, respectively, higher for the AAS biosorbent, when compared with the AS biosorbent. This could explain the difference of (6 and 4) h to reach the equilibrium for RB-5 and RO-16, respectively. This difference in the kinetic behavior is related to differences in the textural properties of the biosorbents after the treatment with acid, as already reported in the literature,[17,18,22,23] and also in agreement with the results discussed above in the characterization of the biosorbents.

In order to continue this work, the contact time between the biosorbents and biosorbates were fixed at (10.0 and 4.0) h using the AS and AAS biosorbents, respectively, for both dyes as biosorbates. This increase in the contact time utilized in this work was to guarantee that for both dyes equilibrium would be attained even at higher biosorbate concentrations.

**Equilibrium Studies.** An adsorption isotherm describes the relationship between the amount of adsorbate taken up by the adsorbent ($q_e$) and the adsorbate concentration remaining in the solution after the system attained the equilibrium ($C_e$). There are several equations to analyze experimental adsorption equilibrium data. The equation parameters of these equilibrium models often provide some insight into the adsorption mechanism, the surface properties and affinity of the adsorbent. In this work, the Langmuir,[36] the Freundlich,[37] and the Sips[38] isotherm models were tested.


dx.doi.org/10.1021/je100866c |J. Chem. Eng. Data 2011, 56, 1857–1868

**Table 6. Comparison of Maxima Adsorption Capacities for RB-5 and RO-16 Adsorbed[a]**

| adsorbent | $Q_{max}$ (mg·g$^{-1}$) RB-5 | RO-16 | ref |
|---|---|---|---|
| carbonized Brazilian pine-fruit shell (C-PW) | | 320 | 15 |
| activated carbon from Brazilian pine-fruit shell (AC-PW) | | 472 | 15 |
| waterworks sludge | | 86.8 | 58 |
| sewage sludge | | 47.0 | 58 |
| landfill sludge | | 114.7 | 58 |
| polysulfone-immobilized protonated *C. glutamicum* biomass | | 94.4 | 59 |
| chitosan cross-linked (beads) | | 30 | 60 |
| chitosan cross-linked (beads) | | 5.6 | 60 |
| chitosan | | 30.4 | 61 |
| chitosan hydrogel beads | 709.3 | | 62 |
| chitosan hydrogel beads | 413.2 | | 62 |
| high lime fly ash | 7.18 | | 63 |
| cetyltrimethylammonium bromide modified zeolite | 12.9 | | 64 |
| powdered activated carbon | 58.52 | | 65 |
| fly ash | 7.93 | | 65 |
| bone char | 157 | | 66 |
| brown seaweed, Laminaria sp | 101.5 | | 67 |
| aqai stalk (AS) | 52.3 | 61.3 | this work |
| acidified aqai stalk (AAS) | 72.3 | 156 | this work |

[a] The values were obtained at the best experimental conditions of each work.

**Table 7. Molecular Properties of RB-5 and RO-16 Calculated by the Software ChemBio 3D Ultra Version 11.0**

| properties | RB-5 | RO-16 | ratio RB-5/RO-16 |
|---|---|---|---|
| Connolly accessible area/nm$^2$ | 11.36 | 7.71 | 1.47 |
| Connolly molecular area/nm$^2$ | 6.42 | 4.20 | 1.53 |
| Connolly solvent excluded volume/nm$^3$ | 5.86 | 3.70 | 1.58 |

The isotherms of adsorption of RB-5 and RO-16 were carried out at 298 K on the AS and AAS biosorbents, using the best experimental conditions described previously (see Table 5 and Figure 6). Based on the $F_{error}$, the Sips model is the best isotherm model for both dyes and biosorbents. The maximum amounts of RB-5 and RO-16 adsorbed were (52.3 and 61.3) mg·g$^{-1}$, respectively, using AS as the biosorbent and (72.3 and 156) mg·g$^{-1}$, respectively using AAS as the biosorbent.

These values indicate that AS and AAS are fairly good biosorbents for the removal of these dyes from aqueous solutions (see Table 6).[15,58−67] For the RB-5 dye, out of ten different adsorbents, AAS presents an adsorption capacity higher than 5, and for RO-16 dye, out of eleven different adsorbents, AAS presents an adsorption capacity higher than eight.

It should be highlighted that the maximum amount adsorbed ($Q_{max}$) of the RB-5 and RO-16 dyes by the biosorbents was 1.38 and 2.54-fold respectively, higher for the AAS biosorbent when compared with the AS biosorbent. Considering that the kinetics of adsorption of both dyes were also faster using the AAS biosorbent (see Table 4), it can be concluded that the acid treatment of aqai stalk promoted the increase of macropore structure on the biomaterial (see Figure 1), contributing to a faster diffusion of the dyes through the pores of the biosorbent, and also allowing higher amounts of the dyes to be adsorbed by the AAS biosorbent. This effect was more pronounced for the RO-16 dye than for RB-5, since the maximum longitudinal length of RB-5 is 2.55 nm, whereas this value for RO-16 is only 1.68 nm (see the Supporting Information, Figure 1). In Table 7 are presented molecular properties of RB-5 and RO-16 dyes calculated by the Sofware ChemBio 3D Ultra version 11.0. According to these values, the Connolly solvent excluded volume of RB-5 is 58% higher than the RO-16 dye, and also the Connolly molecular area and accessible area of the RB-5 dye is higher when compared with the RO-16 dye. The lower is the volume of the dye molecule, the faster is the kinetics of adsorption (see Table 4) and also easier is the arrangement of the dye molecules on the external and internal part of the biosorbent, because lower will be the steric hindrance caused by the adsorbed dye molecule.[68] Therefore, it is expected that smaller dye molecules will allow higher adsorption capacity.

## CONCLUSION

The aqai palm stalk (*Euterpe oleracea*) in natural form (AS) as well as a protonated form (AAS) are good alternative biosorbents to remove the textile dyes C.I. Reactive Black 5 (RB-5) and C.I. Reactive Orange 16 (RO-16) from aqueous solutions. The AS and AAS were characterized by FTIR spectroscopy, SEM, and nitrogen adsorption/desorption curves. It was demonstrated that the OH groups of phenols and alcohols and carboxylate groups presented a shift to lower wavenumbers after contact with both dyes, indicating that these groups should participate in the biosorption mechanism. Both dyes interact with the biosorbents at the solid/liquid interface when suspended in water. The best conditions were established with respect to pH and contact time to saturate the available sites located on the adsorbent surface. Four kinetic models were used to adjust the adsorption and the best fit was obtained with the Avrami (fractionary-order) kinetic model. However, the intraparticle diffusion model gave multiple

linear regions, which suggested that the biosorption may also be followed by multiple adsorption rates. The equilibration time of both dyes were obtained after (10 and 4) h of contact between the dyes and the AS and AAS biosorbents, respectively. The shorter time of contact for AAS biosorbent was attributed to the macropores generated at the aqai fiber after acid treatement. The equilibrium isotherm of these dyes was obtained, that were best fitted to the Sips isotherm model. The maximum amounts of RB-5 and RO-16 adsorbed were (52.3 and 61.3) $mg \cdot g^{-1}$, respectively, using AS as biosorbent and (72.3 and 156) $mg \cdot g^{-1}$, respectively using AAS as biosorbent.

## ■ ASSOCIATED CONTENT

**Supporting Information.** Structural formulae of RB-5 and RO-16 and additional FTIR spectra. This material is available free of charge via the Internet at http://pubs.acs.org.

## ■ AUTHOR INFORMATION

### Corresponding Author

*Fax: +55 (51) 3308-7304. Phone: +55 (51) 3308 7175. E-mail: eder.lima@ufrgs.br; profederlima@gmail.com.

### Funding Sources

The authors are grateful to CNPq, to CAPES and to FAPERGS for financial support and fellowships.

## ■ ACKNOWLEDGMENT

We are grateful to Centro de Microscopia Eletrônica (CME-UFRGS) for the use of the SEM microscope.

## ■ NOMENCLATURE

$C$ constant related with the thickness of boundary layer $(mg \cdot g^{-1})$
$C_e$ dye concentration at the equilibrium $(mg \cdot L^{-1})$
$C_f$ dye concentration at ending of the adsorption $(mg \cdot L^{-1})$
$C_o$ initial dye concentration put in contact with the adsorbent $(mg \cdot L^{-1})$
$h_o$ the initial sorption rate $(mg \cdot g^{-1} \cdot h^{-1})$
$k_{AV}$ is the Avrami kinetic constant $[(h^{-1})]$
$K_F$ the Freundlich equilibrium constant $[mg \cdot g^{-1} \cdot (mg \cdot L^{-1})^{-1/nF}]$
$k_f$ the pseudofirst order rate constant $(h^{-1})$
$k_{id}$ the intraparticle diffusion rate constant $(mg \cdot g^{-1} \cdot h^{-0.5})$
$K_L$ the Langmuir equilibrium constant $(L \cdot mg^{-1})$
$K_S$ the Sips equilibrium constant $(L \cdot mg^{-1})$
$k_s$ the pseudosecond order rate constant $(g \cdot mg^{-1} \cdot h^{-1})$
$n_{AV}$ is a fractionary reaction order (Avrami) which can be related, to the adsorption mechanism
$n_F$ dimensionless exponent of the Freundlich equation
$n_S$ dimensionless exponent of the Sips equation
$q$ amount adsorbed of the dye by the adsorbent $(mg \cdot g^{-1})$
$q_e$ amount adsorbate adsorbed at the equilibrium $(mg \cdot g^{-1})$
$Q_{max}$ the maximum adsorption capacity of the adsorbent $(mg \cdot g^{-1})$
$q_t$ amount of adsorbate adsorbed at time $(mg \cdot g^{-1})$
$t$ time of contact (h)
$X$ biosorbent dosage $(g \cdot L^{-1})$

## ■ REFERENCES

(1) Cardoso, N. F.; Pinto, R. B.; Lima, E. C.; Calvete, T.; Amavisca, C. V.; Royer, B.; Cunha, M. L.; Fernandes, T. H. M.; Pinto, I. S. Removal of remazol black B textile dye from aqueous solution by adsorption. *Desalination* **2011**, *269*, 92–103.

(2) Royer, B.; Cardoso, N. F.; Lima, E. C.; Ruiz, V. S. O.; Macedo, T. R.; Airoldi, C. Organofunctionalized kenyaite for dye removal from aqueous solution. *J. Colloid Interface Sci.* **2009**, *336*, 398–405.

(3) Royer, B.; Cardoso, N. F.; Lima, E. C.; Macedo, T. R.; Airoldi, C. Sodic and acidic crystalline lamellar magadiite adsorbents for removal of methylene blue from aqueous solutions. Kinetic and equilibrium studies. *Sep. Sci. Technol.* **2010**, *45*, 129–141.

(4) Brookstein, D. S. Factors associated with textile pattern dermatitis caused by contact allergy to dyes, finishes, foams, and preservatives. *Dermatol. Clin.* **2009**, *27*, 309–322.

(5) de Lima, R. O. A.; Bazo, A. P.; Salvadori, D. M. F.; Rech, C. M.; Oliveira, D. P.; Umbuzeiro, G. A. Mutagenic and carcinogenic potential of a textile azo dye processing plant effluent that impacts a drinking water source. *Mutat. Res. Genet. Toxicol. Environ. Mutagen.* **2007**, *626*, 53–60.

(6) Carneiro, P. A.; Umbuzeiro, G. A.; Oliveira, D. P.; Zanoni, M. V. B. Assessment of water contamination caused by a mutagenic textile effluent/dyehouse effluent bearing disperse dyes. *J. Hazard. Mater.* **2010**, *174*, 694–699.

(7) Riera-Torres, M.; Gutiérrez-Bouzán, C.; Crespi, M. Combination of coagulation−flocculation and nanofiltration techniques for dye removal and water reuse in textile effluents. *Desalination* **2010**, *252*, 53–59.

(8) Anandan, S.; Lee, G. J.; Chen, P. K.; Fan, C.; Wu, J. J. Removal of Orange II Dye in Water by Visible Light Assisted Photocatalytic Ozonation Using $Bi_2O_3$ and $Au/Bi_2O_3$ Nanorods. *Ind. Eng. Chem. Res.* **2010**, *49*, 9729–9737.

(9) Berberidou, C.; Avlonitis, S.; Poulios, I. Dyestuff effluent treatment by integrated sequential photocatalytic oxidation and membrane filtration. *Desalination* **2009**, *249*, 1099–1106.

(10) Liang, X.; Zhong, Y.; Zhu, S.; Zhu, J.; Yuan, P.; He, H.; Zhang, J. The decolorization of Acid Orange II in non-homogeneous Fenton reaction catalyzed by natural vanadium−titanium magnetite. *J. Hazard. Mater.* **2010**, *181*, 112–120.

(11) Zhang, Y.; Li, D.; Chen, Y.; Wang, X.; Wang, S. Catalytic wet air oxidation of dye pollutants by polyoxomolybdate nanotubes under room condition. *Appl. Catal., B* **2009**, *86*, 182–189.

(12) Raghu, S.; Lee, C. W.; Chellammal, S.; Palanichamy, S.; Basha, C. A. Evaluation of electrochemical oxidation techniques for degradation of dye effluents—A comparative approach. *J. Hazard. Mater.* **2009**, *171*, 748–754.

(13) Novotný, Č.; Svobodová, K.; Benada, O.; Kofroňová, O.; Heissenberger, A.; Fuchs, W. Potential of combined fungal and bacterial treatment for color removal in textile wastewater. *Bioresour. Technol.* **2011**, *102*, 879–888.

(14) Forgacs, E; Cseháti, T; Oros, G. Removal of synthetic dyes from wastewaters: a review. *Environ. Int.* **2004**, *30*, 953–971.

(15) Royer, B.; Lima, E. C.; Cardoso, N. F.; Calvete, T.; Bruns, R. E. Statistical design of experiments for optimization of batch adsorption conditions for removal of reactive red 194 textile dye from aqueous effluents. *Chem. Eng. Commun.* **2010**, *197*, 775–790.

(16) Royer, B.; Cardoso, N. F.; Lima, E. C.; Macedo, T. R.; Airoldi, C. A useful organofunctionalized layered silicate for textile dye removal. *J. Hazard. Mater.* **2010**, *181*, 366–374.

(17) Calvete, T.; Lima, E. C.; Cardoso, N. F.; Dias, S. L. P.; Pavan, F. A. Application of carbon adsorbents prepared from the Brazilian-pine fruit shell for removal of Procion Red MX 3B from aqueous solution - Kinetic, equilibrium, and thermodynamic studies. *Chem. Eng. J.* **2009**, *155*, 627–636.

(18) Calvete, T; Lima, E. C.; Cardoso, N. F.; Vaghetti, J. C. P.; Dias, S. L. P.; Pavan, F. A. Application of carbon adsorbents prepared from Brazilian-pine fruit shell for the removal of reactive orange 16 from aqueous solution: Kinetic, equilibrium, and thermodynamic studies. *J. Environ. Manage.* **2010**, *91*, 1695–1706.

(19) Calvete, T; Lima, E. C.; Cardoso, N. F.; Dias, S. L. P.; Ribeiro, E. S. Removal of Brilliant Green Dye from Aqueous Solutions Using Home Made Activated Carbons. *Clean: Soil, Air, Water* **2010**, *38*, 521–532.

(20) Crini, G. Non-conventional low-cost adsorbents for dye removal: A review. *Bioresour. Technol.* **2006**, *97*, 1061–1085.

(21) Gupta, V. K.; Suhas, I. A. Application of low-cost adsorbents for dye removal − A review. *J. Environ. Manage.* **2009**, *90*, 2313–2342.
(22) Lima, E. C.; Royer, B.; Vaghetti, J. C. P.; Simon, N. M.; da Cunha, B. M.; Pavan, F. A.; Benvenutti, E. V.; Veses, R. C.; Airoldi, C. Application of Brazilian-pine fruit coat as a biosorbent to removal of reactive red 194 textile dye from aqueous solution, Kinetics and equilibrium study. *J. Hazard. Mater.* **2008**, *155*, 536–550.
(23) Royer, B.; Cardoso, N. F.; Lima, E. C.; Vaghetti, J. C. P.; Simon, N. M.; Calvete, T.; Veses, R. C. Applications of Brazilian-pine fruit shell in natural and carbonized forms as adsorbents to removal of methylene blue from aqueous solutions - Kinetic and equilibrium study. *J. Hazard. Mater.* **2009**, *164*, 1213–1222.
(24) Açai Farms, http://www.acaifarms.com/, website visited on January 6th, 2010.
(25) Pacheco-Palencia, L. A.; Duncan, C. E.; Talcott, S. T. Phytochemical composition and thermal stability of two commercial açai species, *Euterpe oleracea* and *Euterpe precatoria*. *Food Chem.* **2009**, *115*, 1199–1205.
(26) Açai Palm- Wikipedia, http://en.wikipedia.org/wiki/A%C3%A7ai, website visited on January 6th, 2011.
(27) de Vasconcelos, M. A. M.; Alves, S. M. Production system of Açai, http://sistemasdeproducao.cnptia.embrapa.br/FontesHTML/Acai/SistemaProducaoAcai_2ed/paginas/intro.htm, website visited on August 21st, 2010.
(28) Arenas, L. T.; Lima, E. C.; dos Santos, A. A., Jr.; Vaghetti, J. C. P.; Costa, T. M. H.; Benvenutti, E. V. Use of statistical design of experiments to evaluate the sorption capacity of 1,4-diazoniabicyclo-[2.2.2]octane/silica chloride for Cr(VI) adsorption. *Colloids Surf. A* **2007**, *297*, 240–248.
(29) Jacques, R. A.; Bernardi, R.; Caovila, M.; Lima, E. C.; Pavan, F. A.; Vaghetti, J. C. P.; Airoldi, C. Removal of Cu(II), Fe(III) and Cr(III) from aqueous solution by aniline grafted silica gel. *Sep. Sci. Technol.* **2007**, *42*, 591–609.
(30) Gay, D. S. F.; Fernandes, T. H. M.; Amavisca, C. V.; Cardoso, N. F.; Benvenutti, E. V.; Costa, T. M. H.; Lima, E. C. Silica grafted with a silsesquioxane containing the positively charged 1,4-diazoniabicyclo-[2.2.2]octane group used as adsorbent for anionic dye removal. *Desalination* **2010**, *258*, 128–135.
(31) Vaghetti, J. C. P.; Lima, E. C.; Royer, B.; Cardoso, N. F.; Martins, B.; Calvete, T. Pecan nutshell as biosorbent to remove toxic metals from aqueous solution. *Sep. Sci. Technol.* **2009**, *44*, 615–644.
(32) Lopes, E. C. N.; dos Anjos, F. S. C.; Vieira, E. F. S.; Cestari, A. R. An alternative Avrami equation to evaluate kinetic parameters of the interaction of Hg(II) with thin chitosan membranes. *J. Colloid Interface Sci.* **2003**, *263*, 542–547.
(33) Largegren, S. About the theory of so-called adsorption of soluble substances. *Kungliga Suensk Vetenskapsakademiens Handlingar* **1898**, *241*, 1–39.
(34) Ho, Y. S.; Mckay, G. M. Pseudo-second order model for sorption process. *Proc. Biochem.* **1999**, *34*, 451–465.
(35) Weber, W. J., Jr.; Morris, J. C. Kinetics of adsorption on carbon from solution. *J. Sanit. Eng. Div. Am. Soc. Civil Eng.* **1963**, *89*, 31–59.
(36) Langmuir, I. The adsorption of gases on plane surfaces of glass, mica and platinum. *J. Am. Chem. Soc.* **1918**, *40*, 1361–1403.
(37) Freundlich, H. Adsorption in solution. *Phys. Chem. Soc.* **1906**, *40*, 1361–1368.
(38) Sips, R. On the structure of a catalyst surface. *J. Chem. Phys.* **1948**, *16*, 490–495.
(39) Vaghetti, J. C. P.; Lima, E. C.; Royer, B.; Brasil, J. L.; da Cunha, B. M.; Simon, N. M.; Cardoso, N. F.; Noreña, C. P. Z. Application of Brazilian-pine fruit coat as a biosorbent to removal of Cr(VI) from aqueous solution. Kinetics and equilibrium study. *Biochem. Eng. J.* **2008**, *42*, 67–76.
(40) Lima, E. C.; Barbosa, F., Jr; Krug, F. J.; Tavares, A. Copper determination in biological materials by ETAAS using W-Rh permanent modifier. *Talanta* **2002**, *57*, 177–186.
(41) Lima, E. C.; Fenga, P. G.; Romero, J. R.; de Giovani, W. F. Electrochemical behaviour of $[Ru(4,4'\text{-}Me_2bpy)_2(PPh_3)(H_2O)](ClO_4)_2$ in homogeneous solution and incorporated into carbon paste electrodes. Application to oxidation of benzylic compounds. *Polyhedron* **1998**, *17*, 313–318.
(42) Lima, E. C.; Krug, F. J.; Nobrega, J. A.; Nogueira, A. R. A. Determination of ytterbium in animal faeces by tungsten coil electrothermal atomic absorption spectrometry. *Talanta* **1998**, *47*, 613–623.
(43) Lima, E. C.; Royer, B.; Vaghetti, J. C. P.; Brasil, J. L.; Simon, N. M.; dos Santos, A. A., Jr.; Pavan, F. A.; Dias, S. L. P.; Benvenutti, E. V.; da Silva, E. A. Adsorption of Cu(II) on Araucaria angustifolia wastes: Determination of the optimal conditions by statistic design of experiments. *J. Hazard. Mater.* **2007**, *140*, 211–220.
(44) Vaghetti, J. C. P.; Lima, E. C.; Royer, B.; da Cunha, B. M.; Cardoso, N. F.; Brasil, J. L.; Dias, S. L. P. Pecan nutshell as biosorbent to remove Cu(II), Mn(II) and Pb(II) from aqueous solutions. *J. Hazard. Mater.* **2009**, *162*, 270–280.
(45) Smith, B. *Infrared spectral Interpretation − A systematic approach*; CRC Press: Boca Raton, FL, 1999.
(46) Kara, S.; Aydiner, C.; Demirbas, E.; Kobya, M.; Dizge, N. Modeling the effects of adsorbent dose and particle size on the adsorption of reactive textile dyes by fly ash. *Desalination* **2007**, *212*, 282–293.
(47) Kumari, P.; Sharma, P.; Srivastava, S.; Srivastava, M. M. Biosorption studies on shelled Moringa oleifera Lamarck seed powder: Removal and recovery of arsenic from aqueous system. *Int. J. Miner. Process* **2006**, *78*, 131–139.
(48) Yurtsever, M.; Sengil, I. A. Biosorption of Pb(II) ions by modified quebracho tannin resin. *J. Hazard. Mater.* **2009**, *163*, 58–64.
(49) Deniz, F.; Saygideger, S. D. Equilibrium, kinetic and thermodynamic studies of Acid Orange 52 dye biosorption by Paulownia tomentosa Steud. leaf powder as a low-cost natural biosorbent. *Bioresour. Technol.* **2010**, *101*, 5137–5143.
(50) Oladoja, N. A.; Akinlabi, A. K. Congo Red Biosorption on Palm Kernel Seed Coat. *Ind. Eng. Chem. Res.* **2009**, *48*, 6188–6196.
(51) El-Khaiary, M. I.; Malash, G. F. Common data analysis errors in batch adsorption studies. *Hydrometallurgy* **2011**, *105*, 314–320.
(52) Cestari, A. R.; Vieira, E. F. S.; Pinto, A. A.; Lopes, E. C. N. Multistep adsorption of anionic dyes on silica/chitosan hybrid 1. Comparative kinetic data from liquid- and solid-phase models. *J. Colloid Interface Sci.* **2005**, *292*, 363–372.
(53) Cestari, A. R.; Vieira, E. F. S.; Vieira, G. S.; Almeida, L. E. The removal of anionic dyes from aqueous solutions in the presence of anionic surfactant using aminopropylsilica. -A kinetic study. *J. Hazard. Mater.* **2006**, *138*, 133–141.
(54) Bascialla, G.; Regazzoni, A. E. Immobilization of anionic dyes by intercalation into hydrotalcite. *Colloids Surf. A* **2008**, *328*, 34–39.
(55) Zubieta, C. E.; Messina, P. V.; Luengo, C.; Dennehy, M.; Pieroni, O.; Schulz, P. C. Reactive dyes remotion by porous $TiO_2$-chitosan materials. *J. Hazard. Mater.* **2008**, *152*, 765–777.
(56) Serna-Guerrero, R.; Sayari, A. Modeling adsorption of $CO_2$ on amine-functionalized mesoporous silica. 2: Kinetics and breakthrough curves. *Chem. Eng. J.* **2010**, *161*, 182–190.
(57) Cardoso, N. F.; Lima, E. C.; Pinto, I. S.; Amavisca, C. V.; Royer, B.; Pinto, R. B.; Alencar, W. S.; Pereira, S. F. P. Application of cupuassu shell as biosorbent for the removal of textile dyes from aqueous solution. *J. Environ. Manage.* **2011**, *92*, 1237–1247.
(58) Won, S. W.; Choi, S. B.; Yun, Y. S. Performance and mechanism in binding of Reactive Orange 16 to various types of sludge. *Biochem. Eng. J.* **2006**, *28*, 208–214.
(59) Vijayaraghavan, K.; Yun, Y. S. Competition of Reactive red 4, Reactive orange 16 and Basic blue 3 during biosorption of Reactive blue 4 by polysulfone-immobilized *Corynebacterium glutamicum*. *J. Hazard. Mater.* **2008**, *153*, 478–486.
(60) Kimura, I. Y.; Laranjeira, M. C. M.; Fávere, V. T.; Furlan, L. The interaction between reactive dye containing vinylsulfone group and chitosan microspheres. *Int. J. Polym. Mater.* **2002**, *51*, 759–768.
(61) Crini, G.; Badot, P. M. Application of chitosan, a natural aminopolysaccharide, for dye removal from aqueous solutions by adsorption processes using batch studies: A review of recent literature. *Prog. Polym. Sci.* **2008**, *33*, 399–447.

(62) Chatterjee, S.; Chatterjee, T.; Woo, S. H. Influence of the polyethyleneimine grafting on the adsorption capacity of chitosan beads for Reactive Black 5 from aqueous solutions. *Chem. Eng. J.* **2011**, *166*, 168–175.

(63) Eren, Z.; Acar, F. N. Equilibrium and kinetic mechanism for Reactive Black 5 sorption onto high lime Soma fly ash. *J. Hazard. Mater.* **2007**, *143*, 226–232.

(64) Karadag, D.; Turan, M.; Akgul, E.; Tok, S.; Faki, A. Adsorption equilibrium and kinetics of Reactive Black 5 and Reactive Red 239 in aqueous solution onto surfactant-modified zeolite. *J. Chem. Eng. Data* **2007**, *52*, 1615–1620.

(65) Eren, Z.; Acar, F. N. Adsorption of Reactive Black 5 from an aqueous solution: equilibrium and kinetic studies. *Desalination* **2006**, *194*, 1–10.

(66) Ip, A. W. M.; Barford, J. P.; McKay, G. Reactive Black dye adsorption/desorption onto different adsorbents: effect of salt, surface chemistry, pore size and surface area. *J. Colloid Interface Sci.* **2009**, *337*, 32–38.

(67) Vijayaraghavan, K.; Yun, Y. S. Biosorption of C.I. Reactive Black 5 from aqueous solution using acid-treated biomass of brown seaweed Laminaria sp. *Dyes Pigm.* **2008**, *76*, 726–732.

(68) Vachoud, L.; Zydowicz, N.; Domard, A. Sorption and desorption studies on chitin gels. *Int. J. Biol. Macromol.* **2001**, *28*, 93–101.

# Anexo 3

Journal of Hazardous Materials xxx (2012) xxx–xxx

Contents lists available at SciVerse ScienceDirect

Journal of Hazardous Materials

journal homepage: www.elsevier.com/locate/jhazmat

# Comparison of *Spirulina platensis* microalgae and commercial activated carbon as adsorbents for the removal of Reactive Red 120 dye from aqueous effluents

Natali F. Cardoso[a], Eder C. Lima[a,*], Betina Royer[a], Marta V. Bach[a], Guilherme L. Dotto[b], Luiz A.A. Pinto[b], Tatiana Calvete[c]

[a] *Institute of Chemistry, Federal University of Rio Grande do Sul, UFRGS, AV. Bento Gonçalves 9500, 91501-970, Porto Alegre, RS, Brazil*
[b] *Unit Operation Laboratory, School of Chemistry and Food, Federal University of Rio Grande, FURG, R. Engenheiro Alfredo Huch 475, 96201-900, Rio Grande, RS, Brazil*
[c] *Universitary Center La Salle (UNILASALLE), Av. Victor Barreto 2288, 92010-000, Canoas, RS, Brazil*

## HIGHLIGHTS

- *Spirulina platensis* (SP) and activated carbon (AC) were used to remove RR-120 dye.
- The maximum adsorption capacities were found at pH 2 and 298 K.
- The values were 482.2 and 267.2 mg $g^{-1}$ for SP and AC, respectively.
- Adsorption was exothermic, spontaneous and favorable.
- SP and AC were effective to treat a simulated dye-house effluent.

## ARTICLE INFO

*Article history:*
Received 25 June 2012
Received in revised form
11 September 2012
Accepted 12 September 2012
Available online xxx

*Keywords:*
Dye removal from aqueous solution
Adsorption
Effluent treatment
Nonlinear fitting
Thermodynamic

## ABSTRACT

*Spirulina platensis* microalgae (SP) and commercial activated carbon (AC) were compared as adsorbents to remove Reactive Red 120 (RR-120) textile dye from aqueous effluents. The batch adsorption system was evaluated in relation to the initial pH, contact time, initial dye concentration and temperature. An alternative kinetic model (general order kinetic model) was compared with the traditional pseudo-first order and pseudo-second order kinetic models. The equilibrium data were fitted to the Langmuir, Freundlich and Liu isotherm models, and the thermodynamic parameters were also estimated. Finally, the adsorbents were employed to treat a simulated dye-house effluent. The general order kinetic model was more appropriate to explain RR-120 adsorption by SP and AC. The equilibrium data were best fitted to the Liu isotherm model. The maximum adsorption capacities of RR-120 dye were found at pH 2 and 298 K, and the values were 482.2 and 267.2 mg $g^{-1}$ for the SP and AC adsorbents, respectively. The thermodynamic study showed that the adsorption was exothermic, spontaneous and favourable. The SP and AC adsorbents presented good performance for the treatment of simulated industrial textile effluents, removing 94.4–99.0% and 93.6–97.7%, respectively, of the dye mixtures containing high saline concentrations.



## 1. Introduction

Population growth increases the demand for industrial products. Dyes are used to colour the final products of different industries, such as textiles, paper and pulp mills, cosmetics, food, leather, rubber, etc. The generation of these products leads to the formation of wastewater contaminated with dyes. The textile industry is responsible for the use of 30% of synthetic dyes [1]. Of all dyed textile fibres, cotton occupies the number one position, and more than 50% of its production is dyed with reactive dyes [2]. It is estimated that about 10–60% of reactive dyes are lost during textile dyeing, producing large amounts of coloured wastewater [1]. The dye-containing wastewater discharged from these industries can adversely affect the aquatic environment by impeding light penetration and, as a consequence, precluding the photosynthesis of aqueous flora [3,4]. Moreover, most of these dyes can cause allergy, dermatitis, skin irritation [5] and also provoke cancer [6] and mutation in humans [6,7]. It is rather difficult to treat reactive dye effluents because the complex aromatic molecular structure of these compounds. The molecular structures of reactive dyes make them more stable and biologically non-degradable [8–10]. Since global regulations have grown more stringent [1], the effluents of the textile industry have to be treated carefully before discharge [11,12]. This has resulted in increased demand for eco-friendly technologies to remove dyes from aqueous effluents [8,11,12].

* Corresponding author. Tel.: +55 51 3308 7175; fax: +55 51 3308 7304.
*E-mail addresses:* profederlima@gmail.com, eder.lima@ufrgs.br (E.C. Lima).

0304-3894/$ – see front matter © 2012 Elsevier B.V. All rights reserved.
http://dx.doi.org/10.1016/j.jhazmat.2012.09.026

Adsorption is one of the most commonly employed methods for the removal of synthetic dyes from aqueous effluents [13,14], due its simplicity and high efficiency, as well as the availability of a wide range of adsorbents that can be applied [11–16]. This process transfers the dyes from the aqueous effluent to a solid phase, remarkably decreasing dye bioavailability to live organisms [11,12]. The decontaminated effluent can then be released to the environment or the water can be reutilised in the industrial process [15]. Subsequently, the adsorbent can be regenerated or stored in a dry place without direct contact with the environment [16]. Different kinds of adsorbents to remove dyes from aqueous solutions have been reported in the literature, such as agricultural wastes (cupuassu shell [3], aqai stalk [4], jujuba seeds [13], Brazilian pine fruit shell [15]), chemically modified lignin [16], chitosan [17], algae [18,19], inorganic silicates [20–22], activated carbons [12,23,24], carbon nanotubes [11,25,26] and others.

The blue-green algae *Spirulina platensis* is available in large quantities, as it is widely cultivated worldwide; its annual production is about 2000 tons [27,28]. Its biomass contains a variety of functional groups such as carboxyl, hydroxyl, sulphate, phosphate and other charged groups which can be mediate pollutant binding [29–31]. This microalgae has been successfully employed to remove heavy metals [28–30] and food dyes [31,32] from aqueous solutions. In spite of this, there are no studies currently available on the use of *S. platensis* biomass for the removal of textile dyes. In addition, it is important to compare *S. platensis* with commercial activated carbon (the main adsorbent used in dye removal [23]) in order to verify the potential of its application.

In this work, a comparison of the adsorbents *S. platensis* microalgae (SP) and commercial activated carbon (AC) for the removal of Reactive Red 120 textile dye (RR-120) from aqueous solutions was performed. This dye is widely used for textile dyeing in the Brazilian cloth industry. An alternative kinetic adsorption model was used to study the adsorption of the dye onto the SP and AC adsorbents. The equilibrium isotherms, determination of the thermodynamic parameters and utilisation of the adsorbents to treat a simulated dye-house effluent were performed for both adsorbents.

## 2. Material and methods

### 2.1. Solutions and reagents

The solutions were prepared with deionised water. Reactive Red 120 dye (RR-120) (C.I. 25810; $C_{44}H_{24}Cl_2N_{14}O_{20}S_6Na_6$, 1469.98 g mol$^{-1}$, see Supplementary Fig. 1) was obtained from Sigma–Aldrich (Switzerland) as a commercially available textile dye, with 80% dye content, and was used without further purification. RR-120 has six sulphonate groups. These groups present negative charges even in highly acidic solutions due to their p$K_a$ values being lower than zero [24]. The main characteristic structural features of a typical reactive dye molecule are [33]:

- the reactive system, enabling the dye to form covalent bonds between the dye and the cotton fibre;
- the chromophoric group, contributing to the colour and much to the substantively for cellulose;
- a bridging group that links the reactive system to the chromophore;
- solubilising groups that make the dye soluble in water.

The stock solution (5.00 g L$^{-1}$) was prepared by dissolving the dye in deionised water. The working solutions were obtained by diluting the dye stock solution to the required concentrations. To adjust the pH of the solutions, 0.50 mol L$^{-1}$ sodium hydroxide or hydrochloric acid were used. The pH of the solutions was measured using a Schott Lab 850 set pH meter (Germany).

### 2.2. Adsorbents preparation and characterisation

In this research, *S. platensis* microalgae and commercial activated carbon were employed as adsorbents. The commercial activated carbon (Merck, Germany) with a particle size of <90 μm was used for comparison with *S. platensis*.

*S. platensis* (strain LEB-52) was cultivated in a 450 L open outdoor photo-bioreactor, under uncontrolled conditions, in the south of Brazil. During these cultivations, water was supplemented with 20% Zarrouk synthetic medium [34]. At the end of cultivation, the biomass was recovered by filtration, washed with distilled water and pressed to recover the biomass with a moisture content of 76% (wet basis). The wet biomass (in cylindrical pellet form with a diameter of 3 mm) was dried in perforated trays using perpendicular air flow. The drying conditions were: air temperature 60 °C, air velocity 1.5 m s$^{-1}$, relative humidity between 7% and 10% and load in the tray of 4 kg m$^{-2}$ [35]. The dried biomass was ground by a mill (Wiley Mill Standard, No. 03, USA) and sieved until the discrete particle size ranged from 68 to 75 μm. *S. platensis* was characterised according to the centesimal chemical composition [36] and energy dispersive X-ray spectroscopy (EDS) (Pioneer).

The SP and AC adsorbents were characterised by vibrational spectroscopy in the infrared region with Fourier transform (FTIR) using a Varian spectrometer, model 640-IR. The spectra were obtained with a resolution of 4 cm$^{-1}$ with 100 cumulative scans. The surface analyses and porosity were carried out with a volumetric adsorption analyser (Nova 1000, Quantachrome Instruments) at 77 K. The samples were pre-treated at 473 K for 24 h under a nitrogen atmosphere in order to eliminate the moisture adsorbed on the solid sample surface. The samples were then submitted to 298 K in a vacuum, reaching a residual pressure of $10^{-4}$ Pa. For area and pore calculations, the multi-point BET and BJH [37] methods were used.

### 2.3. Adsorption studies

Batch contact adsorption experiments were carried out in order to evaluate the SP and AC adsorbents for the removal RR-120 dye from aqueous solutions. For these experiments, 50.0 mg of adsorbent were placed in 50 mL cylindrical polypropylene flasks containing 20.0 mL of the dye solutions (50.00–1200.0 mg L$^{-1}$), which were agitated for a suitable period of time (0.0833–6.00 h) using an acclimatised shaker at temperatures ranging from 298 to 323 K. The pH of the dye solutions ranged from 2.0 to 10.0. Subsequently, in order to separate the adsorbent from the aqueous solutions, the contents of the flasks were transferred to centrifuge tubes and then centrifuged at 10,000 rpm for 10 min. Aliquots of 1–10 mL of the supernatant were properly diluted with an aqueous solution fixed at pH 2.0.

The final dye concentration remaining in the liquid phase was determined by visible spectrophotometry at 534 nm. The adsorption capacity and the percentage dye removal were calculated by Eqs. (1) and (2), respectively:

$$q = \frac{(C_0 - C_f)}{X} \quad (1)$$

$$\%\text{Removal} = \frac{(C_0 - C_f)}{C_0} \times 100 \quad (2)$$

where $q$ is the amount of dye adsorbed by the adsorbent (mg g$^{-1}$), $C_0$ is the initial dye concentration (mg L$^{-1}$), $C_f$ is the dye concentration (mg L$^{-1}$) after the batch adsorption procedure and $X$ is the adsorbent dosage (g L$^{-1}$).

Please cite this article in press as: N.F. Cardoso, et al., Comparison of *Spirulina platensis* microalgae and commercial activated carbon as adsorbents for the removal of Reactive Red 120 dye from aqueous effluents, J. Hazard. Mater. (2012), http://dx.doi.org/10.1016/j.jhazmat.2012.09.026

The desorption experiments were carried out as follows: 50.0 mg $L^{-1}$ of RR-120 dye was shaken with 50.0 mg of either SP or AC for 1 h. Then, the loaded adsorbents were filtered through 0.2 μm cellulose acetate, then washed with water to remove the non-adsorbed dye. Then, the dye adsorbed on the adsorbents were agitated in 20.0 mL of an NaCl solution (0.05–0.50 mol $L^{-1}$) an NaOH solution (0.05–0.50 mol $L^{-1}$) or a mixture of NaCl (0.05–0.50 mol $L^{-1}$) + 0.10 mol $L^{-1}$ NaOH for 15–60 min. The desorbed dye was separated and quantified as described above.

### 2.4. Kinetic adsorption models

Please see the Supplementary material [38–41].

### 2.5. Equilibrium models

Please see the Supplementary material [42–44].

### 2.6. Quality assurance and statistical evaluation of the kinetic and isotherm parameters

Please see the Supplementary material [45–49].

### 2.7. Simulated dye-house effluent

Two synthetic dye-house effluents containing four representative reactive dyes and one direct dye used for colouring fibres and their corresponding auxiliary chemicals were prepared at pH 2.0, using a mixture of different dyes most often applied in the textile fibre industry. According to the practical information obtained from a dye-house, typically 10–50% [1] of reactive dyes and 100% of the dye bath auxiliaries remain in the spent dye bath, and its composition undergoes a 5–30-fold dilution during the subsequent washing and rinsing stages [11,50]. The concentrations of the dyes and auxiliary chemicals selected to imitate an exhausted dye bath are given in Supplementary Table 1.

## 3. Results and discussion

### 3.1. S. platensis and commercial activated carbon characterisation

The FTIR spectrum of *S. platensis* (Fig. 1A) shows O—H bond stretching mixed with the $NH_2$ group at 3370 $cm^{-1}$ (intense and broad band) [12,24]. The bands at 2920 and 2859 $cm^{-1}$ are related to asymmetric and symmetric stretching of $CH_2$ groups, respectively [12,24]. Scissor bending of the $NH_2$ group can be observed at 1659 and 1535 $cm^{-1}$ (sharp and intense bands) [27,30]. The bands at 1224, 1149, 1021 $cm^{-1}$ can be assigned to the C—N stretch of amide or amine groups [28,31]. The adsorption bands in the region 750–900 $cm^{-1}$ can be attributed to P—O, S—O and aromatic C—H stretching vibrations [28]. Fig. 1B shows the FTIR vibrational spectra of the commercial activated carbon. The intense absorption band at 3437 $cm^{-1}$ is assigned to O—H bond stretching [12,24]. The two $CH_2$ stretching bands at 2924 and 2854 $cm^{-1}$ are assigned to asymmetric and symmetric stretching of $CH_2$ groups [12,24]. The sharp band at 1736 $cm^{-1}$ is assigned to the carbonyl group of carboxylic acid [12]. The sharp intense peak observed at 1631 $cm^{-1}$ is assigned to aromatic C=C ring stretching [12,24]. In addition, there are several small bands and shoulders in the range of 1460–1250 $cm^{-1}$ that are assigned to ring modes of the aromatic rings [12,24]. The bands at 1160 and 1098 $cm^{-1}$ are assigned to C—O stretching vibrations. Based on these FTIR results, it is expected that the interaction of RR-120 dye with the SP biosorbent should occur with the OH, $NH_2$, C=O and COO groups and at the aromatic group present in the biomass, as previously reported in the literature [12,24,28,31]. In addition,

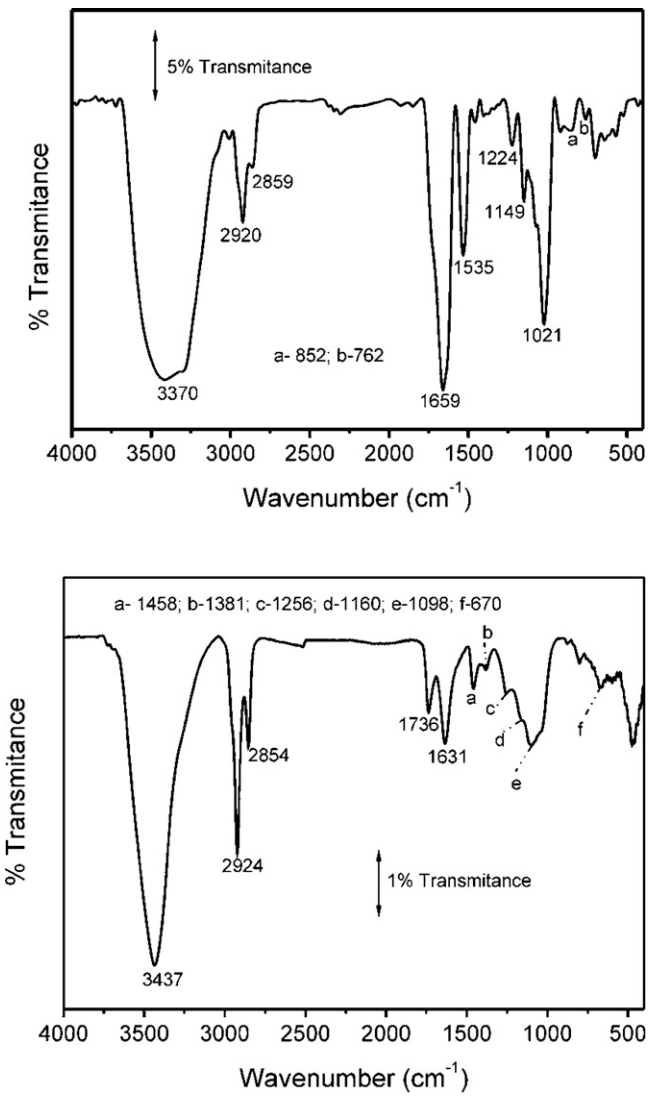


**Fig. 1.** FTIR spectra for: (A) SP; (B) AC.

FTIR spectra were obtained after the adsorption of RR-120 dye on the SP and AC adsorbents. However, the wavenumbers of the vibrational bands were practically the same as seen in the adsorbents without contact with the adsorbate, indicating that the interaction of the dye with the adsorbents presented low energy [24]. This result is consistent with the changes in adsorption enthalpy discussed in Section 3.5.

Supplementary Table 2 shows the proximal and centesimal (obtained from EDS analysis) compositions of *S. platensis* microalgae. As can be seen in Supplementary Table 2, *S. platensis* is composed of a variety of biomolecules, and the major elements on its surface are C, N, O, P and S. The point of zero charge ($pH_{zpc}$) of *S. platensis* microalgae is 7.0, as demonstrated in our recent study [31].

Based on the results of FTIR and EDS analysis, it can be stated that the *S. platensis* adsorbent contains functional groups, such as, carboxyl, hydroxyl, sulphate, phosphate, aldehyde and ketone [27–32]. On the other hand, the commercial activated carbon adsorbent presents OH, COOH and aromatic groups [11,12,23,24]. These chemical groups can mediate the interaction between the RR-120 textile dye and the adsorbent in aqueous solution.

The textural properties of the SP and AC adsorbents are presented in Supplementary Table 3. As expected, the superficial area and total pore volume of the AC adsorbent were much higher

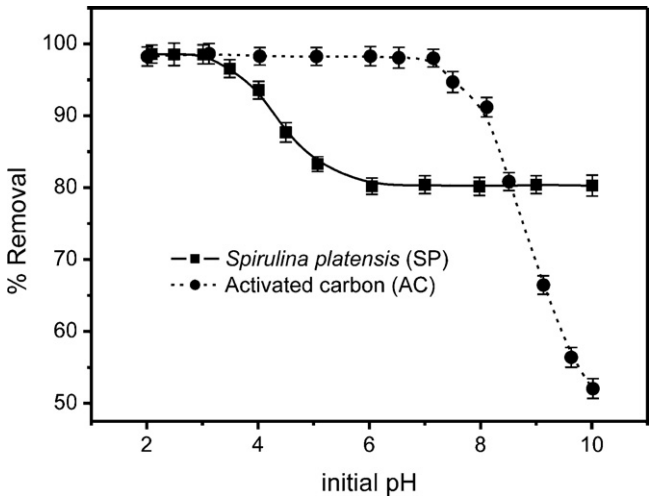


**Fig. 2.** Effect of pH on the adsorption of RR-120 dye on SP and AC adsorbents.

than those of the SP biomass [12]. The activated carbon adsorbent presents several micropore structures that are responsible for its higher superficial area and the greater volume of $N_2$ adsorbed. On the other hand, biomass materials present lower superficial area and lower total pore volume when compared with activated carbons [3,4]. However, biomass adsorbents usually present a larger average pore diameter when compared with activated carbons [3,4,11,12]. This fact could facilitate the accommodation of more dye molecules in the pores of the biomass when compared with activated carbon, as previously reported in the literature [3,4,11,12].

### 3.2. Effects of acidity on adsorption

One of the most important factors that influences the adsorption of a dye on a solid adsorbent is pH [3,4]. Different dyes will present different ranges of suitable pH depending on which adsorbent is used. The effects of initial pH on the percentage of removal of RR-120 dye in solution (50 mg $L^{-1}$) using the SP and AC adsorbents were evaluated within the pH range between 2 and 10 (Fig. 2).

For the SP adsorbent, in the range of pH from 2.0 to 3.0, the percentage of dye removal was practically unchanged. In the range from pH 7.0 to 10.0, the decrease in the percentage of dye removal was only 0.1%, and the percentage of dye removal was also decreased by 18.2% in the range of pH 2.0–10.0. This may have occurred because, under acidic conditions (pH 2.0–3.0), the OH, $NH_2$, C=O and COO groups are protonated [3,4,24]. As consequence, the SP surface was positively charged ($pH_{pzc}$ 7.0). Coupled to this, the RR-120 sulphonate groups (D-$SO_3Na$) were converted to anionic dye ions (D–$SO_3^-$). It should be stated that the RR-120 dye did not present any colour changes in the pH range of 2.0–10.0, since it is a dye that belongs to the reactive dye class. Moreover, RR-120 dye possesses six sulphonate groups that make it readily soluble in water, even in extremely acidic medium, since its $pK_a$ is lower than zero [24]. In this manner, electrostatic attraction occurs between the dye's sulphonate groups and the functional groups on the surface of *S. platensis*.

For the AC adsorbent, the percentage of dye removal decreased by less than 0.1% in the pH interval from 2.0 to 7.0. From pH 7.0 to 10.0, the decrease in the percentage of RR-120 dye removal was 44.3%. These results indicate that the activated carbon could be used within the pH range of 2.0–7.0 without presenting a remarkable difference on the percentage of dye removal, as previously observed in the literature [12,23,24]. On the other hand, the maximum removal of RR-120 dye took place in the pH interval of 2.0–3.0. The decrease

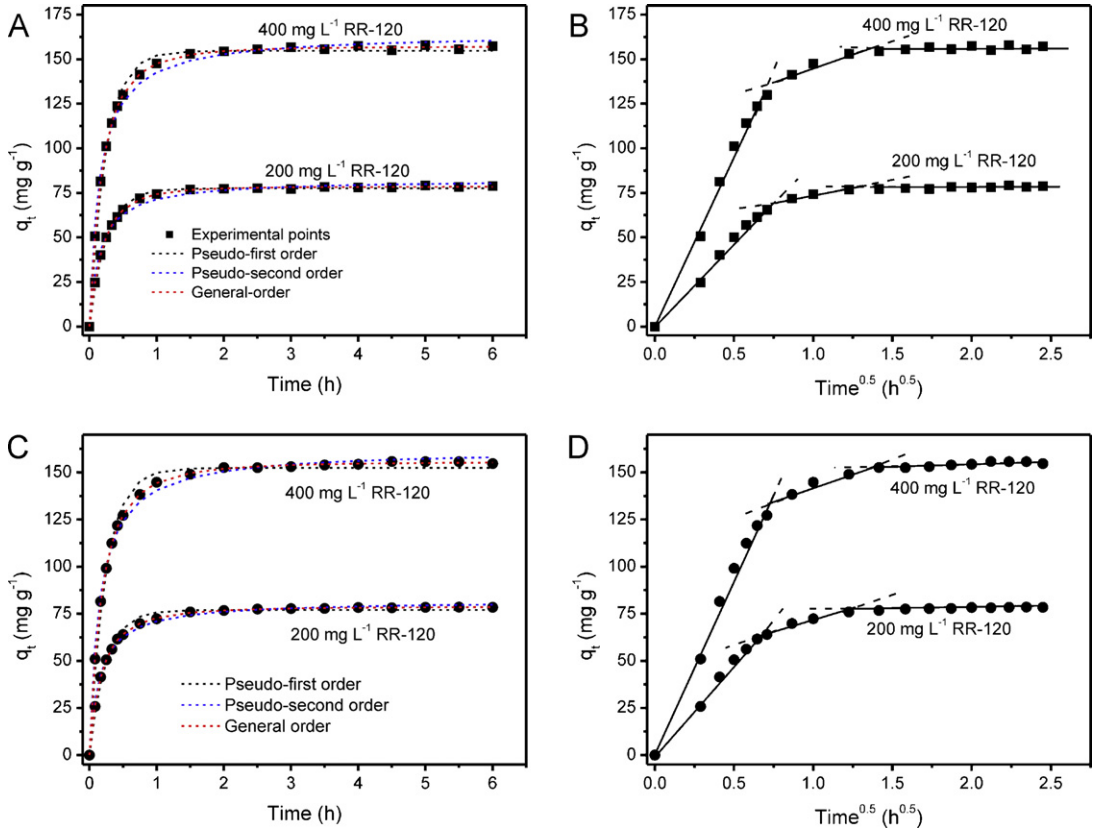


**Fig. 3.** Kinetic adsorption curves for RR-120 uptake at 298 K on SP and AC adsorbents. (A and B) SP; (C and D) AC.

in the percentage of dye removal with an increase in the pH of the dye solution was also previously observed using the alga *Stoechospermum marginatum* with acid orange II dye [19], the adsorption of Reactive Red 120 by the alga *Chara contraria* [51], the removal of Remazol Brilliant Blue R from aqueous solution using the green algae *Scenedesmus quadricauda* immobilised in alginate gel beads [52] and the removal of Lanaset Red G dye from aqueous solution using the alga *C. contraria* [53].

In order to continue this work, the initial pH of the RR-120 dye solution was fixed at pH 2.0 for the SP adsorbent and pH 6.0 for the AC adsorbent.

### 3.3. Kinetic studies

Adsorption kinetic studies are important in the treatment of dye-containing aqueous effluents because they provide valuable information on the mechanism of the adsorption process [50,54].

To evaluate the kinetics of adsorption of RR-120 dye using the SP and AC adsorbents, the non-linear pseudo-first order, pseudo-second order and general order kinetic adsorption models were tested, as shown in Fig. 3. The kinetic parameters for the three kinetic models are listed in Supplementary Table 4. Taking into account that the experimental data were fitted to non-linear kinetic models, an error function ($F_{error}$) was used to evaluate the fitting of the experimental data. A lower $F_{error}$ indicates a smaller difference in the $q$ calculated by the model and the experimentally measured $q$ [21–25,49] (see Supplementary Material, Eq. (20)). It should be pointed out that the $F_{error}$ utilised in this work takes into account the number of fitted parameters (see Supplementary Material, $p$ term of Eq. (20)), since it is reported in the literature [54,55] that the best fit of the results depends on the number of parameters contained in a non-linear equation. For this reason, the number of fitted parameters should be considered in the calculation of $F_{error}$. In addition, the $F_{error}$ values are in agreement with the adjusted $R^2$ values. However $R^2$ values are limited to the range from 0 to 1, so verifying the difference in the experimentally measured $q$ compared to the value of $q$ given by the model is biased [55].

In order to compare the different kinetic models, the $F_{error}$ of each individual model was divided by the $F_{error}$ of the minimum value ($F_{error}$ ratio). It was found that the minimum $F_{error}$ values were obtained with the general order kinetic model. The pseudo-first order kinetic model presented $F_{error}$ ratio values ranging from 3.52 to 4.71 (SP) and 6.34 to 7.33 (AC). Also, for the pseudo-second order model, the $F_{error}$ ratio values ranged from 5.12 to 5.30 (SP) and 4.63 to 4.58 (AC). These results clearly indicate that the general order kinetic model better explains the adsorption process of RR-120 dye using the SP and AC adsorbents.

Taking into account that the general order kinetic equation presents different orders ($n$) when the concentration of the adsorbate is changed (see Supplementary Table 4), it is difficult to compare the kinetic parameters of the model. Therefore, it is useful to use the initial sorption rate $h_0$ [56] to evaluate the kinetics of a given model, using Eq. (3):

$$h_0 = k_n q_e^n \quad (3)$$

where $h_0$ is the initial sorption rate ($mg\,g^{-1}\,h^{-1}$), $k_n$ is the rate constant ($h^{-1}(g\,mg^{-1})^{n-1}$), $q_e$ is the amount adsorbed at equilibrium ($mg\,g^{-1}$) and $n$ is the order of the kinetic model. It should be stressed that when $n=2$, this equation provides the same initial sorption rate first introduced by Ho and McKay [56]. It was observed that the initial sorption rate increased when increasing the initial dye concentration for all kinetic models, as expected, indicating that there is coherence within the experimental data. Taking into account that the kinetic data were better fitted to the general order kinetic model, since the order of an adsorption process should follow the same logic of a chemical reaction where the order is experimentally measured [57] instead of being previously stipulated by a given model, more confident initial sorption rates ($h_0$) were obtained by the general order kinetic model.

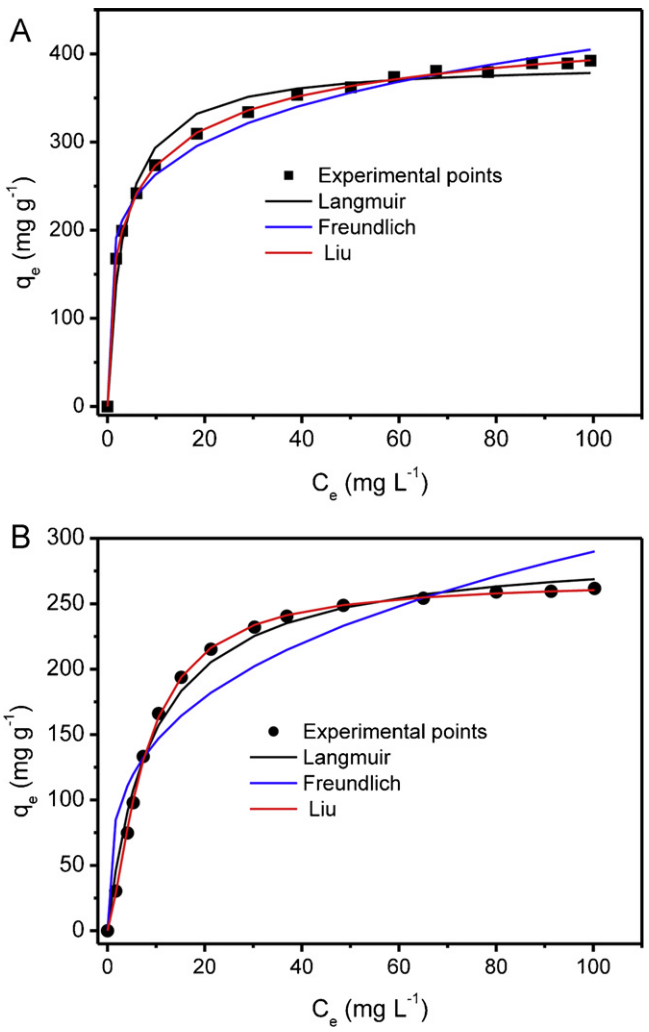


**Fig. 4.** Isotherms of adsorption of RR-120 dye at 298 K. (A) SP; (B) AC.

The intra-particle diffusion model [41] was also used to verify the influence of mass transfer resistance on the binding of RR-120 dye to the SP and AC adsorbents (Supplementary Table 4 and Fig. 3B and D). The intra-particle diffusion constant, $k_{id}$ ($mg\,g^{-1}\,h^{-0.5}$), can be obtained from the slope of the plot of $q_t$ versus the square root of time. These figures show the plots of $q_t$ versus $t^{1/2}$, with three linear sections for the RR-120 dye using the SP and AC adsorbents. These results imply that the adsorption processes involve more than one sorption rate [50]. For both adsorbents, the adsorption process exhibited three stages, which can be attributed to each linear section of the plots in Fig. 3B and D. The first linear section was attributed to the diffusional process of the dye to the adsorbent surface [50]; hence, it was the fastest sorption stage. The second section, ascribed to intra-particle diffusion, was a delayed process [50]. The third stage may be regarded as diffusion through smaller pores, which is followed by the establishment of equilibrium [50].

It was observed in Fig. 4 that the minimum contact time required for RR-120 dye to reach equilibrium with the SP and AC adsorbents was about 2 h for both adsorbents. In order to continue this work, the contact time between the SP and AC adsorbents with RR-120 dye was fixed at 3.0 h using both adsorbents. The increased contact time utilised in this work was used to guarantee

Please cite this article in press as: N.F. Cardoso, et al., Comparison of *Spirulina platensis* microalgae and commercial activated carbon as adsorbents for the removal of Reactive Red 120 dye from aqueous effluents, J. Hazard. Mater. (2012), http://dx.doi.org/10.1016/j.jhazmat.2012.09.026

that RR-120 dye equilibrium would be attained even at higher adsorbate concentrations [11,12].

### 3.4. Equilibrium studies

An adsorption isotherm describes the relationship between the amount of adsorbate adsorbed by the adsorbent ($q_e$) and the adsorbate concentration remaining in the solution after the system attains equilibrium ($C_e$), keeping the temperature of the process constant [15,16]. The adsorption parameters of equilibrium models often provide some insight into the adsorption mechanism, the surface properties and affinity of the adsorbent by the adsorbate. In this study, the Langmuir [42], Freundlich [43] and Liu et al. [44] isotherm models were tested.

The adsorption isotherms were carried out from 298 to 323 K with RR-120 dye on the two adsorbents (SP and AC), and were performed using the best experimental conditions described above (see Supplementary Table 5, and Fig. 4). Fig. 4 shows the adsorption isotherms of RR-120 dye using SP and AC adsorbents at 298 K. Based on the $F_{error}$ (see Supplementary Table 5), the Liu model was the best isotherm model for both adsorbents at all six temperatures studied. The Liu model showed (Supplementary Table 5) the lowest $F_{error}$ values, which means that the q fit by the isotherm model was close to the $q$ measured experimentally.

In order to compare the different equilibrium isotherm models, the $F_{error}$ of each individual model was divided by the $F_{error}$ of minimum value ($F_{error}$ ratio). The Freundlich isotherm presented $F_{error}$ ratio values ranging from 5.50 to 8.82 (SP) and from 13.17 to 23.80 (AC). The Langmuir isotherm model presented $F_{error}$ ratio from 7.01 to 9.01 (SP) and from 4.77 to 12.73 (AC). These results of the $F_{error}$ ratio analysis clearly indicate that the Liu isotherm model best explain the equilibrium of adsorption of RR-120 dye on the SP and AC adsorbents in the temperature range of 298 to 323 K.

The Langmuir isotherm model is based on the following principles [42]: adsorbates are chemically adsorbed at a fixed number of well-defined sites; each site can only hold one adsorbate species; all sites are energetically equivalent; there are no interactions between the adsorbate species. The Freundlich isotherm model assumes that the concentration of the adsorbate on the adsorbent surface increases with the adsorbate concentration. Theoretically, using this expression, an infinite amount of adsorption can occur [43]. The Liu isotherm model is a combination of the Langmuir and Freundlich isotherm models; therefore, the monolayer assumption of Langmuir model is ruled out and the infinite adsorption assumption that originates from the Freundlich model is also discarded. The Liu model [44] predicts that the active sites of the adsorbent cannot present the same energy. Therefore, the adsorbent may present active sites preferred by the adsorbate molecules for occupation [44]; however, saturation of the active sites should occur unlike in the Freundlich isotherm model. Taking into account that the adsorbents presented in this study have different functional groups (see Section 3.1), it is expected that the activate sites of the adsorbent will not have the same energy.

The maximum amount of the RR-120 dye adsorbed ($Q_{max}$ = 482.2 mg g$^{-1}$) by the SP adsorbent was higher than the maximum amount by the adsorbed commercial activated carbon ($Q_{max}$ = 267.2 mg g$^{-1}$). This may be attributed to a higher number of activated sites available in the microalgae when compared with the activated carbon. In the FTIR results (see Fig. 1), it can be noted that the amount of organic functional groups in SP (Fig. 1A) is greater than the residual organic groups present in the AC adsorbent (Fig. 1B). In addition, it was possible to verify that SP possessed protein (65.7%), lipids (7%) and carbohydrates (11.3%); see Supplementary Table 2.

When compared with other adsorbents presented in the literature [3,4,11,13,15,16,20,21,26,32] (see detailed a comparison in Supplementary Table 6), SP presented satisfactory adsorption capacity, and can be alternatively considered for the removal of reactive dyes from aqueous effluents.

### 3.5. Thermodynamics of adsorption

As reported in the literature [11,12,24,25,29,31], the thermodynamic parameters related to the adsorption process, i.e. changes in Gibb's free energy ($\Delta G$, kJ mol$^{-1}$), enthalpy ($\Delta H^\circ$, kJ mol$^{-1}$) and entropy ($\Delta S^\circ$, J mol$^{-1}$ K$^{-1}$) can be estimated by the following equations:

$$\Delta G^\circ = \Delta H^\circ - T\Delta S^\circ \quad (4)$$

$$\Delta G^\circ = -RT\ \ln(K) \quad (5)$$

The combination of Eqs. (4) and (5), gives:

$$ln(K) = \frac{\Delta S^\circ}{R} - \frac{\Delta H^\circ}{R} \times \frac{1}{T} \quad (6)$$

where $R$ is the universal gas constant (8.314 J K$^{-1}$ mol$^{-1}$), $T$ is the absolute temperature (Kelvin) and $K$ represents the equilibrium adsorption constants of the fitted isotherm. It has been reported in the literature that different adsorption equilibrium constants ($K$) are obtained with different isotherm models [11,12,23,24,26,39,50,58–61]. The thermodynamic parameters of adsorption can be estimated from $K_g$ (the *Liu* equilibrium constant), as previously reported in the literature [11,26]. The values of $\Delta H^\circ$ and $\Delta S^\circ$ can be calculated from the slope and intercept of the linear plot of ln ($K$) versus 1/$T$.

The thermodynamic results are shown in Supplementary Table 7. The $R^2$ values of the linear fit were at least 0.99, indicating that the values of enthalpy and entropy calculated for both adsorbents were confident. In addition, the magnitude of enthalpy was consistent with physical sorption for both adsorbents [62]. The type of interaction can be classified, to a certain extent, by the magnitude of the change in enthalpy. Physical sorption such as hydrogen bonding usually proves values <30 kJ mol$^{-1}$ [62]. Other physical sorption mechanisms such as van der Waals forces are usually 4–10 kJ mol$^{-1}$, hydrophobic bond forces about 5 kJ mol$^{-1}$, coordination exchange about 40 kJ mol$^{-1}$ and dipole bond forces 2–29 kJ mol$^{-1}$ [63]. On the other hand, chemical bond forces are usually >80 kJ mol$^{-1}$ [63]. The values of adsorption ($\Delta H^\circ$) obtained in this study (<20 kJ mol$^{-1}$) are consistent with hydrogen bond and dipole bond forces for both adsorbents.

Enthalpy changes ($\Delta H^\circ$) indicate that adsorption followed an exothermic process. Negative values of $\Delta G$ indicate that RR-120 dye adsorption by the SP and AC adsorbents was a spontaneous and favourable process at all the studied temperatures. The positive values of $\Delta S^\circ$ confirmed a high preference of RR-120 molecules for the surface of the SP and AC adsorbents, and also suggested the possibility of some structural changes or readjustments in the dye-carbon adsorption complex occurring during the adsorption process [64].

### 3.6. Treatment of a simulated dye-house effluent

In order to verify the efficiency of SP and AC as adsorbents for the removal of dyes from textile effluents, two simulated dye-house effluents were prepared (see Supplementary Table 1) with different contents of dyes. The UV–vis spectra of the untreated effluents and effluents treated with SP and AC were recorded from 350 to 800 nm (Fig. 5). The area under the absorption bands from 350 to 800 nm were utilised to monitor the percentage of the dye mixture removed from the simulated dye effluents. The SP adsorbent removed 94.4 and 99.0% (Fig. 5) and the AC adsorbent removed 93.6 and 97.7% (Fig. 5) of the dye mixture in effluents A and B,

Please cite this article in press as: N.F. Cardoso, et al., Comparison of *Spirulina platensis* microalgae and commercial activated carbon as adsorbents for the removal of Reactive Red 120 dye from aqueous effluents, J. Hazard. Mater. (2012), http://dx.doi.org/10.1016/j.jhazmat.2012.09.026

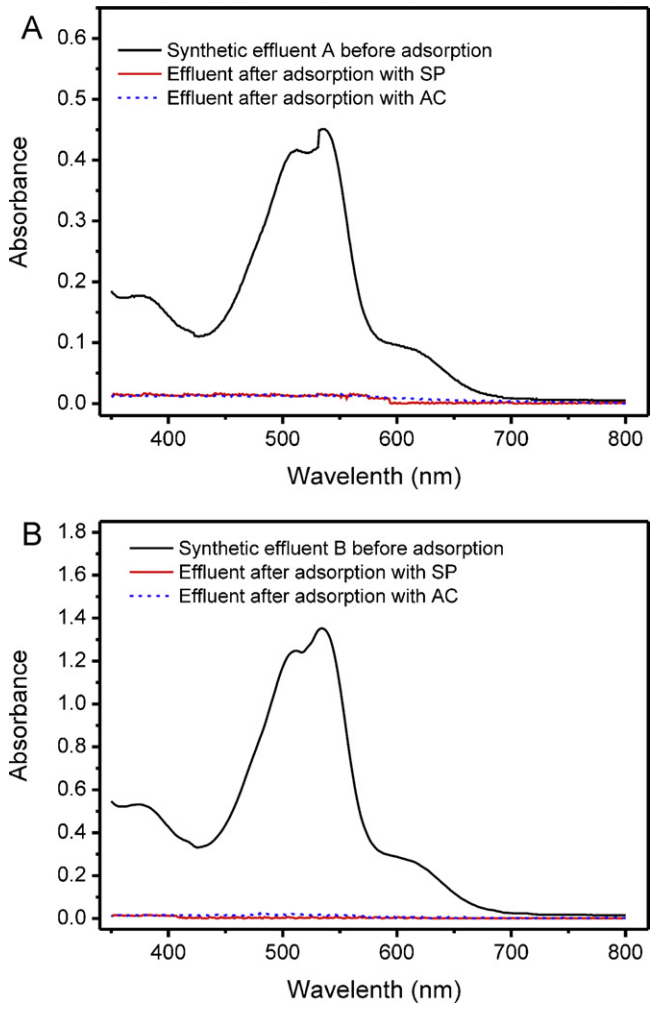


**Fig. 5.** UV–vis spectra of simulated dye effluents before and after adsorption treatment with SP and AC. For composition of effluents, see Supplementary Table 1.

respectively. The efficiency of the SP adsorbent for treating a simulated dye-house effluent presented slightly better performance when compared with the AC adsorbent. This result is in agreement with the previous results obtained in this study (please see Section 3.4). However, although the AC adsorbent presented slightly lower performance for treating a simulated dye-house effluent, it can be used as well as SP for real textile wastewater treatment (see Fig. 5). Based on these simulated effluent data, it is possible to infer that both the SP and AC adsorbents present good efficiency for the treatment of real wastewater effluents.

### 3.7. Desorption experiments

In order to evaluate the reuse of the SP and AC adsorbents, desorption experiments were carried out. Several eluents such as NaCl solutions (0.05–0.50 mol $L^{-1}$), NaOH solutions (0.05–0.50 mol $L^{-1}$) and a mixture of NaCl (0.05–0.50 mol $L^{-1}$) + 0.50 mol $L^{-1}$ NaOH were tested for the regeneration of the loaded adsorbent (see Supplementary Table 8). For SP, it should be mentioned that 0.30–0.50 mol $L^{-1}$ NaOH immediately desorbed the dye taken up by the adsorbent. On the other hand, the recoveries of the adsorbent by aqueous NaCl at different concentrations as the regenerating solution did not occur efficiently even after 1 h of agitation (recoveries < 3%). The mixture containing NaCl (0.05–0.50 mol $L^{-1}$) + 0.10 mol $L^{-1}$ NaOH presented fairly good desorption of the dye from SP (recoveries 70.15–74.36%). The best elution efficiency was obtained with 0.50 mol $L^{-1}$ NaOH. This result confirms the thermodynamic parameters presented in Section 3.5 and the pH studies described above. RR-120 dye at pH 2.0 is electrostatically attracted to SP. This interaction was inhibited by the NaOH solution. For the AC adsorbent, the elution efficiency was lower than 13% for all the eluents tested, indicating that activated carbons could not be reutilised for adsorption purposes. On the other hand, SP eluted with 0.50 mol $L^{-1}$ NaOH was reutilised for the adsorption of RR-120 dye, attaining a sorption efficiency of about 93% in the second cycle, 90% in the third cycle and 88% in the fourth cycle of adsorption/desorption when compared with the first cycle of adsorption/desorption. Therefore, the use of SP for dye adsorption could be economically viable since regeneration of the adsorbent is feasible.

## 4. Conclusions

*S. platensis* and activated carbon were good adsorbents for the removal of Reactive Red 120 (RR-120) textile dye from aqueous solutions. The adsorbent materials were characterised by FTIR spectroscopy, SEM and $N_2$ adsorption/desorption curves.

The most appropriate conditions were established with respect to pH and contact time to saturate the available sites located on the adsorbent surface. Four kinetic models were used to adjust the adsorption, and the best fit was the general order kinetic model. The equilibrium isotherm of the RR-120 dye was obtained, and these data fit best to the Liu isotherm model. The maximum adsorption capacities were 482.2 and 267.2 mg $g^{-1}$ for SP and AC, respectively. The thermodynamic parameters of adsorption ($\Delta H^{\circ}$, $\Delta S^{\circ}$ and $\Delta G$) were calculated. The magnitude of the enthalpy of adsorption was compatible with a physical interaction of the RR-120 dye with both the SP and AC adsorbents. For the treatment of simulated industrial textile effluents, the SP and AC adsorbents presented good performance, removing 97.1 and 96.5%, respectively, of a dye mixture in media containing high saline concentrations.

## Acknowledgements

The authors are grateful to CNPq, and to FAPERGS for financial support and fellowships.

## Appendix A. Supplementary data

Supplementary data associated with this article can be found, in the online version, at http://dx.doi.org/10.1016/j.jhazmat.2012.09.026.

## References

[1] C. Hessel, C. Allegre, M. Maisseu, F. Charbit, P. Moulin, Guidelines and legislation for dye house effluents, J. Environ. Manage. 83 (2007) 171–180.
[2] C. Allègre, P. Moulin, M. Maisseu, F. Charbit, Treatment and reuse of reactive dyeing effluents, J. Membr. Sci. 269 (2006) 15–34.
[3] N.F. Cardoso, E.C. Lima, I.S. Pinto, C.V. Amavisca, B. Royer, R.B. Pinto, W.S. Alencar, S.F.P. Pereira, Application of cupuassu shell as biosorbent for the removal of textile dyes from aqueous solution, J. Environ. Manage. 92 (2011) 1237–1247.
[4] N.F. Cardoso, E.C. Lima, T. Calvete, I.S. Pinto, C.V. Amavisca, T.H.M. Fernandes, R.B. Pinto, W.S. Alencar, Application of aqai stalks as biosorbents for the removal of the dyes Reactive Black 5 and Reactive Orange 16 from aqueous solution, J. Chem. Eng. Data 56 (2011) 1857–1868.
[5] D.S. Brookstein, Factors associated with textile pattern dermatitis caused by contact allergy to dyes, finishes, foams, and preservatives, Dermatol. Clin. 27 (2009) 309–322.
[6] P.A. Carneiro, G.A. Umbuzeiro, D.P. Oliveira, M.V.B. Zanoni, Assessment of water contamination caused by a mutagenic textile effluent/dyehouse effluent bearing disperse dyes, J. Hazard. Mater. 174 (2010) 694–699.
[7] R.O.A. de Lima, A.P. Bazo, D.M.F. Salvadori, C.M. Rech, D.P. Oliveira, G.A. Umbuzeiro, Mutagenic and carcinogenic potential of a textile azo dye

processing plant effluent that impacts a drinking water source, Mutat. Res Genet. Toxicol. Environ. Mutagen. 626 (2007) 53–60.
[8] A. Srinivasan, T. Viraraghavan, Decolorization of dye wastewaters by biosorbents: a review, J. Environ. Manage. 91 (2010) 1915–1929.
[9] Z. Eren, Ultrasound as a basic and auxiliary process for dye remediation: a review, J. Environ. Manage. 104 (2012) 127–141.
[10] E. Hosseini Koupaie, M.R. Alavi Moghaddam, S.H. Hashemi, Investigation of decolorization kinetics and biodegradation of azo dye Acid Red 18 using sequential process of anaerobic sequencing batch reactor/moving bed sequencing batch biofilm reactor, Int. Biodeter. Biodegr. 71 (2012) 43–49.
[11] F.M. Machado, C.P. Bergmann, T.H.M. Fernandes, E.C. Lima, B. Royer, T. Calvete, S.B. Fagan, Adsorption of Reactive Red M-2BE dye from water solutions by multi-walled carbon nanotubes and activated carbon, J. Hazard. Mater. 192 (2011) 1122–1131.
[12] N.F. Cardoso, R.B. Pinto, E.C. Lima, T. Calvete, C.V. Amavisca, B. Royer, M.L. Cunha, T.H.M. Fernandes, I.S. Pinto, Removal of remazol black B textile dye from aqueous solution by adsorption, Desalination 269 (2011) 92–103.
[13] R.M.C. Somasekhara, L. Sivaramakrishna, R.A. Varada, The use of an agricultural waste material, Jujuba seeds for the removal of anionic dye (Congo red) from aqueous medium, J. Hazard. Mater. 203 (2012) 118–127.
[14] A.M.M. Vargas, A.L. Cazetta, A.C. Martins, J.C.G. Moraes, E.E. Garcia, G.F. Gauze, W.F. Costa, V.C. Almeida, Kinetic and equilibrium studies: adsorption of food dyes Acid Yellow 6 Acid Yellow 23, and Acid Red 18 on activated carbon from flamboyant pods, Chem. Eng. J. 181 (2012) 243–250.
[15] B. Royer, N.F. Cardoso, E.C. Lima, J.C.P. Vaghetti, N.M. Simon, T. Calvete, R.C. Veses, Applications of brazilian-pine fruit shell in natural and carbonized forms as adsorbents to removal of methylene blue from aqueous solutions – kinetic and equilibrium study, J. Hazard. Mater. 164 (2009) 1213–1222.
[16] L.G. da Silva, R. Ruggiero, P.M. Gontijo, R.B. Pinto, B. Royer, E.C. Lima, T.H.M. Fernandes, T. Calvete, Adsorption of Brilliant Red 2BE dye from water solutions by a chemically modified sugarcane bagasse lignin, Chem. Eng. J. 168 (2011) 620–628.
[17] J.S. Piccin, G.L. Dotto, M.L.G. Vieira, L.A.A. Pinto, Kinetics, Mechanism of the Food Dye FD&C Red 40 Adsorption onto Chitosan, J. Chem. Eng Data 56 (2011) 3759–3765.
[18] M. Kousha, E. Daneshvar, M.S. Sohrabi, M. Jokar, A. Bhatnagar, Adsorption of acid orange II dye by raw and chemically modified brown macroalga *Stoechospermum marginatum*, Chem. Eng. J. 192 (2012) 67–76.
[19] Ç. Doğar, A. Gürses, M. Açıkyıldız, E. Özkan, Thermodynamics and kinetic studies of biosorption of a basic dye from aqueous solution using green algae Ulothrix sp, Colloid Surf. B 76 (2010) 279–285.
[20] B. Royer, N.F. Cardoso, E.C. Lima, V.S.O. Ruiz, T.R. Macedo, C. Airoldi, Organofunctionalized kenyaite for dye removal from aqueous solution, J.Colloid Interface Sci. 336 (2009) 398–405.
[21] B. Royer, N.F. Cardoso, E.C. Lima, T.R. Macedo, C. Airoldi, A useful organofunctionalized layered silicate for textile dye removal, J. Hazard. Mater. 181 (2010) 366–374.
[22] E.W. de Menezes, E.C. Lima, B. Royer, F.E. de Souza, B.D. dos Santos, J.R. Gregório, T.M.H. Costa, Y. Gushikem, E.V. Benvenutti, Ionic silica based hybrid material containing the pyridinium group used as adsorbent for textile dye, J.Colloid Interface Sci. 378 (2012) 10–20.
[23] T. Calvete, E.C. Lima, N.F. Cardoso, J.C.P. Vaghetti, S.L.P. Dias, F.A. Pavan, Application of carbon adsorbents prepared from Brazilian-pine fruit shell for the removal of reactive orange 16 from aqueous solution– kinetic, equilibrium, and thermodynamic studies, J. Environ. Manage. 91 (2010) 1695–1706.
[24] T. Calvete, E.C. Lima, N.F. Cardoso, S.L.P. Dias, F.A. Pavan, Application of carbon adsorbents prepared from the Brazilian-pine fruit shell for removal of Procion Red MX 3B from aqueous solution – kinetic, equilibrium, and thermodynamic studies, Chem. Eng. J. 155 (2009) 627–636.
[25] S. Chatterjee, T. Chatterjee, S.R. Lim, S.H. Woo, Effect of the addition mode of carbon nanotubes for the production of chitosan hydrogel core–shell beads on adsorption of Congo red from aqueous solution, Bioresour. Technol. 102 (2011) 4402–4409.
[26] F.M. Machado, C.P. Bergmann, E.C. Lima, B. Royer, F.E. de Souza, I.M. Jauris, T. Calvete, S.B. Fagan, Adsorption of Reactive Blue 4 dye from water solutions by carbon nanotubes: experiment and theory, Phys. Chem. Chem. Phys. 14 (2012) 11139–11153.
[27] M. A.Çelekli, M. Yavuzatmaca, Predictive modeling of biomass production by *Spirulina platensis* as function of nitrate and NaCl concentrations, Bioresour. Technol. 100 (2009) 1847–1851.
[28] A. Çelekli, M. Yavuzatmaca, H. Bozkurt, An eco-friendly process: predictive modeling of copper adsorption from aqueous solution on *Spirulina platensis*, J. Hazard. Mater. 173 (2010) 123–129.
[29] A. Seker, T. Shahwan, A. Eroglu, S. Yilmaz, Z. Demirel, M. Dalay, Equilibrium thermodynamic and kinetic studies for the biosorption of aqueous lead(II), cadmium(II) and nickel(II) ions on *Spirulina platensis*, J. Hazard. Mater. 154 (2008) 973–980.
[30] A. Çelekli, H. Bozkurt, Biosorption of cadmium and nickel ions using *Spirulina platensis* – kinetic and equilibrium studies, Desalination 275 (2011) 141–147.
[31] G.L. Dotto, E.C. Lima, L.A.A. Pinto, Biosorption of food dyes onto *Spirulina platensis* nanoparticles: equilibrium isotherm and thermodynamic analysis, Bioresour. Technol. 103 (2012) 123–130.
[32] G.L. Dotto, V.M. Esquerdo, M.L.G. Vieira, L.A.A. Pinto, Optimization, kinetic analysis of food dyes biosorption by *Spirulina platensis*, Colloids Surf. B: Biointerfaces 91 (2012) 234–241.
[33] E. Matyjas, E. Rybicki, Novel reactive red dyes, AUTEX Res. J. 3 (2003) 90–95.
[34] J.A.V. Costa, L.M. Colla, P.F.F. Duarte, Improving *Spirulina platensis* biomass yield using a fed-batch process, Bioresour. Technol. 92 (2004) 237–241.
[35] E.G. Oliveira, G.S. Rosa, M.A. Moraes, L.A.A. Pinto, Characterization of thin layer drying of *Spirulina platensis* utilizing perpendicular air flow, Bioresour. Technol. 100 (2009) 1297–1303.
[36] AOAC, Official Methods of Analysis, AOAC, Washington, DC, 1995.
[37] J.C.P. Vaghetti, M. Zat, K.R.S. Bentes, L.S. Ferreira, E.V. Benvenutti, E.C. Lima, 4-Phenylenediaminepropylsilica xerogel as a sorbent for copper determination in waters by slurry-sampling ETAAS, J. Anal. Atom. Spectrom. 18 (2003) 376–380.
[38] Y. Liu, L. Shen, A general rate law equation for biosorption, Biochem. Eng. J. 38 (2008) 390–394.
[39] Y. Liu, Y.J. Liu, Review– biosorption isotherms, kinetics and thermodynamics, Sep. Purif. Technol. 61 (2008) 229–242.
[40] Y.S. Ho, Review of second-order models for adsorption systems, J. Hazard. Mater. 136 (2006) 681–689.
[41] W.J. Weber-Jr., J.C. Morris, Kinetics of adsorption on carbon from solution, J. Sanit. Eng. Div. Am. Soc. Civil Eng. 89 (1963) 31–59.
[42] I. Langmuir, The adsorption of gases on plane surfaces of glass, mica and platinum, J. Am. Chem. Soc. 40 (1918) 1361–1403.
[43] H. Freundlich, Adsorption in solution, Phys. Chem. Soc. 40 (1906) 1361–1368.
[44] Y. Liu, H. Xu, S.F. Yang, J.H. Tay, A general model for biosorption of $Cd^{2+}$, $Cu^{2+}$ and $Zn^{2+}$ by aerobic granules, J. Biotechnol. 102 (2003) 233–239.
[45] F. Barbosa-Jr., F.J. Krug, E.C. Lima, On-line coupling of electrochemical preconcentration in tungsten coil electrothermal atomic absorption spectrometry for determination of lead in natural waters, Spectrochim. Acta B 54 (1999) 1155–1166.
[46] E.C. Lima, F.J. Krug, J.A. Nobrega, A.R.A. Nogueira, Determination of ytterbium in animal faeces by tungsten coil electrothermal atomic absorption spectrometry, Talanta 47 (1998) 613–623.
[47] E.C. Lima, P.G. Fenga, J.R. Romero, W.F. de Giovani, Electrochemical behaviour of $[Ru(4,4'\text{-}Me_2bpy)_2(PPh_3)(H_2O)](ClO_4)_2$ in homogeneous solution and incorporated into carbon paste electrodes:application to oxidation of benzylic compounds, Polyhedron 17 (1998) 313–318.
[48] E.C. Lima, J.L. Brasil, A.H.D.P. Santos, Evaluation of Rh, Ir, Ru, W-Rh, W-Ir, and W-Ru as Permanent Modifiers for the determination of Lead in Ashes, Coals, Sediments, Sludges, Soils, and Freshwaters by Electrothermal Atomic Absorption Spectrometry, Anal. Chim. Acta 484 (2003) 233–242.
[49] R.C. Jacques, E.C. Lima, S.L.P. Dias, A.C. Mazzocato, F.A. Pavan, Yellow passionfruit shell as biosorbent to remove Cr(III) and Pb(II) from aqueous solution, Sep. Purif. Technol. 57 (2007) 193–198.
[50] W.S. Alencar, E.C. Lima, B. Royer, B.D. dos Santos, T. Calvete, E.A. da Silva, C.N. Alves, Application of aqai stalks as biosorbents for the removal of the dye Procion Blue MX-R from aqueous solution, Sep. Sci. Technol. 47 (2012) 513–526.
[51] A. Çelekli, G. Ilgün, H. Bozkurt, Sorption equilibrium, kinetic, thermodynamic, and desorption studies of Reactive Red 120 on Chara contraria, Chem. Eng. J. 191 (2012) 228–235.
[52] A. Ergene, K. Ada, S. Tan, H. Katırcıoğlu, Removal of Remazol Brilliant Blue R dye from aqueous solutions by adsorption onto immobilized Scenedesmus quadricauda– equilibrium and kinetic modeling studies, Desalination 249 (2009) 1308–1314.
[53] A. Çelekli, B. Tanrıverdia, H. Bozkurtb, Predictive modeling of removal of Lanaset Red G on Chara contraria; kinetic, equilibrium, and thermodynamic studies, Chem. Eng. J. 169 (2011) 166–172.
[54] M.I. El-Khaiary, G.F. Malash, Y.S. Ho, On the use of linearized pseudo-second-order kinetic equations for modeling adsorption systems, Desalination 257 (2010) 93–101.
[55] M.I. El-Khaiary, G.F. Malash, Common data analysis errors in batch adsorption studies, Hydrometallurgy 105 (2011) 314–320.
[56] Y.S. Ho, G. Mckay, Sorption of dye from aqueous solution by peat, Chem. Eng. J. 70 (1988) 115–124.
[57] R. Chang, General Chemistry: The Essential Concepts, 6th ed, McGraw-Hill, New York, 2011.
[58] Y. Wang, X.J. Wang, M. Liu, X. Wang, Z. Wu, L.Z. Yang, S.Q. Xia, J.F. Zhao, Cr(VI) removal from water using cobalt-coated bamboo charcoal prepared with microwave heating, Ind. Crops Prod. 39 (2012) 81–88.
[59] W. Zhang, H. Li, X. Kan, L. Dong, H. Yan, Z. Jiang, H. Yang, A. Li, R. Cheng, Adsorption of anionic dyes from aqueous solutions using chemically modified straw, Bioresour. Technol. 117 (2012) 40–47.
[60] V.K. Gupta, B. Gupta, A. Rastogi, S. Agarwal, A. Nayak, A comparative investigation on adsorption performances of mesoporous activated carbon prepared from waste rubber tire and activated carbon for a hazardous azo dye-Acid Blue 113, J. Hazard. Mater. 186 (2011) 891–901.
[61] S.S. Vieira, Z.M. Magriotis, N.A.V. Santos, M.D. Cardoso, A.A. Saczk, Macauba palm (*Acrocomia aculeata*) cake from biodiesel processing: an efficient and low cost substrate for the adsorption of dyes, Chem. Eng. J. 183 (2012) 152–161.
[62] C.L. Sun, C.S. Wang, Estimation on the intramolecular hydrogen-bonding energies in proteins and peptides by the analytic potential energy function, J. Mol. Struct. 956 (2010) 38–43.
[63] B.V. Oepen, W. Kordel, W. Klein, Sorption of nonpolar and polar compounds to soils: processes, measurement and experience with the applicability of the modified OECD-guideline, Chemosphere 22 (1991) 285–304.
[64] D.D. Asouhidou, K.S. Triantafyllidis, N.K. Lazaridis, K.A. Matis, S.S. Kim, T.J. Pinnavaia, Sorption of reactive dyes from aqueous solutions by ordered hexagonal and disordered mesoporous carbons, Microporous Mesoporous Mater. 117 (2009) 257–267.

Please cite this article in press as: N.F. Cardoso, et al., Comparison of *Spirulina platensis* microalgae and commercial activated carbon as adsorbents for the removal of Reactive Red 120 dye from aqueous effluents, J. Hazard. Mater. (2012), http://dx.doi.org/10.1016/j.jhazmat.2012.09.026

**Supplementary Material**

*2.4. Kinetic adsorption models*

As reported previously [38,39], in the sense of a chemical reaction or process, a rate law's exponents are generally unrelated to the chemical equation's coefficients, but they sometimes are the same by coincidence. This means that there is no way to predict the reaction order without experimental data. In order to establish a general rate law equation for adsorption, the adsorption process on the surface of adsorbent is assumed to be rate controlling step. In this case, attention is turned from adsorbate concentration in bulk solution to change in the effective number of adsorption sites at the surface of adsorbent during adsorption. If the reaction rate law is applied to Eq. 1, following rate expression for adsorption can be obtained:

$$\frac{dq}{dt}=k_N\left(q_e\text{-}q_t\right)^n \tag{1}$$

in which $k_N$ is the rate constant and n is the adsorption reaction order with regard to the effective concentration of the adsorption sites available on the surface of adsorbent, $q_e$ is the amount adsorbed at the equilibrium and $q_t$ is the amount adsorbed at any time. Eq. 1 is the result of application of the universal rate law to an adsorption process, and can be used without any further assumption [38,39]. Theoretically, the exponent n in Eq. 1 can be integral or rational non-integral numbers [38,39].

The effective number of the available adsorption sites ($\theta_t$) on the adsorbent surface is defined by following equation:

$$\theta_t = 1 - \frac{q_t}{q_e} \quad (2)$$

By definition of *k*:

$$k = k_N (q_e)^{n-1} \quad (3)$$

The Eq.4 describes the rate of adsorption in function of variable ($\theta_t$).

$$\frac{d\theta_t}{dt} = -k.\theta_t^{\,n} \quad (4)$$

Where:

For a virgin adsorbent $\theta_t$ equals 1, and it tends to decrease during adsorption. When adsorption process reaches its equilibrium, $\theta_t$ tends to a fixed value. If the saturation of the adsorbent occurs, $\theta_t$ would become zero.

Making the integration of Eq. 4,

$$\int_1^{\theta} \frac{d\theta_t}{\theta_t^{\,n}} = -k \int_0^t dt \quad (5)$$

It leads to:

$$\frac{1}{1-n}.\left[\theta_t^{\,1-n} - 1\right] = -k.t \quad (6)$$

This results in:

$$\theta_t = \left[1 - k.(1-n).t\right]^{1/(1-n)} \quad (7)$$

Applying the Eq 2 and Eq. 3 on Eq.7, it is obtained:

$$q_t = q_e - \frac{q_e}{\left[k_N (q_e)^{n-1}.t.(n-1)+1\right]^{1/(n-1)}} \quad (8)$$

Eq. 8 is the General kinetic adsorption equation that is valid for n≠1.

The pseudo-first order kinetic model is a special case of Eq. 4, when n=1 [38,39].

$$\frac{d\theta_t}{dt} = -k.\theta_t^{\,1} \quad (9)$$

Integrating Eq. 9 , it gives:

$$\theta_t = exp(-k.t) \quad (10)$$

Substituting Eq. 2 and Eq.3 on Eq. 10, it is obtained the pseudo-first order kinetic model

$$q_t = q_e\left[1-exp(-k_1.t)\right] \quad (11)$$

Therefore, the pseudo-first order kinetic equation is a special case of general kinetic adsorption.

The pseudo-second order kinetic model [40] is a special case of Eq. 8 (General order kinetic equation), when *n*=2. Therefore:

$$q_t = q_e - \frac{q_e}{\left[k_2 (q_e).t+1\right]} \quad (12)$$

Rearranging this equation it leads to:

$$q_t = \frac{q_e^2 k_2 t}{\left[k_2(q_e).t+1\right]} \quad (13)$$

The Intra-particle diffusion equation was early defined [41] as:

$$q_t = k_{id}.\sqrt{t} + C \quad (14)$$

Where $k_{id}$ is the intra-particle diffusion rate constant (mg $g^{-1}$ $h^{-0.5}$); C is a constant related with the thickness of boundary layer (mg $g^{-1}$).

In this work the pseudo-first order (Eq. 11), pseudo-second order (Eq.13), general order equation (Eq. 8) and intra-particle diffusion (Eq. 14) models were utilized for evaluation of the dye adsorption kinetics.

*2.5. Equilibrium models*

The adsorption equilibrium was evaluated by using the following isotherm models.

*Langmuir Isotherm model* [42]:

$$q_e = \frac{Q_{max}.K_L.C_e}{1+K_L.C_e} \quad (15)$$

Where $q_e$ is amount adsorbate adsorbed at the equilibrium (mg $g^{-1}$); $Q_{max}$ is the maximum adsorption capacity of the adsorbent (mg $g^{-1}$); $K_L$ is the Langmuir equilibrium constant (L $mg^{-1}$); $C_e$ is dye concentration at the equilibrium (mg $L^{-1}$).

*Freundlich isotherm model* [43]:

$$q_e = K_F . C_e^{1/nF} \quad (16)$$

Where $K_F$ is the Freundlich equilibrium constant [mg $g^{-1}$ (mg $L^{-1}$)$^{-1/nF}$]; $n_F$ is dimensionless exponent of the Freundlich equation.

*Liu isotherm model* [44]:

$$q_e = \frac{Q_{max.}(K_g . C_e)^{n_L}}{1 + (K_g . C_e)^{n_L}} \quad (17)$$

Where $K_g$ is the Liu equilibrium constant (L $mg^{-1}$); $n_L$ is dimensionless exponent of the Liu equation, $Q_{max}$ is the maximum adsorption capacity of the adsorbent (mg $g^{-1}$).

*2.6. Quality assurance and statistical evaluation of the kinetic and isotherm parameters*

To establish the accuracy, reliability and reproducibility of the collected data, all the batch adsorption measurements were performed in triplicate. Blanks were run in parallel and they were corrected when necessary [45].

All dye solutions were stored in glass flasks, which were cleaned by soaking in 1.4 mol $L^{-1}$ $HNO_3$ for 24 h [46], rinsing five times with de-ionized water, dried, and stored in a flow hood.

For analytical calibration, standard solutions with concentrations ranging from (5.00 to 150.0) mg $L^{-1}$ of the dyes were employed, running against a blank solution of water adjusted to pH 2.0. The linear analytical calibration of the curve was furnished by the UVWin software of the T90+ PG Instruments spectrophotometer (England). The detection limit of the method, obtained with a signal/noise ratio of 3 [47], was 0.20 mg $L^{-1}$ of RR-120. All the analytical measurements were performed in triplicate, and the precision of the standards was better than 3 % (n=3). For checking the accuracy of the RR-120 dye sample solutions during the

spectrophotometric measurements, standards containing dyes at 50.0 mg $L^{-1}$ were employed as a quality control every five determinations [48].

The kinetic and equilibrium *models were fitted by employing a nonlinear method, with successive interactions calculated by the method of Levenberg-Marquardt and also interactions calculated by the Simplex method, using the nonlinear fitting facilities of the software Microcal Origin 7.0. In addition, the models were also evaluated by determination coefficient ($R^2$); adjusted determination coefficient ($R^2$ adj), as well as by an error function ($F_{error}$) [49], which measures the differences in the amount of dye taken up by the adsorbent predicted by the models and the actual q measured experimentally. $R^2$, $R^2_{adj}$ and $F_{error}$ are given* below, in Eqs. 18, 19 and 20 respectively:

$$R^2 = \left( \frac{\sum_i^n \left( q_{i,exp} - \overline{q}_{i,exp} \right)^2 - \sum_i^n \left( q_{i,exp} - q_{i,model} \right)^2}{\sum_i^n \left( q_{i,exp} - \overline{q}_{i,exp} \right)^2} \right) \quad (18)$$

$$R^2_{adj} = 1 - \left( 1 - R^2 \right) . \left( \frac{n-1}{n-p} \right) \quad (19)$$

$$F_{error} = \sqrt{\left( \frac{1}{n-p} \right) . \sum_i^n \left( q_{i,exp} - q_{i,model} \right)^2} \quad (20)$$

where $q_{i,\ model}$ is each value of q predicted by the fitted model, $q_{i,\ exp}$ is each value of *q* measured experimentally, $\overline{q}_{exp}$ is the average of *q* experimentally measured, *n* is the number of experiments performed, and *p* is the number of parameters of the fitted model [49].

**Supplementary Table 1**. Chemical composition of the simulated dyehouse effluent.

| | | Concentration (mg $L^{-1}$) | |
|---|---|---|---|
| **Dye** | **λ (nm)** | **Effluent A** | **Effluent B** |
| **Reactive Dyes** | | | |
| Reactive Red 120 | 534 | 20.0 | 60.0 |
| Reactive Orange 16 | 493 | 5.00 | 15.0 |
| Reactive Black 5 | 598 | 5.00 | 15.0 |
| Cibacron Brilliant Yellow 3G-P | 402 | 5.00 | 15.0 |
| **Direct dye** | | | |
| Direct Blue 53 | 607 | 5.00 | 15.0 |
| **Auxiliary chemical** | | | |
| $Na_2SO_4$ | | 100.0 | 100.0 |
| NaCl | | 100.0 | 100.0 |
| $Na_2CO_3$ | | 150.0 | 150.0 |
| $CH_3COONa$ | | 150.0 | 150.0 |
| $CH_3COOH$ | | 600.0 | 600.0 |
| pH | | 2.0* | 2.0* |

* pH of the solution adjusted with 0.10 mol $L^{-1}$ HCl and NaOH

**Supplementary Table 2.** Centesimal chemical composition and elemental composition of *Spirulina platensis*.

| Centesimal composition | (%, wet basis)[a] |
|---|---|
| Moisture content | 10.0 ± 0.7 |
| Ash | 6.0 ± 0.4 |
| Protein | 65.7 ± 0.5 |
| Lipids | 7.0 ± 0.1 |
| Carbohydrate [b] | 11.3 ± 0.5 |
| **Elemental composition** | **(%)[c]** |
| C | 56.3 ± 0.4 |
| N | 31.7 ± 0.6 |
| O | 8.0 ± 0.2 |
| P | 2.3 ± 0.1 |
| S | 1.7 ± 0.1 |

[a] mean ± standard error in triplicate. [b] by difference. [c]values ± standard error obtained from EDS analysis of five surfaces.

**Supplementary Table 3.** Textural properties of SP and AC adsorbents.

| Adsorbents | Surface Area ($m^2/g$) | Total pore Volume ($cm^3/g$) | Average pore diameter (nm) |
|---|---|---|---|
| SP | 3.51 | 0.00395 | 4.51 |
| PAC | 728.7 | 0.641 | 3.52 |

**Supplementary Table 4**. Kinetic parameters for RR-120 removal using SP and AC adsorbent. Conditions: temperature of 298 K; pH 2.0 for SP and pH 6.0 for AC; mass of adsorbent 50.0 mg.

| | SP | | AC | |
|---|---|---|---|---|
| Pseudo-first order | 200.0 mg $L^{-1}$ | 400.0 mg $L^{-1}$ | 200.0 mg $L^{-1}$ | 400.00 mg $L^{-1}$ |
| $k_1$ ($h^{-1}$) | 4.054 | 4.100 | 4.103 | 4.109 |
| $q_e$ (mg $g^{-1}$) | 77.51 | 154.6 | 76.97 | 152.3 |
| $h_0$ (mg $g^{-1}$ $h^{-1}$) | 314.2 | 634.0 | 315.8 | 625.9 |
| $R^2_{adj}$ | 0.9961 | 0.9942 | 0.9905 | 0.9916 |
| $F_{error}$ | 1.366 | 3.311 | 2.095 | 3.899 |
| Pseudo-second order | | | | |
| $k_2$ (g $mg^{-1}$ $h^{-1}$) | 0.07815 | 0.03970 | 0.07965 | 0.04030 |
| $q_e$ (mg $g^{-1}$) | 82.42 | 164.4 | 81.88 | 162.0 |
| $h_0$ (mg $g^{-1}$ $h^{-1}$) | 530.9 | 1073.3 | 534.0 | 1058.2 |
| $R^2_{adj}$ | 0.9911 | 0.9931 | 0.9962 | 0.9956 |
| $F_{error}$ | 2.056 | 3.597 | 1.325 | 2.814 |
| General order | | | | |
| $K_n$ [$h^{-1}$.(g $mg^{-1}$)$^{n-1}$] | 1.236 | 0.7168 | 0.5575 | 0.4521 |
| $q_e$ (mg $g^{-1}$) | 78.41 | 157.1 | 78.82 | 155.7 |
| N | 1.312 | 1.386 | 1.591 | 1.488 |
| $h_0$ (mg $g^{-1}$ $h^{-1}$) | 377.1 | 793.4 | 424.3 | 827.2 |
| $R^2_{adj}$ | 0.9997 | 0.9997 | 0.9998 | 0.9998 |
| $F_{error}$ | 0.3881 | 0.7028 | 0.2860 | 0.6151 |
| Intraparticle | | | | |
| $k_{id}$ (mg $g^{-1}$ $h^{-0.5}$)* | 15.54 | 33.09 | 24.82 | 33.83 |
| $R^2$ | 0.9864 | 0.9854 | 0.9856 | 0.9875 |

* second stage

**Supplementary Table 5.** Isotherm parameters for RR-120 adsorption, using SP and AC adsorbents. Conditions: adsorbent mass 50.0 mg; pH fixed at 2.0 for SP and 6.0 for AC, contact time 3 h.

| | SP | | | | | | AC | | | | | |
|---|---|---|---|---|---|---|---|---|---|---|---|---|
| | 298 K | 303 K | 308 K | 313 K | 318 K | 323 K | 298 K | 303 K | 308 K | 313 K | 318 K | 323 K |
| Langmuir | | | | | | | | | | | | |
| $Q_{max}$ (mg $g^{-1}$) | 390.7 | 364.7 | 341.4 | 314.9 | 293.5 | 258.4 | 293.1 | 287.7 | 280.8 | 275.5 | 274.4 | 274.1 |
| $K_L$ (L $mg^{-1}$) | 0.3085 | 0.2710 | 0.2332 | 0.2201 | 0.1992 | 0.2190 | 0.1101 | 0.1025 | 0.09023 | 0.08087 | 0.07140 | 0.06229 |
| $R^2_{adj}$ | 0.9815 | 0.9826 | 0.9834 | 0.9809 | 0.9821 | 0.9735 | 0.9896 | 0.9803 | 0.9773 | 0.9752 | 0.9637 | 0.9476 |
| $F_{error}$ | 15.11 | 13.61 | 12.34 | 12.38 | 11.17 | 11.92 | 9.122 | 11.17 | 12.17 | 12.54 | 14.93 | 17.57 |
| Freudlich | | | | | | | | | | | | |
| $K_F$ (mg $g^{-1}$ (mg $L^{-1})^{-1/n_F}$) | 171.7 | 154.2 | 138.5 | 121.2 | 108.2 | 101.0 | 72.53 | 75.51 | 67.09 | 60.45 | 54.49 | 50.66 |
| $n_F$ | 5.362 | 5.157 | 4.977 | 4.656 | 4.490 | 4.716 | 3.325 | 3.485 | 3.329 | 3.156 | 2.973 | 2.892 |
| $R^2_{adj}$ | 0.9886 | 0.9880 | 0.9867 | 0.9833 | 0.9830 | 0.9848 | 0.9011 | 0.8899 | 0.8853 | 0.8828 | 0.8716 | 0.8515 |
| $F_{error}$ | 11.85 | 11.29 | 11.03 | 11.55 | 10.89 | 9.029 | 28.15 | 26.43 | 27.37 | 27.25 | 28.08 | 29.58 |
| *Liu* | | | | | | | | | | | | |
| $Q_{max}$ (mg $g^{-1}$) | 482.2 | 447.6 | 413.9 | 386.1 | 359.4 | 333.2 | 267.2 | 255.3 | 247.4 | 239.5 | 230.6 | 223.9 |
| $K_g$ (L $mg^{-1}$) | 0.1698 | 0.1539 | 0.1412 | 0.1257 | 0.1142 | 0.1048 | 0.1313 | 0.1201 | 0.1095 | 0.1001 | 0.09239 | 0.08364 |
| $n_L$ | 0.5235 | 0.5424 | 0.5658 | 0.5781 | 0.5890 | 0.5313 | 1.412 | 1.605 | 1.661 | 1.712 | 1.9535 | 2.196 |
| $R^2_{adj}$ | 0.9996 | 0.9997 | 0.9998 | 0.9996 | 0.9998 | 0.9996 | 0.9995 | 0.9994 | 0.9993 | 0.9997 | 0.9998 | 0.9997 |
| $F_{error}$ | 2.154 | 1.684 | 1.369 | 1.892 | 1.234 | 1.450 | 1.911 | 2.007 | 2.140 | 1.359 | 1.180 | 1.380 |

**Supplementary Table 6**. Maximum sorption capacities of different adsorbents used to remove dyes.

| Adsorbent | Adsorbate | $Q_{max}$ (mg $g^{-1}$) | Reference |
|---|---|---|---|
| *S. platensis* | Reactive red 120 | 482.2 | This work |
| Commercial activated carbon | Reactive red 120 | 267.2 | This work |
| Cupuassu shell | Reactive red 194 | 64.1 | [3] |
| Akai stalks | Reactive black 5 | 52.3 | [4] |
| Multi-walled carbon nanotubes | Reactive red M-2BE | 335.7 | [11] |
| Jujuba seeds | Congo red | 55.56 | [13] |
| Brazilian-pine fruit shell | Methylene blue | 252.0 | [15] |
| modified sugarcane bagasse | Brilliant Red 2BE | 73.6 | [16] |
| Organofunctionalized kenyaite | Sumifix Brilliant Orange 3R | 70.7 | [20] |
| octosilicate Na-RUB-18 | Reactive Black 5 | 76.8 | [21] |
| Single-wall carbon nanotubes | Reactive Blue 4 | 567.7 | [26 |
| *S. platensis* | FD&C red n°40 | 400.3 | [32] |

**Supplementary Table 7.** Thermodynamic parameters of the adsorption of RR-120 dye on SP and AC adsorbents. Conditions: mass of adsorbent 50.0 mg, pH fixed at 2.0 for SP and 6.0 for AC; contact time of 3 h.

| | Temperature (K) | | | | | |
|---|---|---|---|---|---|---|
| | 298 | 303 | 308 | 313 | 318 | 323 |
| SP | | | | | | |
| $K_g$ (L $mol^{-1}$) | $2.496.10^5$ | $2.259.10^5$ | $2.076.10^5$ | $1.848.10^5$ | $1.679.10^5$ | $1.540.10^5$ |
| $\Delta G$ (kJ $mol^{-1}$) | -30.79 | -31.06 | -31.35 | -31.56 | -31.81 | -32.08 |
| $\Delta H°$ (kJ $mol^{-1}$) | -15.64 | - | - | - | - | - |
| $\Delta S°$ (J $K^{-1}$ $mol^{-1}$) | 50.89 | - | - | - | - | - |
| $R^2$ | 0.9982 | - | - | - | - | - |
| AC | | | | | | |
| $K_g$ (L $mol^{-1}$) | $1.930.10^5$ | $1.765.10^5$ | $1.610.10^5$ | $1.472.10^5$ | $1.358.10^5$ | $1.230.10^5$ |
| $\Delta G$ (kJ $mol^{-1}$) | -30.15 | -30.43 | -30.70 | -30.97 | -31.25 | -31.47 |
| $\Delta H°$ (kJ $mol^{-1}$) | -14.31 | - | - | - | - | - |
| $\Delta S°$ (J $K^{-1}$ $mol^{-1}$) | 53.20 | - | - | - | - | - |
| $R^2$ | 0.9989 | - | - | - | - | - |

**Supplementary Table 8**. Desorption of RR-120 dye loaded on SP and AC adsorbents. Conditions for adsorption: initial RR-120 concentration 50 mg $L^{-1}$; mass of adsorbent 50.0 mg, pH 2.0; time of contact 1 h.

| | % Desorption | |
|---|---|---|
| Conditions for desorption (mol $L^{-1}$) | SP | AC |
| 0.05 NaCl | 1.25 | 0.94 |
| 0.10 NaCl | 1.34 | 1.24 |
| 0.20 NaCl | 1.95 | 1.37 |
| 0.30 NaCl | 2.36 | 1.98 |
| 0.40 NaCl | 2.64 | 2.02 |
| 0.50 NaCl | 2.85 | 2.16 |
| 0.05 NaOH | 44.32 | 7.36 |
| 0.10 NaOH | 65.36 | 9.56 |
| 0.20 NaOH | 78.36 | 11.35 |
| 0.30 NaOH | 95.42 | 12.34 |
| 0.40 NaOH | 94.34 | 11.52 |
| 0.50 NaOH | 98.36 | 12.01 |
| 0.05 NaCl + 0.10 NaOH | 70.15 | 9.85 |
| 0.10 NaCl + 0.10 NaOH | 71.14 | 9.45 |
| 0.20 NaCl + 0.10 NaOH | 70.87 | 10.15 |
| 0.30 NaCl + 0.10 NaOH | 72.35 | 10.33 |
| 0.40 NaCl + 0.10 NaOH | 74.36 | 10.25 |

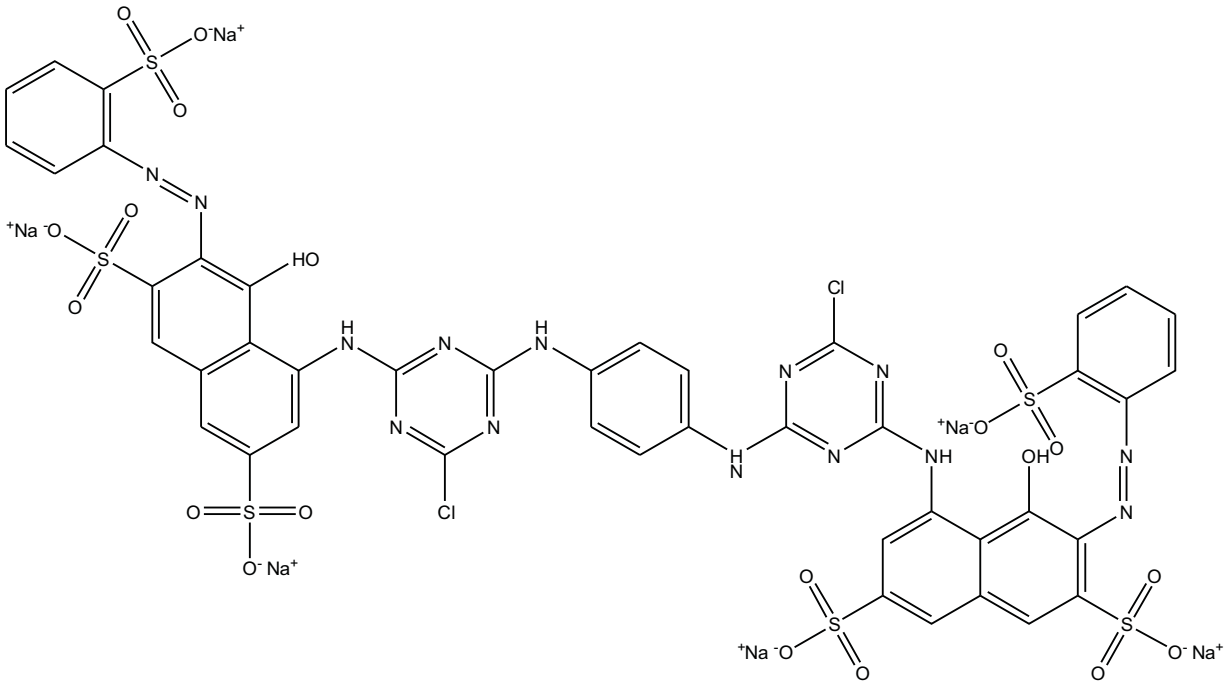


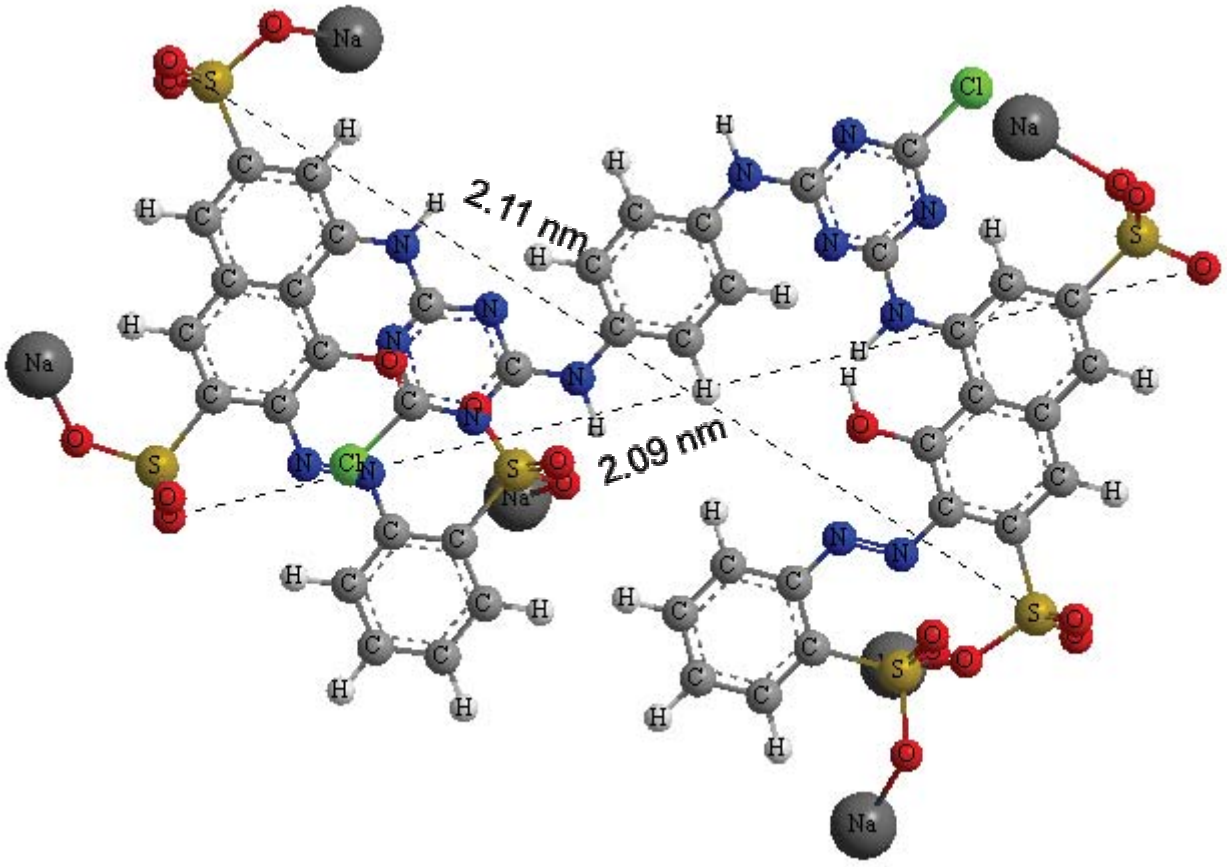


Supplementary Fig 1. A) Structural formulae of RR-120
B) Optimized three-dimensional structural formulae of RR-120. The dimensions of the chemical molecule were calculated using ChemBio 3D Ultra version 11.0.